INFORMATION TO USERS

This material was produced from a microfilm copy of the original document. While the most advanced technological means to photograph and reproduce this document have been used, the quality is heavily dependent upon the quality of the original submitted.

The following explanation of techniques is provided to help you understand markings or patterns which may appear on this reproduction.

1. The sign or "target" for pages apparently lacking from the document photographed is "Missing Page(s)". If it was possible to obtain the missing page(s) or section, they are spliced into the film along with adjacent pages. This may have necessitated cutting thru an image and duplicating adjacent pages to insure you complete continuity.

2. When an image on the film is obliterated with a large round black mark, it is an indication that the photographer suspected that the copy may have moved during exposure and thus cause a blurred image. You will find a good image of the page in the adjacent frame.

3. When a map, drawing or chart, etc., was part of the material being photographed the photographer followed a definite method in "sectioning" the material. It is customary to begin photoing at the upper left hand corner of a large sheet and to continue photoing from left to right in equal sections with a small overlap. If necessary, sectioning is continued again — beginning below the first row and continuing on until complete.

4. The majority of users indicate that the textual content is of greatest value, however, a somewhat higher quality reproduction could be made from "photographs" if essential to the understanding of the dissertation. Silver prints of "photographs" may be ordered at additional charge by writing the Order Department, giving the catalog number, title, author and specific pages you wish reproduced.

5. PLEASE NOTE: Some pages may have indistinct print. Filmed as received.

Xerox University Microfilms
300 North Zeeb Road
Ann Arbor, Michigan 48106

76-27,509

KAPLAN, Allan Steven, 1942-
KINETICS OF FLOCCULATION IN A LAMINAR SHEAR FIELD.

The University of Michigan, Ph.D., 1976
Chemistry, pharmaceutical

Xerox University Microfilms, Ann Arbor, Michigan 48106

KINETICS OF FLOCCULATION

IN A LAMINAR SHEAR FIELD

by

Allan Steven Kaplan

A dissertation submitted in partial fulfillment
of the requirements for the degree of
Doctor of Philosophy
(Pharmaceutical Chemistry)
in The University of Michigan
1976

Doctoral Committee:

Professor William I. Higuchi, Chairman
Professor Walter R. Debler
Associate Professor Gordon L. Flynn
Adjunct Professor Everett N. Hiestand
Associate Professor Norman F. H. Ho
Associate Professor Norman D. Weiner

To

My Wife, Eileen,

and My Children,

Nicole, Andrew, Lisa, and Michael

ACKNOWLEDGMENTS

The author desires to take this opportunity to express his appreciation to the interested individuals who have unselfishly contributed their time and effort toward the successful completion of this research project.

It has been my privilege to have been associated with Dr. William I. Higuchi and Dr. Norman F. H. Ho. Their personal dedication and depth of physical insight were reflected in their guidance and encouragement throughout my graduate career.

To Dr. Walter R. Debler for his contributions to the development of the couette cell and his insight into the problem of Taylor vortices.

To Dr. Toshi Yotsuyanagi for his aid in computer technology.

To the other members of the Doctoral Committee for their valuable suggestions during the preparation of this manuscript.

To Gregory Amidon for his assistance in the laboratory.

To the United States Public Health Service, National Institute of Dental Research, The National Institutes of Health, Bethesda, Maryland, I am grateful for continuous financial support through Training Grant DE-00204-08.

To my wife, Eileen, I shall be forever grateful for her encouragement, understanding, and love.

TABLE OF CONTENTS

DEDICATION ii

ACKNOWLEDGEMENTS iii

LIST OF TABLES viii

LIST OF FIGURES x

LIST OF APPENDICES xiv

INTRODUCTION 1

LITERATURE REVIEW AND THEORETICAL CONSIDERATIONS . . . 2

Kinetics of Perikinetic Flocculation 3

Fundamental flocculation equations 3
The stability factor-electrical and hydrodynamic considerations 5
Kinetics of a monodispersed system 8

Kinetics of Orthokinetic Flocculation 9

Fundamental flocculation equations 9
The stability factor W^* - electrical and hydrodynamic considerations 11
Kinetics of a monodispersed system 15

Kinetics of Perikinetic and Orthokinetic Flocculation of a Relatively Monodispersed Particle System 18

Pertinent Experimental Considerations and Results 20

Pertinent Experimental Investigations of Orthokinetic Theory 26

STATEMENT OF THE PROBLEM 33

CONSIDERATIONS IN THE PRESENT APPROACH TO THE PROBLEM 35

Experimental Methodology 37

Materials 37
Apparatus 41
Preparation of the suspension 44
Procedure of the flocculation experiments . 45
Particle size analysis 46
Dilution technique 54

NUMERICAL ANALYSIS 60

The Computer Program 60

The equations 60
The program 61

Computer Simulation Studies 65

Analysis of normalized plots 66
Effect of initial particle size distribution on the rate plot 66
Effect of the total interaction barrier on the rate plot 70
Effect of rate of shear on the rate plot . 73
Effect of the radius of a singlet on the rate plot 75
Effect of the total initial number of particles on the rate plot 77
Effect of alpha and epsilon on the rate plot 77

KINETIC STUDIES 86

Theoretical Estimations of the Performance of the Shear Cell and Flocculating Particle System 86

Electrolyte Effects 89

Surfactant Effects 92

Rate of Shear Effects 95

Particle Size Distribution Effects 100

Particle Density Effects 107

Total and Individual Particle Size Distribution Changes with Time 109

Orthokinetic studies 111
Effect of alpha and epsilon 111
Effect of particle size distribution . . 114

THE TAYLOR SHEAR CELL 120

Introduction 120

Electrolyte Effects 123

Rate of Shear Effects 123

Total and Individual Particle Size Distribution Changes 126

Fitting of the Data 128

DIFFUSION-CONTROLLED FLOCCULATION 133

Introduction 133

Electrolyte and Surfactant Effects 134

Total and Individual Particle Size Distribution Changes 141

Comparison of Orthokinetic and Perikinetic Studies 143

DISCUSSION 145

General 145

Clarification of the Literature and Future Studies 145

Application to Pharmaceutics 147

Theoretical Considerations of Curtis and Hocking 148

APPENDIX 152

BIBLIOGRAPHY 177

LIST OF TABLES

Tables		Page
I.	Dimensions of Couette Cell	43
II.	Evaluation of Day-To-Day Variation Within and Between Coulter Counter Model A and the RIDL Pulse Height Analyzer	55
III.	Evaluation of Dilution Technique Using 2.02 μ Latices and the Coulter Counter Model A	56
IV.	Initial Particle Size Distributions Chosen for the Computer Simulation Presented in Figure 10	69
V.	Calculated Parameters of the Particle System in the Shear Cell at 25°C and Relative Contribution of Laminar Shear-Induced Flocculation to Diffusion Controlled Flocculation	87
VI.	Flocculation Rate Constants and Apparent Stability Factors $W^*_{app.}$ at Various Salt Concentrations at 25°C and G = 31.3 . .	91
VII.	Flocculation Rate Constants and Apparent Stability Factors $W^*_{app.}$ with and without Surfactant at 25°C and G = 31.3	96
VIII.	Flocculation Rate Constants and Apparent Stability Factors $W^*_{app.}$ at Various Rates of Shear at 25°C with NaCl Concentration = 1.50%, TTAB Concentration = 5×10^{-6} M	99
IX.	Important Parameters of Figures 22 and 23 .	101
X.	Flocculation Rate Constants and Apparent Stability Factors $W^*_{app.}$ at Various Rates of Shear for Different Initial Particle Size Distributions at 25°C NaCl Concentration = 1.50%, TTAB Concentration = 5×10^{-6} M	106
XI.	Dimensions of the Taylor Shear Cell	122
XII.	Rate Constants Obtained from Various Perikinetic Systems	136

Tables Page

XIII. Mass Balance at Each Sample Interval for the Laminar Shear-Controlled Experiment Pictured in Figure 42 156

XIV. Parameters Used for Model Simulations 170

XV. Parameters Used for Model Simulations 171

XVI. Parameters Used for Model Simulations 172

XVII. Parameters Used for Model Simulations 173

LIST OF FIGURES

Figure		Page
1.	Laminar Shear Cell Giving Couette Flow	42
2.	Experimental Flow Chart	47
3.	Coulter Counter System	48
4.	Standard Curve for Coulter Count Correction .	51
5.	Calibration Curves of Ultrasonified and Aggregated Samples of 2.02 Micron Latex . . .	53
6.	Comparison of Dilution Techniques	58
7.	Flow Chart of the Computer Program	63
8.	Continuation of the Computer Program Flow Chart	64
9.	Normalized Plot of the Theoretical Simulation of Rapid Flocculation with an Arbitrary Size Distribution to Demonstrate the Utility of the Treatment of Orthokinetic Data by Smoluchowski Type Kinetics	67
10.	Normalized Plot Depicting the Theoretical Simulation of Rapid Flocculation with Arbitrary Polydispersed Particle Size Distributions	68
11.	Normalized Plot Depicting Theoretical Simulations of Identical Particle Size Distributions for Three Distinct Values of the Total Interaction Barrier, W^*_{ij}	71
12.	Plot of Theoretical Simulations of Initially Monodispersed Particle Size Distributions for Two Distinct Values of the Rate of Shear, G	74
13.	Plot of Theoretical Simulations of Initially Monodispersed Particle Size Distributions for Two Distinct Particle Radii	76
14.	Plot of Theoretical Simulations of Initially Monodispersed Particle Size Distributions for Two Different Particle Concentrations	78

Figure Page

15. Normalized Plot Depicting Theoretical Simulations of an Initially Monodispersed Particle Size Distribution with Various Values of Alpha 80

16. Normalized Plot of Theoretical Simulations of an Initially Monodispersed Particle Size Distribution for Three Different Values of Epsilon 82

17. Normalized Plot Depicting Theoretical Simulations of an Initially Monodispersed Particle Size Distribution for Two Different Values of Alpha and Epsilon in Each Curve . . 84

18. Normalized Plot of Various Orthokinetic Systems Depicting the Effect of Salt Concentration on the Rate of Reaction (Modification of Electrical Double Layer) . . 90

19. Normalized Plot Depicting the Effect of Quaternary Ammonium Compound on Reaction Rate (Modification of Surface Charge Density) 93

20. Normalized Plot Depicting the Effect of Quaternary Ammonium Compound on Reaction Rate (Modification of Surface Charge Density) 94

21. Plot Showing the Rate of Shear Effects on the Rate of Reaction 97

22. Normalized Plot Depicting the Effect of Polydispersity on the Reaction Rate of an Orthokinetic System 102

23. Normalized Plot Depicting the Effect of Polydispersity on the Reaction Rate of an Orthokinetic System 103

24. Normalized Plot Depicting the Effect of Particle Density on Experimental Artifacts in Orthokinetic Reactions 108

25. Pictures of Differential Particle Distribution Taken from the Oscilloscope of the Multichannel Pulse Height Analyzer . . . 110

Figure Page

26. Normalized Plot of the Total and Individual Particle Size Distribution Change with Time in the Maximum Rate Case for a Laminar Shear-Controlled System 112

27. Normalized Plot of the Total and Individual Particle Size Distribution Change with Time in the Maximum Rate Case for a Laminar Shear-Controlled System 113

28. Normalized Plot of the Total and Individual Particle Size Distribution Change with Time in the Maximum Rate Case for a Laminar Shear-Controlled System with Various Alphas and Epsilons 115

29. Normalized Plot of the Total and Individual Particle Size Distribution Change with Time in the Maximum Rate Case for a Laminar Shear-Controlled System 116

30. Normalized Plot of the Total and Individual Particle Size Distribution Change with Time in the Maximum Rate Case for a Laminar Shear-Controlled System 117

31. Normalized Plot of the Total and Individual Particle Size Distribution Change with Time in the Maximum Rate Case for a Laminar Shear-Controlled System 118

32. Shear Cell Producing Taylor Vortices 121

33. Normalized Plot of Various Taylor Vortex Systems Depicting the Effect of Salt Concentration on the Rate of Reaction 124

34. A Plot Depicting the Effect of the Theoretical Rate of Shear on the Reaction Rate of a Taylor Vortex System 125

35. Normalized Plot of the Total and Individual Particle Size Distribution Change with Time in the Maximum Rate Case for a Taylor Vortex System 127

36. Plot of Various Computer Simulations Versus Experimental Data Obtained from the Taylor Shear Cell 131

Figure Page

37. Apparatus for Diffusion-Controlled Flocculation of Particles 135

38. Normalized Plot of Various Perikinetic Systems Showing the Effect of Salt Concentration on the Rate of Reaction 138

39. Normalized Plot Depicting the Effect of Particle Density on Experimental Artifacts in Perikinetic Reactions 140

40. Normalized Plot of the Total and Individual Particle Size Distribution Changes with Time in the Maximum Case for a Diffusion-Controlled System 142

41. The Slip of One Particle Around an Aggregate 149

42. Normalized Plot of the Total and Individual Particle Size Distribution Changes with Time in the Maximum Rate Case for a Laminar Shear-Controlled System Depicting the Loss of Mass Balance 156

LIST OF APPENDICES

APPENDIX I 152

Theoretical and Experimental Considerations of Extraneous Factors in Laminar-Shear Induced Flocculation Studies 152

APPENDIX II 159

Additional Considerations Pertaining to the Taylor Vortex System 159

APPENDIX III 165

Sample Calculations Plus Discussion of the Modification of Smoluchowski's Basic Equation to Include Alpha and Epsilon 165

APPENDIX IV 171

Tabulated Data for All Computer Simulations . 171

INTRODUCTION

In the field of colloid science, an important problem has been the treatment of the kinetics of flocculation of dispersed systems in a laminar shear field. Significant progress in this area has been limited by experimental, quantitative, and theoretical difficulties.

It was only recently that a numerical analysis approach to the handling of the rate equations has been developed, in which the effects of polydispersity, and electrical and hydrodynamic barriers were included. This approach, along with suitable experimental techniques, should provide significantly new avenues in our physical understanding of particle-particle interactions during laminar shear flocculation.

This thesis concentrates on the development of the necessary methodology required for quantitative study of discrete particle size interactions during laminar shear flocculation. As will be seen, the results of this investigation should be useful in future mechanistic studies of the kinetic behavior of emulsions and suspensions.

LITERATURE REVIEW AND THEORETICAL CONSIDERATIONS

The literature review will show that most of the rigorous experimental work dealing with colloid systems has been performed on systems under Brownian control. For this reason it is helpful and instructive to review pertinent Brownian as well as laminar shear studies to better understand colloid systems under laminar shear control. The literature review will be presented in sections dealing with theory, experimental approaches, and results in order to facilitate the flow of understanding.

Kinetics of Perikinetic Flocculation

Fundamental flocculation equations

The basic theory of the perikinetic flocculation of colloidal particles was first given by Smoluchowski (1916, 1917). Thereafter, refinements of the theory were made in the direction of the inclusion of the potential energy of interaction between two mutually approaching particles (Kruyt 1952, Verwey 1948) and a more rigorous description of the hydrodynamics in the collision process (Spielman 1970; Honig, et al., 1971).

The fundamental expression that describes the rate of change in particle concentration of size k in a discrete size distribution is given by

$$\frac{dN_k}{dt} = \frac{1}{2} \sum_{\substack{i=1 \\ j=k-i}}^{i=k-1} \frac{4\pi D_{ij} R_{ij} N_i N_j}{W_{ij}} - N_k \sum_{i=1}^{\infty} \frac{4\pi D_{ik} R_{ik} N_i}{W_{ik}} \qquad (1)$$

This is a set of nonlinear ordinary differential equations where the first term on the right side of Equation 1 describes the concentration of spherical particles of size k formed by the flocculation of smaller spherical particles of size i and j and the second term describes the concentration of particles of size k lost by the

collision with particles of all other sizes. The terms N_i, N_j and N_k denote the particle concentrations of size class i, j and k. The W_{ij}, W_{ik} are the stability factors. The D_{ij} is the mutual diffusion coefficient of two particles independent of interparticle distance and R_{ij} is the collision radius. Here,

$$D_{ij} = D_i + D_j = \frac{kT}{6\pi\eta}\left(\frac{1}{a_i} + \frac{1}{a_j}\right) \tag{2}$$

and

$$R_{ij} = a_i + a_j \tag{3}$$

where D_i and D_j are the diffusion coefficients as given by the Stokes-Einstein equation for spheres, kT is the thermal energy, η is the viscosity of the liquid medium, and a_i and a_j are the radii of the respective spheres.

To account for the rate of change of the total particle concentration irrespective of size, Equation 1 becomes

$$\frac{d\sum_{k=1}^{\infty} N_k}{dt} = \frac{dN_\infty}{dt} = \frac{-1}{2}\sum_{i=1}^{\infty}\sum_{j=1}^{\infty}\frac{4\pi D_{ij} R_{ij} N_i N_j}{W_{ij}} \tag{4}$$

where N_∞ is the concentration of particles of all sizes.

The stability factor - electrical and hydrodynamic considerations

In Smoluchowski's (1916) rapidly flocculating system the stability factor, W, is taken to be unity. In the latter system the amount of electrolyte in solution may determine whether flocculation will be rapid. The rate of flocculation is diminished when a repulsive force is acting between the particles, i.e., diffuse electrical double layer interactions. The stability factor defines the system:

$$W = (a_i + a_j) \int_{(a_i + a_j)}^{\infty} \frac{D_{ij}}{D^*_{ij}} \exp\left(\frac{V_T}{kT}\right) \frac{dR}{R^2} \qquad (5)$$

The mathematical description of the effect of hydrodynamic or viscous interactions between mutually diffusing particles was developed by Spielman (1970) and independently by Honig, et al. (1971). D^*_{ij} is the mutual diffusion coefficient between two particles of sizes, a_i and a_j, and is a function of interparticle distance, H. Under the conditions of $H<a_i$ and a_j,

$$D^*_{ij} \simeq D_{ij} \left(\frac{6U^2 + 4U}{6U^2 + 13U + 2}\right)$$

$$\text{where } U = \frac{H(a_i + a_j)}{2a_i a_j} \qquad (6)$$

D_{ij} is the mutual diffusion coefficient which is independent of interparticle distance. The variable $R = (a_i + a_j + H)$.

These authors predicted that the correct diffusion controlled rate is 0.6 to 0.7 (Spielman) or 0.4 to 0.6 (Honig) of Smoluchowski's maximum rate. While performing flocculation studies utilizing latices, Higuchi (1963) noted this effect, and proposed that the correct diffusion controlled rate was between 0.5 and 0.8 of Smoluchowski's maximum rate. Other workers (Mathai 1966, Matthews 1968a, 1970) have also reported less than Smoluchowski maximum rate constants.

The theory predicts the electrical energy requirements of a colloidal dispersion in a dilute electrolyte solution for stability against coagulation. The basis of the theory is that the dispersed particles are subject to long-range attractive and electrical repulsive forces. The energy of attraction (V_A) is due to the London-van der Waals dispersion energy and the electrostatic repulsion energy (V_R) is due to the overlapping of electrical double layers. They are a function of interparticle distance, H. The total interaction energy is

$$V_T = V_A + V_R \tag{7}$$

If $V_A > V_R$ at all distances, an unstable system results, and the dispersion flocculates as rapidly as diffusion permits. If $V_R > V_A$, however, an energy barrier determines whether the aggregation is negligible (which is the case if the energy >>kT) or whether the aggregation is slowed, but not stopped, which is the case if the energy ≈kT.

The attractive energy (Kruyt 1952) between two spherical particles of radii a_i and a_j is given by:

$$V_A = -\left(\frac{A\, a_i a_j}{6(a_i + a_j)\, H}\right)\left(\frac{\lambda}{\lambda + 11.116\, H}\right) \qquad (8)$$

$$(H < a_i \text{ and } a_j)$$

where λ is the characteristic wavelength of the intrinsic oscillations of the atoms and H is the closest separation between particle surfaces, and A is the Hamaker constant. It should be noted that the attractive energy is independent of the electrical properties of the particle surfaces and the electrolyte concentration.

The approximate expression for the potential energy of electrical repulsion is:

$$V_R = \left(\frac{a_i a_j}{a_i + a_j}\right) \varepsilon \psi_0^2 \quad \ln\left(1 + \exp(-\kappa H)\right) \qquad (9)$$

Equation 9 is valid for low surface potentials (ψ_0 <<25 mv), and for spheres much larger than the electrical double layer thickness, i.e., $\kappa a > 1$ and for

$H<a_i$ and a_j. Another assumption in Equation 9 is that the surface potential is constant. ε is the dielectric constant of the medium.

$$\kappa = \left(\frac{\varepsilon kT}{4\pi\varepsilon^2 \Sigma \gamma_i Z_i^2} \right)^{-\frac{1}{2}} \tag{10}$$

where γ_i is the total number of ions of species i per cm^3 of solution, and Z_i is the valence of ions, i.

A more rigorous equation for the surface potential model was developed by Jones and Levine (1969) and Muller (1969), which account for all values of ψ_0. Another model, that of surface charge constant, has appeared in the literature (Jones 1969, Muller 1969, Ho 1970) and seems to provide a more appropriate explanation of the behavior of silver iodide sols (Frens 1969). Most recently Ho, et al. (1970, 1973) derived relatively simple quantitative expressions which describe the constant surface charge model for interactions between spheres.

Kinetics of a monodispersed system

In the special case where the dispersed system is essentially monodispersed in size and the particles are spherical, Equation 4 reduces to

$$\frac{dN_\infty}{dt} = -\frac{4\pi DR}{W} N_\infty^2 = -\frac{4kT}{3\eta W} N_\infty^2 \tag{11}$$

The integrated form is

$$\frac{1}{N_\infty} = \frac{1}{N_0} + \frac{4kT}{3\eta W} t \qquad (12)$$

where N_0 is the initial concentration of particles. A plot of $1/N_\infty$ versus t yields a linear relationship. At 25°C the term $4kT/3\eta$ is equal to 6.14×10^{-12} cm.^{3} sec.$^{-1}$. The half-life for rapid flocculation (W is taken as unity) is

$$\tau = \frac{3\eta}{4kTN_0} \qquad (13)$$

and, with Equation 13, the Smoluchowski equation is transformed into dimensionless concentration and time parameters, i.e.,

$$\frac{N_0}{N_\infty} = 1 + \frac{t}{W\tau} \qquad (14)$$

The suspension is considered to be sufficiently dilute so that multiple collision is precluded.

Kinetics of Orthokinetic Flocculation

Fundamental flocculation equations

The basic theory of laminar shear-induced flocculation of colloidal particles was also developed by Smoluchowski (1916, 1917). The general mathematical expression, which is a set of non-linear ordinary

differential equations that describe the rate of change in the particle concentration of size k in a discrete distribution, is:

$$\frac{dN_k}{dt} = \frac{1}{2} \sum_{\substack{i=1 \\ j=k-i}}^{i=k-1} \frac{4G}{3W^*_{ij}} (a_i + a_j)^3 N_i N_j$$

$$- N_k \sum_{i=1}^{\infty} \frac{4G}{3W^*_{ik}} (a_i + a_k)^3 N_i \qquad (15)$$

where the first term on the right of the equation describes the number of particles of size k formed by the flocculation of smaller particles and the second term describes the number of particles of size k lost by flocculation with particles of all other sizes; G is the shear rate with dimensions of reciprocal time, and W^*_{ij} and W^*_{ik} are the stability factors.

The rate of change in the total particle size distribution is:

$$\frac{d \sum_{k=1}^{\infty} N_k}{dt} = \frac{dN_\infty}{dt} = - \frac{1}{2} \sum_{i=1}^{\infty} \sum_{j=1}^{\infty} \frac{4G}{3W^*_{ij}} (a_i + a_j)^3 N_i N_j \qquad (16)$$

where N_∞ equals the concentration of particles of all sizes. The W^* will be discussed in a separate section.

The stability factor W^* - electrical and hydrodynamic considerations

Albers and Overbeck (1960) made theoretical calculations that demonstrated that water-in-oil emulsions cannot be sufficiently protected against flocculation by an absorbed layer of amphipolar molecules with an oleophilic chain of about 20 A^o. But most importantly they showed through viscosity measurements that such flocculated emulsions can be redispersed by shear forces. They were also able to calculate effective van der Waals constants between the water droplets. They wanted to know the minimum rate of shear required to surmount the van der Waals attraction between particles when the minimum distance between the surfaces is twice the length of the hydrocarbon chain (40 A^o). They determined whether the period during which the shearing force is acting lasted long enough to allow the redispersed particle to be removed to such a distance from the aggregate that it will not be caught back during the rotation of the aggregate. In studying the case of two equal spheres they concluded that when the rate of shear, G, exceeds the value

$$G_{crit.} > \frac{A}{36\pi\eta a H^2 \sin(2\alpha_{crit.})} \qquad (17)$$

where $\alpha_{crit.}$ is taken to be 30°, agglomerates will be broken up into single particles in less time than

required for half a revolution i.e., in less than $2\pi/G$. They showed that droplets of 1 μ protected by an oleophilic layer of 20 A° each, may be separated by a rate of shear of about 1000 $sec.^{-1}$ when the Hamaker constant is low. For a high value of this constant the rate of shear must be even higher.

In their paper Manley and Mason (1952) made microscopic observations of flocculated glass spheres of equal size, and observed that they appeared to be in true contact. Referring to Equation 17 one notes, as H goes to zero, G goes to infinity. This would indicate that extremely large shear rates would be required to separate the flocculated particles. Significantly, if one considers a range of Hamaker constants of 10^{-12} to 10^{-14} erg and a nominal distance of surface separation to be 40 A°, then the rate of shear required for deflocculation would be approximately 10^{5} to 10^{3} $sec.^{-1}$. This is a difference of two to four magnitudes over the largest shear rates employed during the experimental procedures described in this dissertation; therefore, shear-induced deflocculation is of no consequence for initially monodispersed systems at early times.

Swift and Friedlander (1964) performed a series of Brownian and shear-induced experiments utilizing polyvinylstyrene latex. They showed that the collision efficiency in both Brownian and shear-induced

flocculating systems is essentially the same. This is significant because although one would intuitively expect electrical interactions to be the same in either system, the fact that the hydrodynamics are the same is not intuitively obvious. Intuitively, one might suspect the existence of some "slippage" in a shear-induced system. Slippage is defined as the case where the overlap of two particles about to collide is slight, and the interparticulate hydrodynamic forces cause a great enough shift in trajectory, as the particles approach, to cause the particles to miss one another.

Lin, Lee and Sather (1969) took "slippage" into account in the derivation of their equations. They reported some results from the exact solution of the Stokes equations for the quasi-static motion of two spherical particles in the shear field of a viscous fluid. Their solution is obtained by an extension of an exact procedure employing spherical bipolar coordinates that has been developed by several previous investigators. The first application of the bipolar coordinate method was to the class of axisymetric flows associated with the translation and rotation of spheres in a quiescent fluid. Jeffrey (1915) analyzed the flow in the vicinity of two spheres rotating slowly about their line of centers and the corresponding problem of the rotation of a sphere about an axis perpendicular to a plane boundary. Stimson and Jeffrey (1926) considered the creeping

motion of two spheres moving without rotation along their line-of-centers. The quasi-steady translation of a sphere perpendicular to a wall was determined independently by Brenner (1961) and Maude (1961). The application of the method to non-axisymetric motions was initiated by Dean and O'Neill (1963), who studied the rotation of a sphere about an axis parallel to a wall. The problem of the translation of a sphere parallel to a wall was solved by O'Neill (1964). Because of the linearity of the Stokes equations the results for simple motions can be combined to generate solutions of more complex cases. In this way Goldman, Cox and Brenner (1966) determined the motion of two arbitrarily oriented spheres through a quiescent fluid, and Wakiya (1967) considered the more general problem of two spheres moving in a non-uniform velocity field. Wakiya's results are for overall flows having a plane of symmetry and so do not describe the sphere and fluid motions when the particles are oriented arbitrarily with respect to a shear field as reported by Lin, Lee and Sather (1969).

Curtis and Hocking (1970) carried the analysis one step further by taking into account the London Hamaker forces. Devising an experimental system in which the particles are electrically neutral, so that there is no repulsive force due to interaction of electrical double layers, they concerned themselves theoretically with the

motion of the particles which was governed by three forces. These are the effect of the shearing motion on the particles, which drags them along in the fluid, the hydrodynamic forces which result from the translation and rotation of two particles immersed in a fluid, and the London force of attraction. It was shown by Curtis and Hocking that the collision efficiency in laminar shear-induced flocculation does not remain constant. Rather it is a function of the shear rate, particle radius, and Hamaker constant. They also demonstrated that over a wide range of shear rates the collision efficiency remains essentially constant (15 percent decrease in collision efficiency over a three fold increase in shear rate), and perhaps fortuitously for Swift and Friedlander, at a numerical value which happens to be essentually equivalent to the collision efficiency for the maximum rate of a diffusion controlled flocculation system. It is also apparent from the attempted calculation of an estimated Hamaker's constant in the Curtis and Hocking paper, that there was not consistent agreement between theory and experimental results.

Kinetics of a monodispersed system

In the special case of a relatively narrow distribution of spherical particles

$$(a_i + a_j)^3 \simeq (2a_i)^3 = 8a_i^3 \qquad (18)$$

and Equation 16 reduces to

$$\frac{dN_\infty}{dt} = \frac{16Ga_i^3}{3W_{ij}^*} N_\infty^2 \tag{19}$$

The integrated form is

$$\frac{1}{N_\infty} = \frac{1}{N_0} + \frac{16Ga_i^3}{3W_{ij}^*} t \tag{20}$$

where N_0 is the initial concentration of particles. The plot of $1/N_\infty$ versus t predicts a linear relationship with a slope of $16Ga_i^3/3W_{ij}^*$ and an intercept of $1/N_0$. The half-life for rapid flocculation (when W_{ij}^* is taken as unity) is defined as

$$\tau^* = \frac{3}{16Ga_i^3 N_0} \tag{21}$$

Using the half-life expression with Equation 20, the Smoluchowski orthokinetic equation is transformed into dimensionless concentration and time parameters, i.e.,

$$\frac{N_0}{N_\infty} = 1 + \frac{t}{W^*\tau^*} \tag{22}$$

An alternate treatment of the theory, as used by Swift and Friedlander (1964) gives rise to another expression for the overall kinetics of the shear-controlled system. When particles are in laminar shear-control,

Smoluchowski specified that:

$$\phi = \int_0^\infty n(v)\,dv \tag{23}$$

and for an essentially monodispersed system

$$\phi \simeq N_\infty \bar{V} \tag{24}$$

where ϕ equals the volume fraction of suspended particles; $n(v)$ is the number concentration of sizes v and v + dv; N_∞ is the number concentration of particles and $\bar{V}$ is the mean size of the singlet particles, or $4/3\pi a_1^3$.

Therefore, making the proper substitutions into Equation 19 one obtains:

$$\frac{dN_\infty}{dt} = - \frac{4G\phi}{\pi W^*_{ij}} N_\infty \tag{25}$$

and the solution to Equation 25 is:

$$\ln \frac{N_\infty}{N_0} = - \frac{4G\phi}{\pi W^*_{ij}} t \tag{26}$$

Therefore, when flocculation is laminar shear-controlled, the kinetics of coagulation are first order with respect to total particle concentration when the distribution is relatively narrow. The rate constant is proportional to the shear rate.

Kinetics of Perikinetic and Orthokinetic Flocculation of a Relatively Monodispersed Particle System

When the initial particle size distribution is essentially monodispersed spheres and is dilute, the decrease in the particle concentration with time due to collision in a diffusional and laminar shear field (Swift and Friedlander 1964) may be described as:

$$\frac{dN_\infty}{dt} = - (K + K^*)N_\infty^2 \tag{27}$$

where

$$K = \frac{4kT}{3\eta W_{ij}} \tag{28}$$

$$K^* = \frac{16Ga_i^3}{3W^*_{ij}s} \tag{29}$$

where K and K* are the second order rate constants for Brownian collision and collision in a laminar shear field, respectively; s is the efficiency of collision between two interacting particles in a laminar shear field; it is noted here that the stability factor, W, was assumed to be the same for both Brownian, as well as, laminar shear-induced collision, since s is segregated.

Equation 27 is adequate only at relatively initial time periods. As the system becomes increasingly polydispersed with time, the fundamental equations of Smoluchowski (1917) should be utilized.

Integrating Equation 27 gives

$$\frac{1}{N_\infty} = \frac{1}{N_0} + (K + K^*)t \tag{30}$$

where N_0 is the total initial concentration of particles. There are two extreme situations. In a non-shear field the flocculation process is diffusion controlled. If the shear rate is sufficiently large, it follows that $K^*>K$ and the flocculation rate is laminar shear-controlled. To assess the relative contributions of Brownian and laminar shear-induced collisions in a flocculating system of relatively monodispersed particles at initial time, the ratio of Equations 28 and 29 may be used; thus,

$$\frac{K^*}{K} = \frac{4G\eta a_i^3}{kTs} \tag{31}$$

According to Swift and Friedlander (1964), Equation 27 can be alternatively expressed by

$$\frac{dN_\infty}{dt} = - KN_\infty^2 - K^{*\prime}N_\infty \tag{32}$$

where

$$K^{*\prime} = \frac{4G\phi}{\pi W^*_{ij} s} \tag{33}$$

The solution to Equation 32 is

$$\ln \left[\frac{N_0}{N_\infty} \left[\frac{N_\infty + P}{N_0 + P} \right] \right] = \frac{4G\phi}{\pi W^*_{ij} s} t \tag{34}$$

where

$$P = \frac{3G\phi\eta}{\pi kTs} \tag{35}$$

When the ratio of K* to K is large (for example, greater than ten) the first term on the right side of Equation 32 can be neglected; thus,

$$\ln \frac{N_\infty}{N_0} = - \frac{4G\phi}{\pi W^*_{ij} s} t \tag{36}$$

Pertinent Experimental Considerations and Results

The literature shows that the theoretical model dictates that a quantitative study of shear-induced flocculation requires that the particles be spherical and initially monodisperse. In addition, the system must be dilute enough to insure that binary (rather than tertiary) collisions predominate. Also required is that the sole driving force of flocculation be laminar shear, which necessitates the elimination of stirring or other turbulence producing shear mechanisms. Finally, creaming or sedimentation must be absent, and therefore the density of the dispersed phase must be a critical factor in the choice of the colloid. For this reason the literature review focuses on papers concerning experi-

mental design and approach, treatment of data in handling rate equations, and interpretation of results.

Due to the listed restrictions in experimental design, little quantitative work on laminar shear systems has been reported in the literature. Most of the work has dealt with Brownian studies performed on solid sols or latex suspensions since they are relatively monodisperse; and a few studies have involved emulsions. Bernstein (1971a) investigated the discrete particle size distribution, and this was for the Brownian situation. All other authors have only concerned themselves with the overall particle concentration, which in itself is a formidable problem.

Insuring a laminar flow in the shear cell is of primary importance. In his classic paper, Taylor (1923) described the conditions under which laminar flow might be expected in a system of flow between concentric cylinders. He explained that under certain circumstances there would be departure from laminar flow with the resultant axial formation of vortices which became known as Taylor vortices. It is worth pointing out that the heart of the mechanism of Taylor vortex formation is a kind of gyroscopic precession in the fluid. Suppose that the tangential velocity is initially non-uniform in the axial direction, so that the fluid is locally rotating about a line which is not quite parallel to the

cylinder axis. The radial pressure gradient and the centripetal accelerations arising from the curvature of the main flow field are also non-uniform, and exert a net torque (about a tangent) causing the axis of the local vorticity to precess into the tangential direction. The precession generates radial velocities in a meridional plane, and these in turn are coupled to tangential Coriolis accelerations which maintain the non-uniformity of the tangential velocity, thereby closing the circle. The condition of stability exists between two concentric vertical coaxial cylinders if the inner cylinder is stationary and the outer cylinder rotated. If the inner cylinder is rotated while holding the outer cylinder stationary, the onset of secondary flow (Taylor vortices) would develop after a certain Taylor number (T_a, dimensionless) had been exceeded. Under narrow gap conditions (when the gap is much less than the sum of the cell radii)

$$T_a = \frac{4R_1 d^3}{R_1 + R_2} \left[\frac{\Omega}{\nu}\right]^2 \qquad (37)$$

where ν is the kinematic viscosity of the fluid; Ω the angular velocity; d the gap between the cylinders; and R_1 and R_2 the respective radii of the inner and outer cylinders. He also denoted the critical value of the Taylor number by T_{ac}. When T_a is such that $T_{ac}<T_a<1.5T_{ac}$ the pattern of vortices is unaltered but their intensity

increases as T_a increases. Taylor found that $T_{ac} = 3414$. When the assumption of narrow gap geometry is no longer valid, $T_{ac}>3414$, the extent of the inequality increases with d/R_1 according to

$$T_{ac} = 3414/[(1-0.652d/R_1) + 0.0098(1-0.652d/R_1)^{-1}] \tag{38}$$

Taylor verified his predictions visually by injecting dye into the moving fluid from small holes drilled in the surface of the inner cylinder.

Schlichting (1955) verified Taylor's results and further enumerated the importance of concentricity between the cylinders. So long as this is the case, no limit of stability can exist when the inner cylinder is at rest and the outer cylinder rotates about its axis.

Bird, Curtis, and Lightfoot (1960) pointed out that when the inner cylinder is rotating at an angular velocity of Ω_i (and the outer one stationary), a transition Reynolds number (R_{trans}) may be expressed approximately as

$$R_{trans} = \frac{\Omega_i R_1^2}{\nu} \simeq \frac{41.3}{d^{3/2}} \tag{39}$$

Schultz-Grunow (1959) performed experiments with an arrangement in which particular attention was paid to making sure that the cylinders were exactly concentric and free from vibrations induced by imperfect balancing.

It was established that although transition does occur during the starting process, the flow reverts to a laminar pattern when a steady-state has been established (instantaneous reversion to stability).

This is very important because it shows that stop-and-go type of experiments as will be used in this study can be performed with relatively little error.

The two different hydrodynamic systems described above would be expected to give rise to vastly different data due to the difference in the number of collisions experienced in the laminar system versus the Taylor vortex system. Higuchi (1963, 1962) first investigated parameters of aggregation by differentiating the relative amounts of aggregates. Higuchi (1963) noted the singlet-singlet flocculation rate constant of 1.83 micron diameter latex differed from the Smoluchowski theoretical maximum rate by a factor of two. He explained that the deviation was due to a neglect of particle-particle hydrodynamic interactions when the particles are in close proximity. Subsequent studies were peformed by Lemberger (1965). Swift and Friedlander (1964), using latex particles studied both laminar shear-induced and diffusion-controlled systems. Applying similarity of self-preserving functions, to the Smoluchowski theory, they found results similar to that of Higuchi for the diffusion-controlled case. Their results for the laminar shear-controlled case was the most quantitative study

produced to date, and was in good agreement with theory. Matthews and Rhodes (1968a, 1968b) demonstrated the use of the Coulter Counter in the investigation of the flocculation of monodispersed latices. They found flocculation times (half-lives) to be about one and one-half times that predicted by Smoluchowski theory. Thus, the rate constants were about 67 percent of the Smoluchowski maximum rate, i.e., 5.6×10^{-12} cm.^{3} sec.$^{-1}$ at 30°C. This was in good agreement with Higuchi's work (1963). In their study they also did a critical evaluation of the Coulter Counter, pointing out advantages and disadvantages, as well as limitations of the instrument. They also demonstrated that the particle size distribution of polyvinyltoluene latices used was greater than that designated by the manufacturer.

Previous experiments concerned with the effect of a flow field on flocculation, although mostly qualitative in nature, demonstrated that there is indeed such an effect (Mason et al., 1951, 1952, 1955). Gillespie and Langstroth (1951) strove to measure the effect of a rotating paddle on aerosol coagulation, but the flow field was very complicated, and the resulting data difficult to interpret.

Several theoretical and experimental papers have dealt with coagulation in a turbulent fluid (Levich, 1962).

Saffman and Turner (1966) calculated the collision frequency of raindrops in turbulent clouds. Clay (1940) studied the size distributions of emulsions in turbulent pipe flows and turbulent Couette flows in which both particle coagulation and particle breakup by shear were significant.

Studies of coagulation and drop breakup were made by Shinner and Church (1960) and Vermeulen, Williams and Langlois (1955) using emulsions in baffled tanks. Shinner and Church used the concept of local isotropy of the turbulent fluid in determining the maximum size drop. Vermeulen, Williams, and Langlois correlated average drop size with stirring speed, geometry, and physical properties.

Pertinent Experimental Investigations of Orthokinetic Theory

The pertinent experimental investigations of orthokinetic flocculation has come from relatively few laboratories. Albers and Overbeek (1960) showed that flocculated water-in-oil emulsions can be redispersed (confirmed by viscosity measurements) at rates of shear ≥ 1000 sec.$^{-1}$. They were not interested in deflocculation as it relates to the progression of flocculation, but rather as it affects the estimation of the effective Hamaker's constant between water droplets. However, they developed

mathematical expressions to determine the criteria for deflocculation. Based on their equations it would take rates of shear many orders of magnitude greater (>3) than those they employed to cause deflocculation. They pointed out that under the influence of increasing hydrodynamic force, i.e., by increasing the rate of shear, a floc redisperses gradually. In other words, large aggregates break up into smaller and smaller aggregates until one reaches the monomer size. Since their calculations were based on the spontaneous breakup of the floc to the totally redispersed state, large aggregates could, in reality, begin to break up at less than the calculated shear rates. Breaking up of doublets and triplets was extremely difficult. This portion of their work demonstrated the importance of using monodispersed particle size distributions and only following initial rates so that large flocs do not accumulate.

One assumes that their viscosity measurements were truly indicative of the physical situation of the agglomerated emulsions they were studying. They plotted rate of shear versus shear stress and assumed that once they were in a linear region, complete redispersion would result. They assumed that when they were in the linear region the flocculated particles would deagglomerate to monomers, but this may not be necessarily so.

Deagglomeration could have stopped in the doublets, triplet, etc. stage. The only way to really be sure would have been to determine the individual particle size distribution of the emulsion. They, in fact, did not even know what the total number of particles were prior to agglomeration, after agglomeration, or after deagglomeration.

On the other hand, Swift and Friedlander (1964) did make an attempt to ascertain the degree of poly-dispersity in the latices they used for their flocculation studies. It is difficult to believe that they had greater than 95 percent of the singlet species when both Higuchi (1963) and Matthews and Rhodes (1968a), using exhaustive techniques found it difficult to achieve greater than about 90 percent, of the singlet species. This is extremely important since the degree of polydispersity enters into their calculations. Importantly, Swift and Friedlander were able to determine that the sampling disturbances due to stop-and-go experimentation (stopping to take samples) lasted approximately one second, which is about 0.2 percent of the time between data samplings. They sampled through a 1 mm. bore hypodermic needle and the samples were diluted to prevent further coagulation. Swift and Friedlander performed a calculation which indicated that the maximum change in the particle concentration due to shear in the needle was less than 1 percent. They did not include the

equations for the estimation of shear-induced flocculation or deflocculation in their paper. It should be noted that the amount of shear is very much dependent on the velocity of the fluid traversing the syringe. They did not say how they controlled the velocity (kept it constant, or nearly constant) nor did they present any data showing the effect of velocity during the sampling process. The shear cell used to perform their experiments was of the rotating inner cylinder type. Calculations show that their experiments were performed in the stable region, and not in the Taylor vortex region. Swift and Friedlander did shear flocculation experiments with a monodispersed polystyrene latex, but only looked at the total number of particles and not the individual particle size distributions. They also attempted to examine shear-induced flocculation with oil-in-water emulsions. Attempts to prepare an emulsion of uniform size were unsuccessful, therefore coagulation experiments with heterogeneous emulsions were performed. Total counts and size distribution were measured using the Coulter Counter. In general, their experiments with homogeneous polystyrene dispersions appeared to confirm the Smoluchowski theory of coagulation in a shear field. Yet, their experiments with hydrosols did not necessarily agree with the data from polystyrene dispersion experiments.

Curtis and Hocking (1970) offered a different theoretical, but essentially the same experimental approach to orthokinetic flocculation by focusing upon the influence of the London van der Waals forces on orthokinetic flocculation. In order to insure that unaggregated particles were essentially all of the same size, their suspensions of latices were subjected to density gradient centrifugation in a sucrose medium to separate the different size classes of particles. This was done subsequent to stabilization of the suspension with 0.1 percent sodium dodecyl sulphate. The excess surfactant was removed by subsequent washings with NaCl solutions. They also found it necessary to treat the washed and sized latex suspension in an ultrasonic bath to break up aggregates which formed during storage. The electrophoretic mobility of their latices was less than 2 mv. They also used a Coulter Counter to measure the total number of particles at all times. In a manner similar to Swift and Friedlander they used Smoluchowski's relationships to determine an experimental stability factor.

The theoretical determination of the stability factor for two equal spheres was based on a knowledge of the forces acting on the spheres at arbitrary positions and velocities, the differential equations determining the trajectories of the spheres, and lastly, the solution of these equations for enough different initial conditions to enable the collision efficiency to be calculated. Their theoretical treatment is much more rigorous than the basic Smoluchowski theory. The results they obtained were very interesting; they showed that from slow (0.6-8 $sec.^{-1}$) to moderate rates of shear there is a marked change in the collision efficiency, but when moderate rates of shear (30-112 $sec.^{-1}$) are achieved the stability factor remains essentially constant. As pointed out earlier, it was strictly by chance that Swift and Friedlander were doing orthokinetic flocculation studies which gave them stability factors that coincided with those obtained from their perikinetic flocculation studies. The paper by Curtis and Hocking makes this quite clear.

Although Bernstein's (1971b) work is concerned with the perikinetic flocculation of oil-in-water emulsions, it has great relevance to the approaches taken with respect to experimental technique, analysis of the particle size distribution, and the approach to the numerical analysis. Bernstein stressed the importance of methodology and

pointed out a number of artifacts that should be avoided. He showed that the particle size distribution could be determined with equal accuracy using both the Coulter Counter and a multi-channel pulse height analyzer and obtained good agreement between his experimental results and the theoretical predictions.

STATEMENT OF THE PROBLEM

As observed in the literature review, the evaluation of existing concepts on the flocculation of particles in a laminar shear field have not been rigorously pursued. The lack of such studies can be attributed to both difficulties in experimental design and suitable methods for the analysis of the particle size distribution changes with time.

Therefore, the objectives of this investigation are threefold:

1. To develop experimental techniques based on the Coulter Counter and RIDL 400-channel pulse height analyzer for measuring particle size distribution changes with time of a flocculating system under laminar shear.
2. To develop the numerical analysis approach for handling the theoretical particle size distribution changes with time, using Smoluchowski theory as a starting point, as well as producing some simulation studies.
3. Application of Sections 1 and 2 above in the assessment of the application of

Smoluchowski theory to the study of laminar shear flocculation of latex particles.

4. The study of flocculation under the influence of Taylor vortices with an attempt to theoretically correct for vortex effects.

5. A comparative study of perikinetic and orthokinetic flocculation.

The emphasis is on the accomplishment of items 1 through 3, the consequence of which would then permit one to begin to assess the mechanism of particle interactions.

CONSIDERATIONS IN THE PRESENT APPROACH TO THE PROBLEM

It is implicit in the literature review that cell design is of great importance in order to obtain laminar flow. In addition, experiments must be conducted at rates of shear of such magnitude as to preclude any significant perikinetic contribution to the reaction rates. The latex was carefully chosen so that it could provide an essentially non-sedimenting flocculating system. If this were not the case, one would have to account for sedimentation and/or sedimentation-flocculation. In order to meet the theoretical assumption of an essentially monodispersed particle size distribution, the particles were classified and segregated according to size. In addition, the latices and glassware were scrupulously cleaned to prevent the introduction of ionic contaminants into the system which would affect the electrical charge on the latex particle surface. The experiments must be conducted at such rates of shear as to preclude any shear-induced deflocculation. Sample retrieval and manipulation was accomplished in such a way as to prevent any shear-induced flocculation or deflocculation. The initial particle size distribution and the changes in the discrete particle size distribution with time were determined as accurately as possible in order

to provide a quantitative test of the Smoluchowski theory.

Experimental Methodology

Materials

Polyvinyltoluene[1] latices (PVT), essentially monosized 2.02 (±0.0135) microns in diameter were cleaned according to the method of Higuchi, et al. (1963). They were centrifuged in a Sorvall SS-3 Automatic Centrifuge[2] at 4080 relative centrifugal force (rcf) for twenty minutes. The latices were then washed with double distilled water, centrifuge again as before, and were next washed three times with 70 percent ethanol, and centrifuged at 2000 rcf for twenty minutes. Two subsequent washings with water at 4080 rcf for twenty minutes were then performed. Prior to centrifugation, the latices were resuspended in water with ultrasonification[3] until all particles had been redispersed. Finally, the PVT was redispersed in water at a concentration of about 10 percent solids and dialyzed using Visking[4] tubing. The tubing was placed in a 500 ml.

---

[1]PVT is polyvinyltoluene as uniform latex particles from the Dow Chemical Company, Midland, Michigan, 48640.

[2]Ivan Sorvall, Incorporated, Newtown, Connecticut, 06470.

[3]Acoustica 500 Sonifier, Los Angeles, California, at a frequency of 22 kilocycles and 7 amperes.

[4]Visking Dialysis Tubing, 6 cm. circumference, Union Carbide Corporation, Food Product Division, 6733 West 65th Street, Chicago, Illinois, 60638.

portion of water at 45°C which was changed daily according to the method of van den Hul and Vanderhoff (1968). Dialysis was carried out on the suspension for at least 30 days or until the electrophoretic mobility of the PVT was constant. Once the mobility was constant, it was found that the latex particles could be stored in a centrifuge tube so long as they were washed three times with double distilled water prior to use in an experiment. The washing procedure removed any residual surfactant (used during the polymerization step by the manufacture) leached out of the latex spheres. After washing, the mobility of particles stored in the centrifuge tube was the same as the mobility for particles stored in the Visking tubing.

It was found that the suspension contained about 85 percent singlets after the clean-up procedure. In order to increase the percentage of monomers, the particle suspensions were centrifuged at 1469 rcf for 7 minutes, and the upper half of the suspended particles removed and recentrifuged. This procedure was repeated a number of times to remove as many aggregates as possible. The Svedburg-Nichols modification of Stokes' Law for separation in a centrifuge was used to calculate times and distances to affect separation;

$$t = \frac{\eta \ln \left[\frac{X_2}{X_1}\right]}{F_s \omega^2 r_p^2 (\rho_p - \rho_m)} \qquad (40)$$

where X_1 is the rotating radius to the beginning of the path of travel in cm.; X_2 is the rotating radius to the end point of the path of travel in cm.; F_s is the particle shape factor, and is equal to 2/9 for a sphere; r_p is the radius of the particle in cm.; ρ_p is density of the particle; ρ_m is the density of the medium; t is time in seconds; η is the viscosity of the liquid in poise; and ω is the angular velocity in radians per second. Using this methodology, suspensions containing 90-95 percent singlets were obtained; and these were used for the flocculation studies.

Sodium chloride solutions used in the reactions were prepared by mixing particle-free sodium chloride[5] solutions and water for injection[5] and ranged in concentration from 0.5 to 1.5 percent. The content of the sodium chloride solutions was analyzed by use of the Buchler-Collove Chloridometer-Automatic Titrator[6].

The quaternary ammonium compound used was tetradecyltrimethylammonium bromide (TTAB)[7]. It was purified in a Soxhlet extractor using anhydrous benzene (freshly distilled) for two hours. It was then filtered and

---

[5]Abbott Laboratories, North Chicago, Illinois, 60064.

[6]Buchler Instruments, Fort Lee, New Jersey.

[7]K and K Laboratories, Incorporated, Plainview, New York, 11803.

recrystallized (Hauser 1941) by dissolving in absolute ethanol (two grams in 10 ml.).

Five times this amount of anhydrous diethyl ether was added to the solution which was cooled on ice to 0°C and then vacuum filtered. It was dried at 35°C under vacuum for two hours. The melting point was taken and found to be 257-258°C.

$\overline{\text{TTAB}}$ was used to neutralize the surface charge of the latex spheres. The amount of TTAB added was critical since too little would not reduce the charge enough and too much would cause charge reversal and/or stearic hindrance. The surface charge density of a latex sphere was calculated using the Gouy-Chapman relationship (Kruyt 1952)

$$\sigma = \left[\frac{\varepsilon b k T}{2\pi}\right]^{\frac{1}{2}} \cdot \sinh \left[\frac{Ze\psi_0}{2kT}\right] \qquad (41)$$

with ψ_0 being determined experimentally and where b is is an electrolyte characterized by $b = b_+ = b_-$. With a knowledge of σ and the concentration of particles, the appropriate molar concentration of TTAB could be estimated. This was determined to be 5×10^{-6} M. With this concentration of TTAB the zeta potential, which was equated to ψ_0, was found to be negative 2 millivolts.

Apparatus

All glassware used in these experiments were washed thoroughly in dilute Alconox[8], rinsed six times with tap water and three times with double distilled water, then oven dried prior to use. Pipets were subjected to four wash-rinse cycles, and three double distilled water rinses, and oven-dried. Scrupulous care was taken to minimize the presence of adsorbed surface active materials from beakers and pipets used in the preparation of the reaction vessel. These were washed and rinsed as described, immersed in concentrated nitric acid for 24 hours, then rinsed and dried as described to insure that no residual surface active material from the washing steps remained.

The Couette apparatus was constructed with a rotating cup and a stationary bob. The latter was constructed of aluminum and stainless steel (Figure 1). The Couette cell was water jacketed and maintained at 25°C during all experimentation. The dimensions (Table I) were chosen to optimize laminar flow while minimizing the reaction volume required. A variable speed motor was used to rotate the cup via a shaft mounted in a double bearing clamp. This clamp prevented wobbling of the cup.

---

[8]Alconox, Incorporated, New York, New York, 10003.

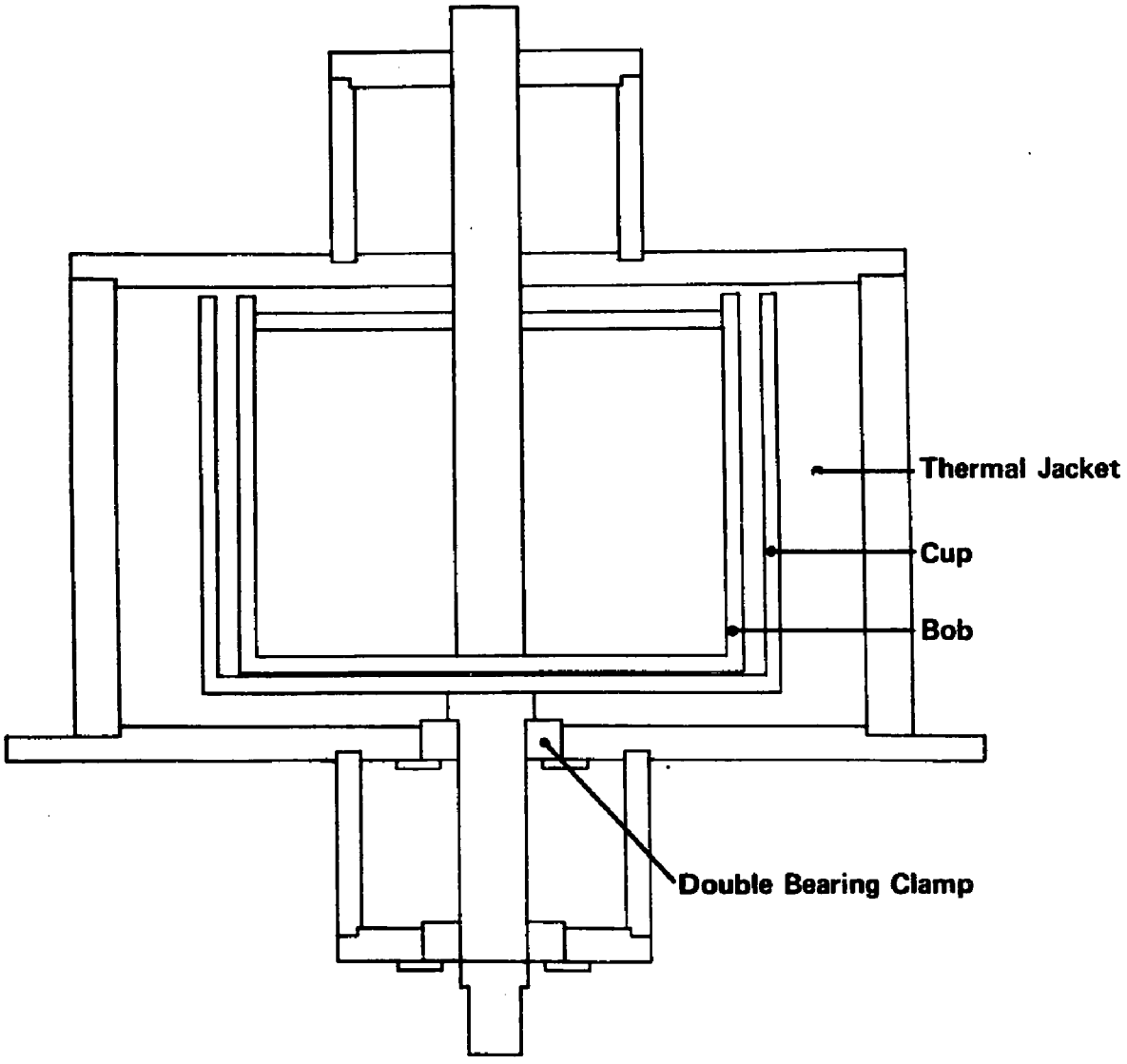

Figure 1. Laminar Shear Cell Giving Couette Flow

TABLE I

Dimensions of Couette Cell

Radius of the Cup	10.0 cm. ±0.01 mm.
Radius of the Bob	9.2 cm. ±0.01 mm.
Gap Between the Cup and Bob	0.8 cm. ±0.01 mm.
Height of the Cup	15.0 cm.
Height of the Bob	14.5 cm.

The rpm was set and checked at the beginning of each experiment using both the Hasler speed indicator[9] and the Monsanto Preset/Variable Time Base Counter Model 104A[10]. During the experiments the rpm was continuously monitored using the Monsanto 104A.

Preparation of the Suspension

To obtain an initially dilute suspension of an essentially monodispersed particle size distribution, clean latex particles were transferred into a volumetric flask containing sterile water and ultrasonified for one hour to further deagglomerate large aggregates formed during the centrifugation step of the particle cleaning. It was found through trial and error that a minimum of 45 minutes of sonification is required for deagglomeration, and that the number of particles per milliliter did not increase after one hour of sonification. In fact, sonification for periods significantly greater than one hour causes a reduction in the number of particles below the maximum. This procedure produced a particle size distribution of about 90 percent singlets, 6 percent doublets, 1 percent triplets, and 3 percent larger sizes. Since sonification caused a rise in temperature, the

---

[9]Hasler-Tel Company, 30 Vesey Street, New York, New York, 10007.

[10]Monsanto Electronic Instruments, 620 Passaic Avenue, West Cladwell, New Jersey, 07006.

volumetric containing the particles was placed into a 25°C water bath for approximately 20 minutes to bring the particle suspension to the proper temperature. The final volume of the suspension was adjusted with 5 percent sodium chloride solution at (25°C) and/or surfactant to get the desired electrolyte and/or surfactant concentration for the flocculation experiments. The total particle concentration range was 3×10^6 to 3×10^7 particles per milliliter.

Procedure of the flocculation experiments

To perform laminar shear-induced experiments the particle suspension was poured into the gap between the cup and bob, to a height below that of the bob (to prevent turbulence). The initial sample was taken and the motor started. Samples were always taken at a depth of 5 cm. beneath the top of the suspension, at the midpoint between the cup and bob. In each instance one milliliter of the reaction mixture was removed slowly (approximately 15 seconds) using a wide-bore pipet to assure minimal shear-induced flocculation or deflocculation. The dilution solution of 0.9 percent sodium chloride was swirled slowly with a pipet, prior to transfer, to induce motion in the solution to assure adequate mixing of the aliquot without unnecessary shear. The 1.0 ml. aliquot was then transferred over a period of 15 seconds to a point just beneath the surface of the

diluent, and was stirred slowly two or three times to assure homogeneity of the mixture. This aliquot was then counted and sized (Figure 2). Prior to taking each sample the motor was turned off and 10 seconds were allowed for the system to come to rest in order to prevent undue turbulence to the system when pipeting. The total sampling time was no more than 25 seconds. Then the motor was started again.

During initial experiments, samples were taken from alongside the cup and bob walls to determine if there was a detectable difference in the number of large particles. None was found.

Particle size analysis

Particle concentrations and size distributions were determined using the Coulter Counter, Model A[11] (CCA), equipped with a 50 micron aperture tube, in conjunction with a RIDL[12] 400-channel pulse height analyzer. The 50 micron aperture tube was stored in sulfuric acid-dichromate solution between experiments to prevent clogging.

The operation of the Coulter Counter may be followed by referring to Figure 3. A controlled vacuum

---

[11]Coulter Electronics, Incorporated, 590 West 20th Street, Hialeah, Florida, 33010.

[12]Radiation Instrument Development Laboratories, Incorporated, Melrose Park, Illinois.

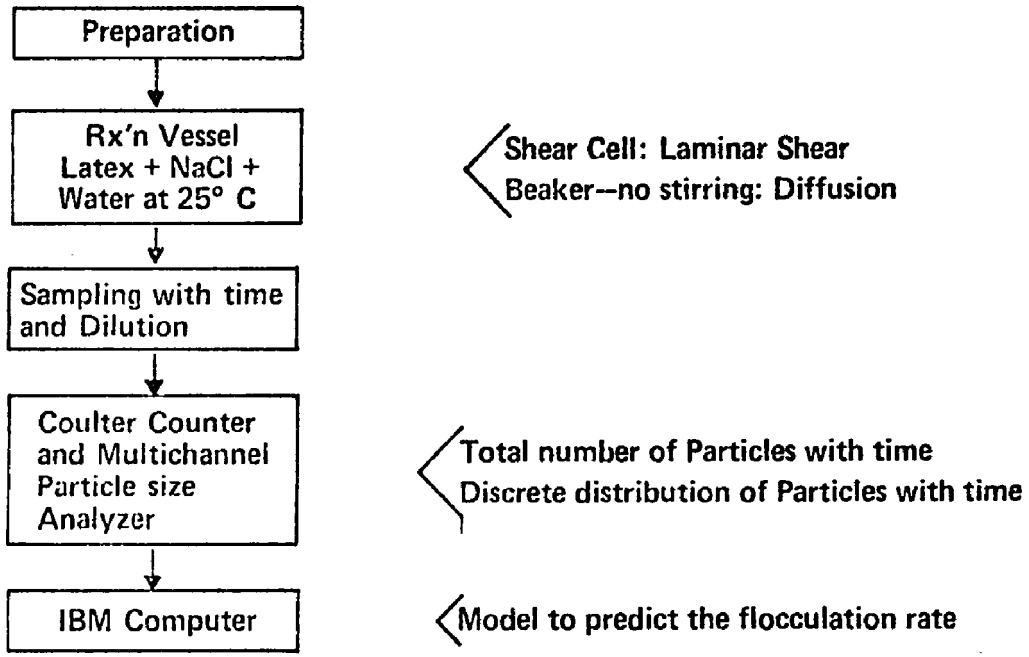

Figure 2. Experimental Flow Chart

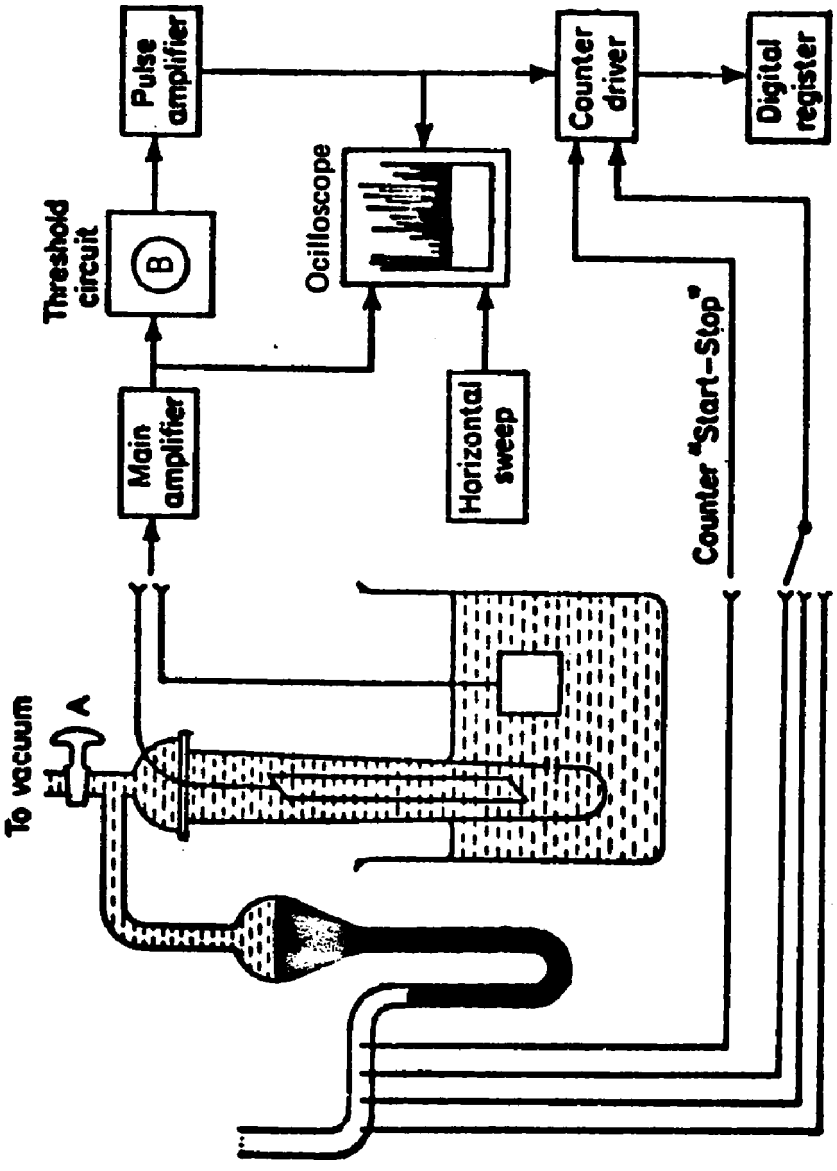

Figure 3. Coulter Counter System

pulls the flow through a sapphire orifice in the aperture tube and unbalances a mercury siphon. The system is then isolated from the vacuum by closing tap A and the flow continues due to the balancing action of the mercury siphon. The advancing mercury starts and stops the counter by means of probe switches placed in such a position that the count is carried out on known volumes of electrolyte (0.05, 0.5, 2.0 ml.). The resistance across the orifice is monitored by means of immersed electrodes on either side. As each particle passes through the orifice it changes the resistance, thus generating a voltage pulse which is amplified, sized, and counted.

Calibration of the 50 micron aperture tube was achieved with polyvinyltoluene latices of 1.857, 2.02, and 3.49 micron diameter in concentrations of about 12,000 particles per 0.05 ml. Spot check calibrations were performed at regular intervals to check electronic drift and background (electrical) noise. The manometer tube apparatus was completely shielded by copper screening to eliminate electronic noise.

It should be noted that when the Model A is electronically set so that zero threshold equalled true zero, a linear relationship between volume and threshold exists and gives the appropriate diameters of particles at a given threshold (B) for all experimental work.

The theory assumes only one particle will be found in the volume defined by the orifice at any one instant of time. There is a distinct possibility of two or more particles passing through simultaneously and being counted as a single particle. At high particle concentrations, the actual number of particles per volume unit will be significantly larger than the number counted.

Determination of the maximum number of particles per sample volume yielding no significant coincidence was made by taking a suspension containing 100,000 particles per 0.05 ml. of sample volume and counting repeated two-fold dilutions. A comparison of the true counts with the measured or apparent counts was made as shown in Figure 4. The point at which the line generated began to deviate from a slope of 1.0 was taken to be the upper limit where coincidence could be neglected for our studies. This value was 15,000 particles per 0.05 ml. sample volume. There was less than 10 percent coincidence up to 25,000 particles per 0.05 ml.

Coulter's laboratory manual (1966 ed.) claims that with a 50 micron aperture tube, the instrument can detect particles having an equivalent sphere diameter of 1.0 micron.

Experiments were performed at threshold settings of 7, 8, and 9. The threshold setting of 8 was chosen to minimize background noise and to optimize total particle

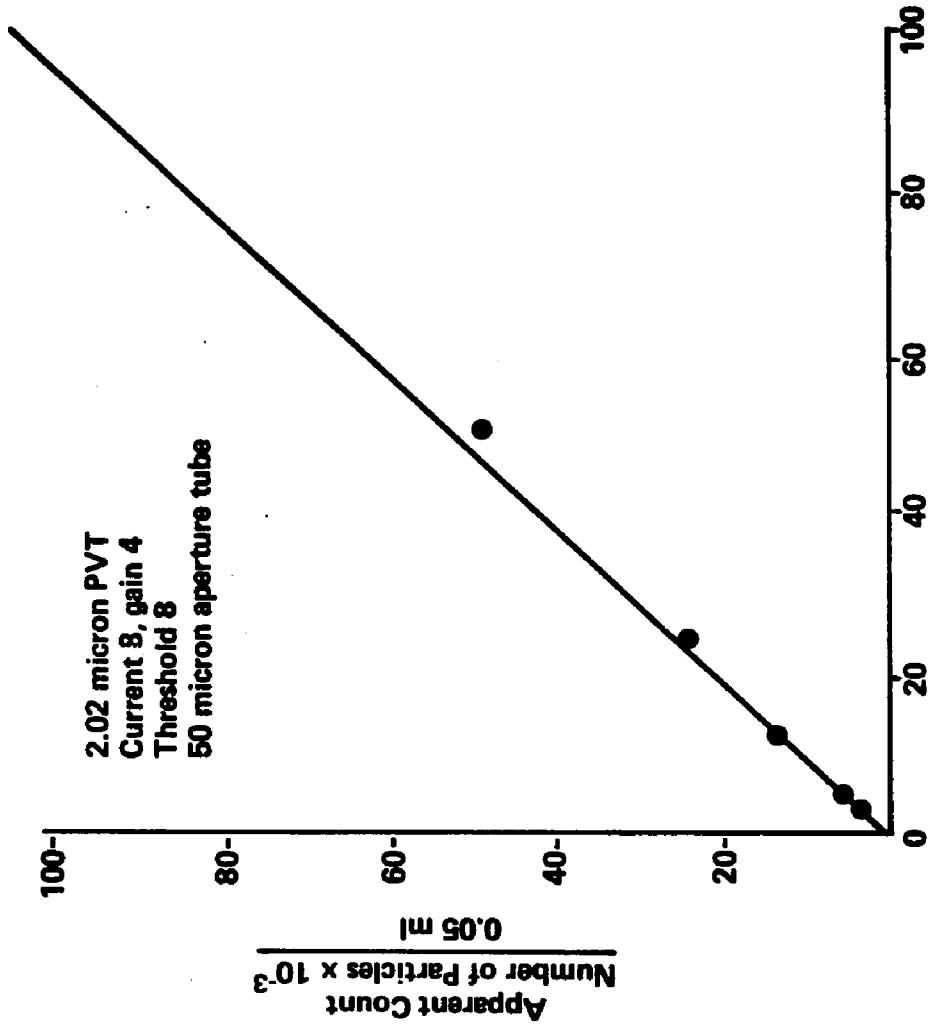

Figure 4. Standard Curve for Coulter Count Correction.

counts of 2.02 micron PVT. Figure 5 is a calibration curve for the 2.02 micron latex. A sample in water was ultrasonified and a distribution taken. A distribution was also taken on the unsonified latex. Below threshold 2, there is a large increase in counts attributable to instrument noise since the background counts of a solution of 0.9 percent NaCl were negligible (approximately 1 percent of the latex count).

The pulses generated by the particles passing through the aperture tube orifice can be directed into the RIDL 400-channel pulse height analyzer where they are grouped according to magnitude. The RIDL then provides a depiction of the differential distribution on its oscilloscope. The location where singlets, doublets, etc. are found on the screen is determined by calibration with known-sized particles. Polaroid pictures are taken of the differential oscilloscope curves, which are subsequently integrated to determine the number of various sizes of particles. The calculations are based on scale expansion factors and the volume of suspension sampled.

In order to evaluate day-to-day variation within and between the Coulter Counter Model A (CCA) and the RIDL pulse height analyzer, a suspension of 2.02 micron latex particles was stabilized using 0.1 percent TTAB. Readings were taken morning and evening for three days. The stock solution was sonified 15 minutes before

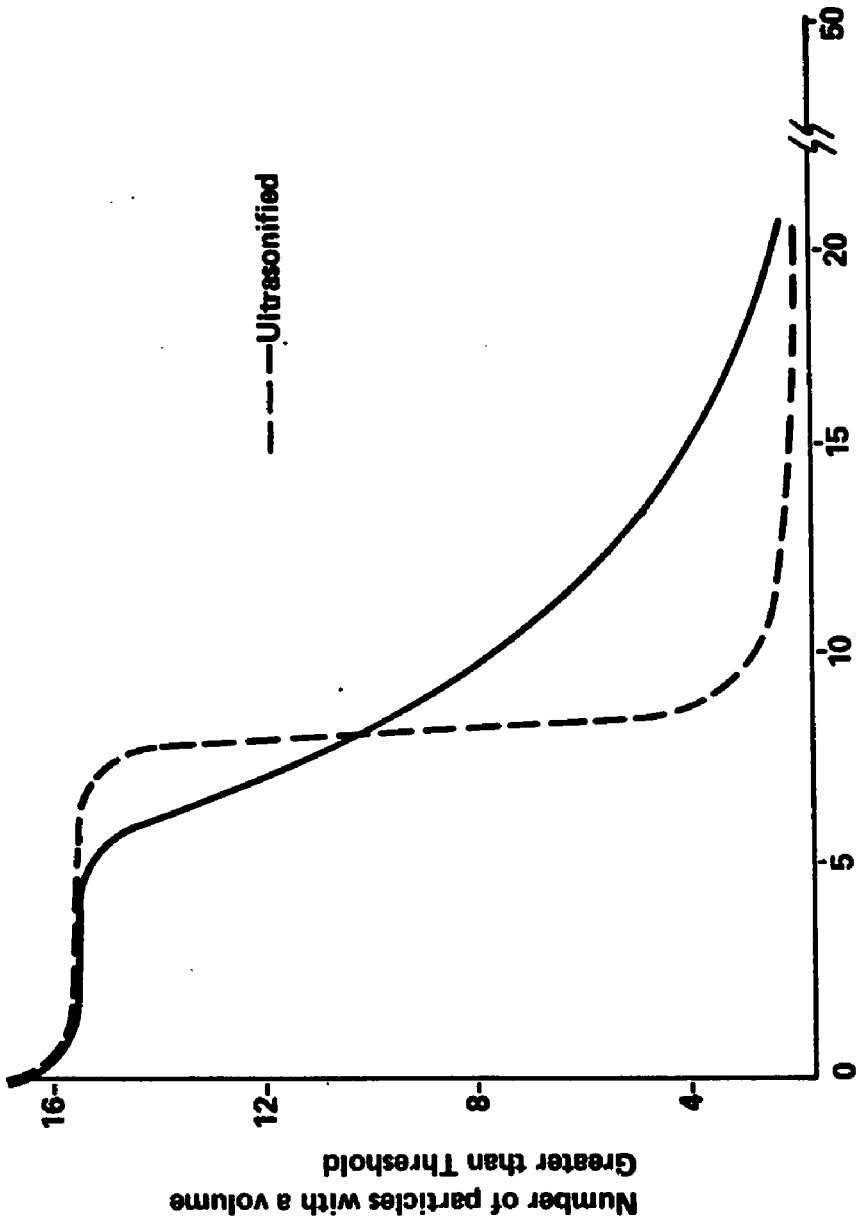

Figure 5. Calibration curves of ultrasonified and aggregated samples of 2.02 micron latex.

removing an aliquot and diluting to sample concentrations (Tables II and III). It was shown that at 95 percent confidence limits the RIDL was ±10 percent and the CCA ±5 of the mean. It was also shown that the readings on the CCA were approximately 9 percent greater than those on the RIDL for a dilute monodispersed suspension of latex particles. The greater variance in the RIDL data is to be expected due to the manual integration of the curves. The 9 percent deviation in total number of particles between instruments appears reasonable for instrumentation of this type.

Dilution technique

Since the Coulter Counter can count a maximum of $3x10^5$ particles per ml. without coincidence, and the concentration of particles required for reaction was $3x10^6$ to $3x10^7$ particles per ml., it was evident that a 100-fold dilution would be required to eliminate coincidence counts. Previously, using latex suspensions, Higuchi, et al. (1963) reported that the method of dilution did not influence their results. Mathews and Rhodes (1970) found no significant difference in absolute counts obtained when transfer pipets of 0.3 and 0.5 mm. bore diameter were used. Dilutions of 20/250 up to 1/250 were performed and the coincidence corrected counts were practically identical. They also reported that either the 30, 50 or 70 micron aperture

TABLE II

Evaluation of Day-To-Day Variation

Within and Between

Coulter Counter Model A and

the RIDL Pulse Height Analyzer

Total Number of Particles x 10^6

Day	RIDL AM	RIDL PM	CCA AM	CCA PM
1	6.7084	6.6256	7.50632	7.36088
	7.1710	6.9488	7.70226	7.48612
2	7.0700	6.8680	7.33462	7.36694
	7.1710	6.8084	7.45380	7.50430
3	6.5448	6.5044	7.58308	7.54268
	6.7468	6.6256	7.62550	7.57298

RIDL mean = 6.8411 ± 0.2324

95% Confidence = ± 10%

CCA mean = 7.5033 ± 0.1175

95% Confidence = ± 5%

$\frac{\text{RIDL mean}}{\text{CCA mean}}$ = 0.912 = 8.8% Higher Readings by CCA

TABLE III

Evaluation of Dilution Technique

Using 2.02 μ Latices and the

Coulter Counter Model A

Total Number of Particles

A	B	C
5894	2488	674
5990	2374	683
5982	2462	666
6027	2425	675
6073	2508	701
5915	2490	677
6066	2562	683
6003	2511	670
*Avg. 5036 ± 1%	2420 ± 2%	620 ± 2%
% Theory 100	102	104

*Average includes subtraction of the blank.

A = Undiluted solution.

B = 40 ml. of solution A diluted to 100 ml.

C = 25 ml. of solution B diluted to 100 ml.

tubes gave equivalent results. A technique for dilution of emulsions was developed by Bernstein, et al. (1971b), where many of these conclusions were independently reached.

It was found during our preliminary studies that the dimension of the pipet bore, withdrawal and delivery rates, as well as degree of agitation during mixing would all affect the amount of scatter in the data. These preliminary studies were performed on a diffusion-controlled system employing the typical Smoluchowski 1/N vs time plot. As can be seen in Figure 6, when prestirring was not performed, a great deal of scatter was generated. When a 1.0 ml. "to deliver" small bore pipet was used to transfer a sample from the reaction mixture to the diluting solution there was generally a loss of counts as compared to the wide-bore, blow-out type serological pipets[13] giving an apparent increase in rate. Likewise, the rate of withdrawal or release of sample caused a transient decrease in the number of particles. The decrease in the number of counts was actually due to shear-induced flocculation of the particles. Although not depicted in Figure 6, highly aggregated systems of particles exhibited shear-induced deflocculation under the same circumstances. These artifacts were avoided by using the transfer

---

[13] Kimax No. 37034-B.

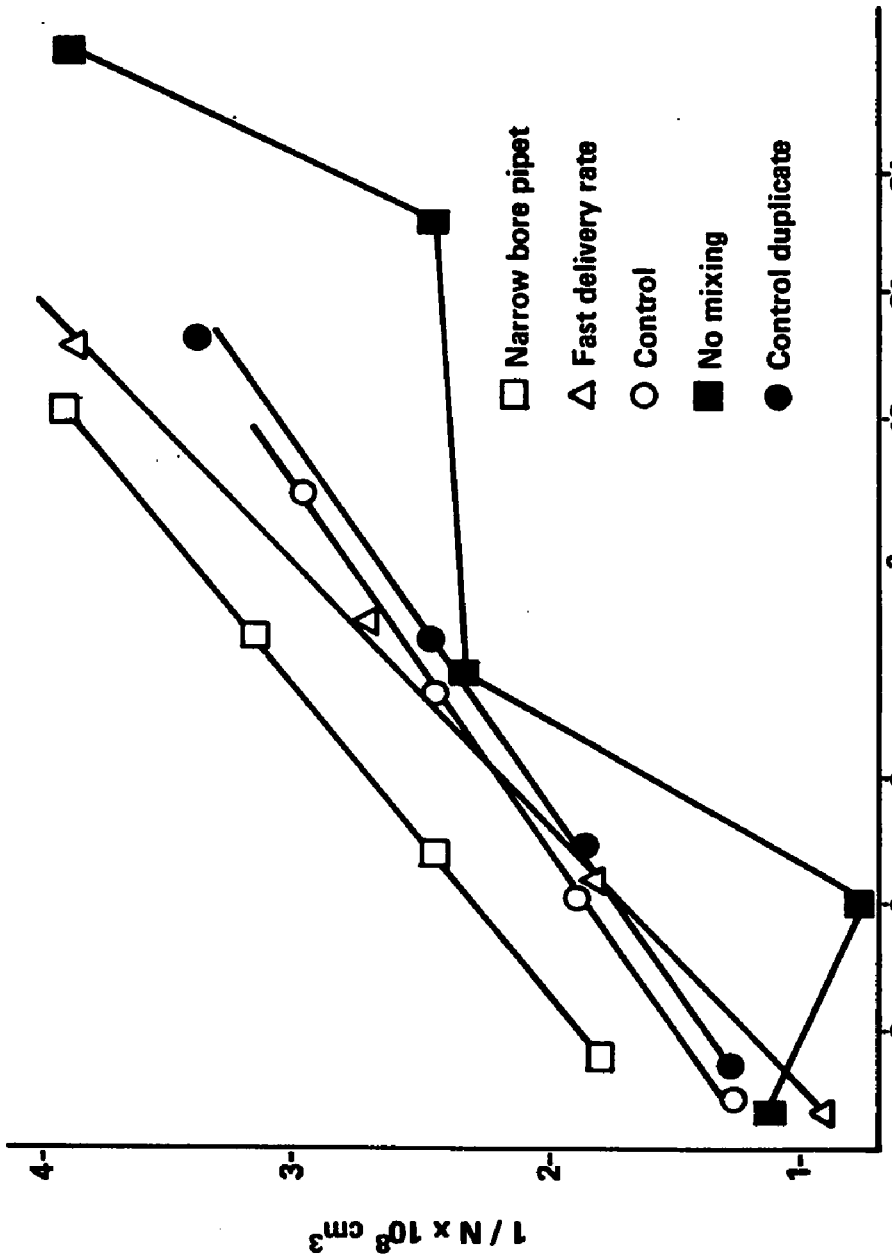

Figure 6. Comparison of dilution techniques.

techniques and apparatus discussed earlier. As demonstrated by the control duplicate, reproducibility was excellent using the developed technique.

NUMERICAL ANALYSIS

The Computer Program

The equations

The general problems of interfacing the fundamental orthokinetic flocculation equation (Equation 15) with the IBM 360 computer was solved and tested. The program could not be tested in the conventional manner by allowing it to make known calculations since there were no known calculations. It had to be tested by performing simulation studies and determining if the results were consistent with the basic Smoluchowski theory, and if the computer experienced computational difficulties. This makes it now possible to directly relate time changes in particle size distribution of suspensions to quantitative theories.

To make the numerical integration of the known linear differential equations more efficient, let us reduce Equations 15 and 16 in terms of dimensionless variables:

$$\sigma^*_{ij} = \frac{1}{8} \left(i^{\frac{1}{3}} + j^{\frac{1}{3}}\right)^3 \tag{42}$$

$$X^* = \frac{t}{\tau^*} \tag{43}$$

$$Y^*_k = \frac{N_k}{N_0} \qquad Y^*_i = \frac{N_i}{N_0} \qquad Y^*_j = \frac{N_j}{N_0} \tag{44a,b,c}$$

$$\tau^* = \frac{3}{16 G a_i^3 N_0} \tag{45}$$

$$\frac{dY_k^*}{dX^*} = \sum_{\substack{i=1 \\ j=k-i}}^{i=k-1} \frac{\sigma_{ij}^* Y_i^* Y_j^*}{W_{ij}^*} - 2 \sum_{i=1}^{\infty} \frac{\sigma_{ik}^* Y_i^* Y_k^*}{W_{ik}^*} \tag{46}$$

In order to relate the fundamental theory, i.e., the rate of change of individual class particles to the usual treatment of experimental flocculation data, i.e., the rate of change of the total number of particles irrespective of size, it is useful to extend Equation 46 for all particle sizes; consequently,

$$\frac{d \sum_{k=1}^{\infty} Y_k^*}{dX^*} = \frac{dY_\infty^*}{dX^*} = - \sum_{i=1}^{\infty} \sum_{j=1}^{\infty} \frac{\sigma_{ij}^*}{W_{ij}^*} Y_i^* Y_j^* \tag{47}$$

The program

Figures 7 and 8 are a flow chart of the computer program. Much thought went into the program writing to preclude computational errors. The first step is of extreme importance, since it is here that all constants, system parameters, and the initial particle size concentrations are entered. These data are subsequently used to calculate other system parameters such as τ^*, and σ^* (i,j).

One extremely important feature of the program design was the inclusion of a volume fraction ratio

calculation to account for mass balance at all times. This was necessitated because the choice of the total number of particle classes is part of the input data. Optimally, the size of the largest aggregate is chosen so that this program dimensional limitation will produce the least computational underflow. Underflow will cause a reduction in the computed reaction rate because the interactions of a significant number of large particles are not taken into consideration. For this reason the total volume fraction was calculated after each integration step, and the result was part of the output. Throughout all simulations the volume fraction was never allowed to go below 0.99. If during a series of calculations the volume fraction fell below 0.99, the calculation was repeated using a larger estimate for the biggest aggregate.

The time increment used for the successive numerical integration was an automatic part of the program, and it depended upon the theoretical flocculation rates. The subroutine for the numerical integration was DVDQ, a double precision variable order integration subroutine for the solution of ordinary differential equations. It was developed at the Jet Propulsion Laboratory, Pasadena, California.

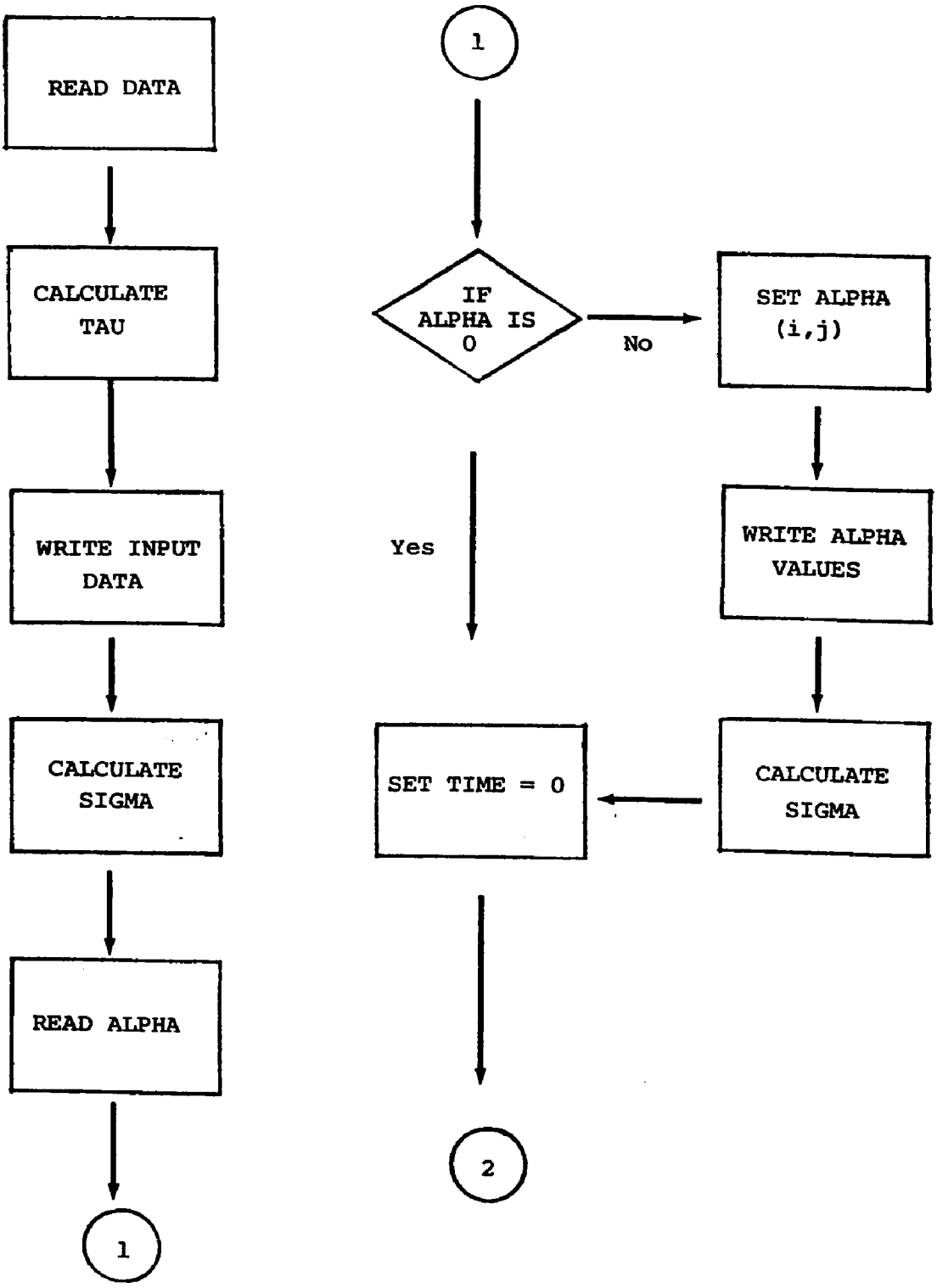

Figure 7. Flow Chart of the Computer Program

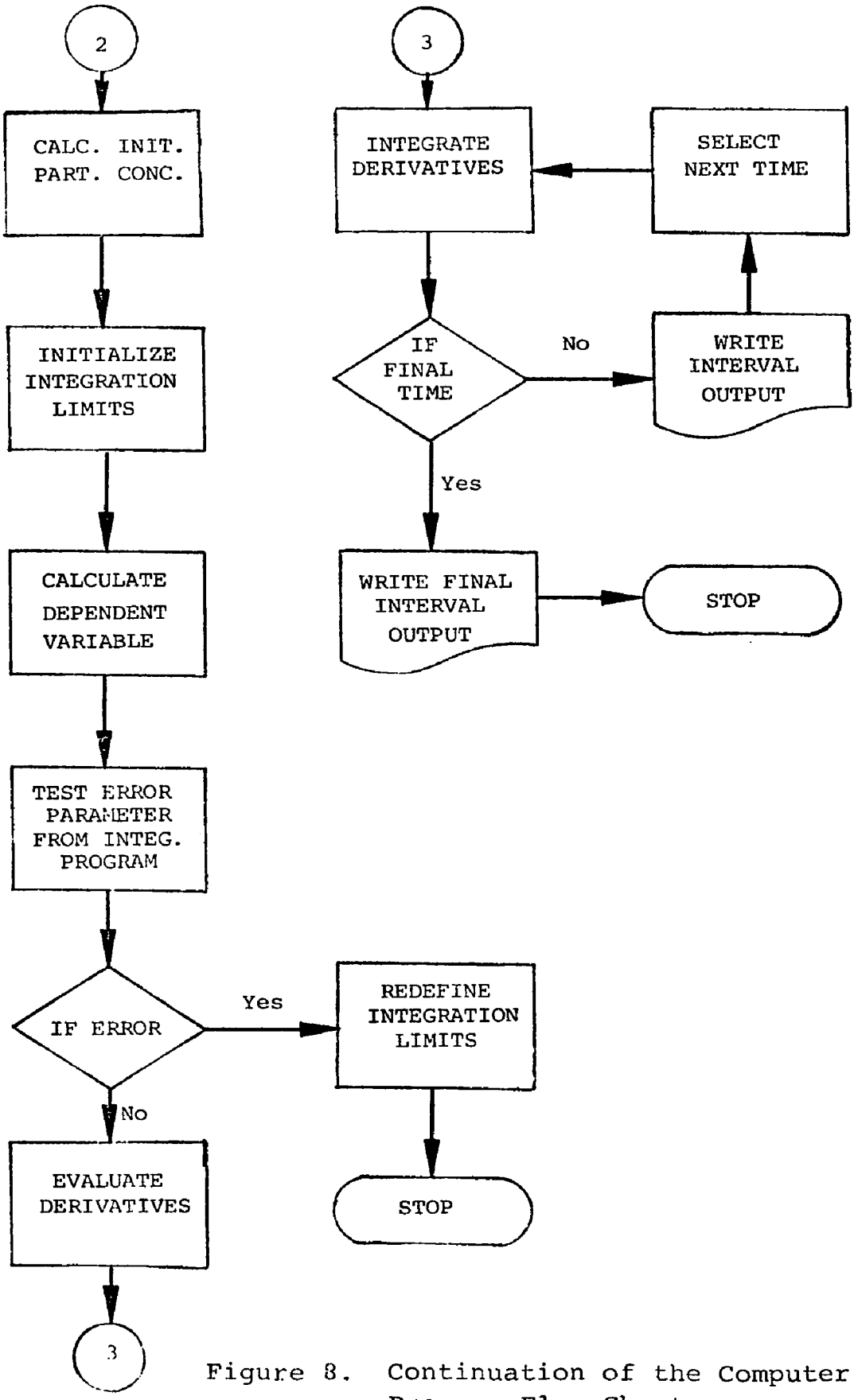

Figure 8. Continuation of the Computer Program Flow Chart

Computer Simulation Studies

In suspensions and emulsions, the roles played by particle-particle interactions are most important. The fundamental perikinetic equations of Smoluchowski have been studied for various particle size distributions, including in the computations the polydispersity effect and the effect of particle-particle potential energy barriers (Suzuki, et al. 1969). A similar approach has now been taken with the fundamental orthokinetic equations of Smoluchowski.

It is the purpose of this section to present the results of computer simulation studies for orthokinetic flocculation. As will be seen, the flocculation model yields a stability factor which is constant with time because the radii of curvature at the points of collision should be nearly the same for any two particles independent of floc size.

Extension of the firm baselines established in the previous sections will permit an in-depth investigation into the factors influencing the particle size distribution changes with time. The computer studies concentrate on substantiating many of the results presented in the kinetic investigations as well as providing insights into

the mechanism of particle-particle interactions in a laminar shear field.

Analysis of normalized plots

Figure 9 shows the results of simulation studies for two orthokinetic systems. In both cases, monodispersed particle size distributions were used. The diameters chosen were 1.01 and 2.02 microns, respectively. This has added significance since these are multiples of the diameters of the latex spheres actually used during experimentation. Even though the system with the larger initial particle diameter was flocculating at a much more rapid rate, both systems could be depicted in the same plot. This type of representation was useful when comparing different systems. It also readily allows comparison of kinetic results between experimental runs.

Effect of the initial particle size distribution on the rate plot

Figure 10 is a normalized plot of a theoretical simulation of the rapid flocculation case with three different arbitrary polydispersed initial particle size distributions. Table IV lists the distributions employed. The effect of polydispersity is readily apparent in Figure 10. With an increase in the heterogeneity of the system there is a marked increase in the rate of reaction.

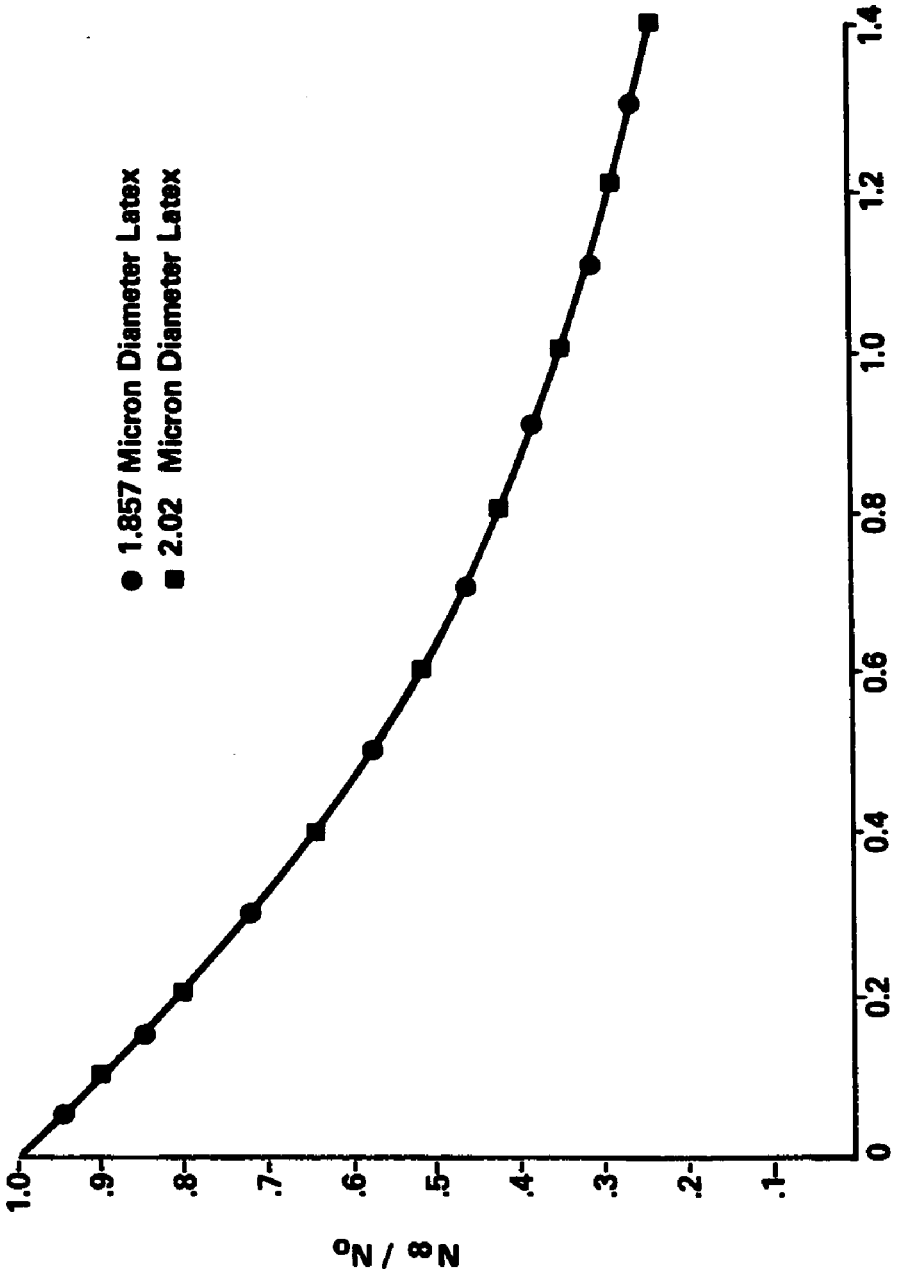

Figure 8. Normalized plot of the theoretical simulation of rapid flocculation with an arbitrary particle size distribution to demonstrate the utility of the treatment of orthokinetic data by Smoluchowski-type kinetics.

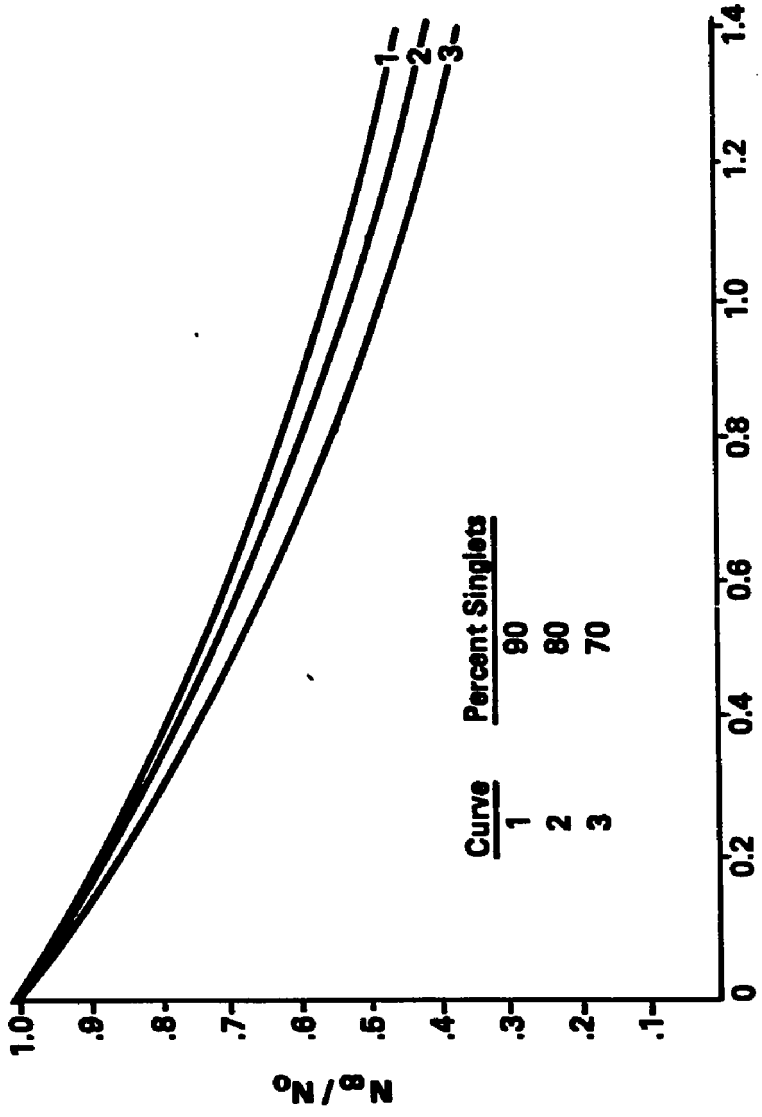

Figure 10. Normalized plot depicting the theoretical simulation of rapid flocculation with arbitrary polydispersed particle size distributions.

TABLE IV

Initial Particle Size Distributions

Chosen for the Computer Simulation

Presented in Figure 10

	Percent of Each Size		
Particle Sizes	Top	Middle	Bottom
Singlets	90.00	80.00	70.00
Doublets	6.85	10.85	15.85
Triplets	1.00	3.5	6.00
4-mers	0.50	2.00	3.00
5-mers	0.50	2.00	3.00
6-mers	0.25	0.50	0.75
7-mers	0.25	0.50	0.75
8-mers	0.25	0.25	0.25
9-mers	0.20	0.20	0.20
10-mers	0.20	0.20	0.20

Singlet size is 1.01 micron radius.

This is stated mathematically in Equation 47, where σ^*_{ij} is the polydispersity function and W^*_{ij} expresses the effect of the total interaction barrier. If there is no interaction barrier ($W^*_{ij} \simeq 1$) and the size distribution is polydispersed; flocculation will proceed more rapidly with time since the mean σ^*_{ij} will become greater as the reaction continues. This was neatly laid out by Muller (1928).

Effect of the total interaction barrier on the rate plot

Figure 11 is the normalized plot of theoretical simulations of flocculation for three different values of the total interaction barrier, W^*_{ij}. The values chosen for W^*_{ij} were 1 for the rapid case where there is no barrier to flocculation, 2 for intermediate reaction rates, and 4 to represent the case of slow flocculation. It is seen that the rate of change in the reaction rate becomes progressively more rapid as W^*_{ij} is reduced (top to bottom in Figure 11). It should also be noted that this parallels events in the preceding section of polydispersity. As it turns out, W^*_{ij} is also dependent upon particle size through both electrical and hydrodynamical considerations. The electrical effect is constant if the assumption that the radii of curvature at the points of collision are nearly the same for any two particles independent of floc size. Therefore,

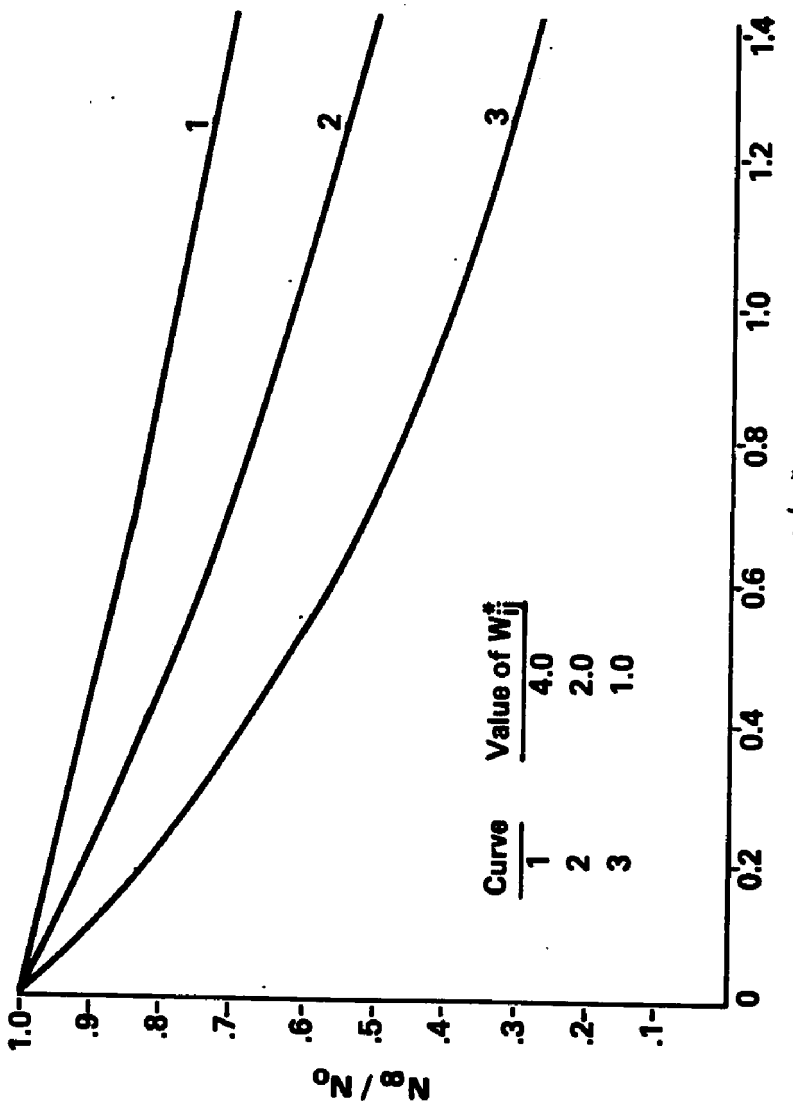

Figure 11. Normalized plot depicting theoretical simulations of identical particle size distributions for three distinct values of the total interaction barrier, W_{ij}^*

there is a psuedo net reduction in the hydrodynamic barrier caused by the "sweeping-out" effect of the large particle radii on the smaller particles. Equation 47 can be rearranged to determine the mean value σ^*_{ij}/W^*_{ij} at dimensionless time X^*.

$$\left\{\frac{\sigma^*_{ij}}{W^*_{ij}}\right\}_{X^*} = \frac{\sum_{i=1}^{\infty} \sum_{j=1}^{\infty} \frac{\sigma^*_{ij}}{W^*_{ij}} Y^*_i Y^*_j}{Y^{*2}_{\infty}} \tag{48}$$

for

$$\left\{\frac{\sigma^*_{ij}}{W^*_{ij}}\right\}_{X^*} > 0$$

Inserting Equation 48 into Equation 47 yields the total rate

$$\frac{dY^*_{\infty}}{dX^*} = - \left\{\frac{\sigma^*_{ij}}{W^*_{ij}}\right\}_{X^*} Y^{*2}_{\infty} \tag{49}$$

and if one considers the mean values for σ^*_{ij} and $1/W^*_{ij}$ at time X^*; that is,

$$\langle\sigma^*_{ij}\rangle_{X^*} = \sum_{i=1}^{\infty} \sum_{j=1}^{\infty} \frac{\sigma^*_{ij} Y^*_i Y^*_j}{Y^{*2}_{\infty}} \tag{50}$$

for

$$\langle\sigma^*_{ij}\rangle_{X^*} \geq 1$$

$$\left\{\frac{1}{W_{ij}^{*}}\right\}_{X^{*}} = \frac{\sum_{i=1}^{\infty}\sum_{j=1}^{\infty}\frac{\sigma_{ij}^{*}}{W_{ij}^{*}}Y_{i}^{*}Y_{j}^{*}}{\sum_{i=1}^{\infty}\sum_{j=1}^{\infty}\sigma_{ij}^{*}Y_{i}^{*}Y_{j}^{*}}$$

for (51)

$$0 < \left\{\frac{1}{W_{ij}^{*}}\right\}_{X^{*}} \leq 1$$

It can be seen from Equations 50 and 51 that the mean polydispersity and the effect of the total interaction are mutually dependent through particle size as the theoretical simulations point out.

Effect of rate of shear on the rate plot

The extremes of rates of shear employed during experimentation were chosen to demonstrate the effect of rate of shear on the rate plot. A dimensionless format could not be used since normalization mathematically negates the effect of G, since G is part of tau (the theoretical half-life). Shear rates of 15.65 $sec.^{-1}$ and 62.60 $sec.^{-1}$ were used for the simulation as well as an initially monodispersed particle size distribution. Figure 12 depicts the marked difference in the rates of reaction on a scale of absolute time. The effect of the larger G is not only felt as a multiple of 4 but also in the manner that a more rapidly proliferated polydispersed system has on the rate of reaction.

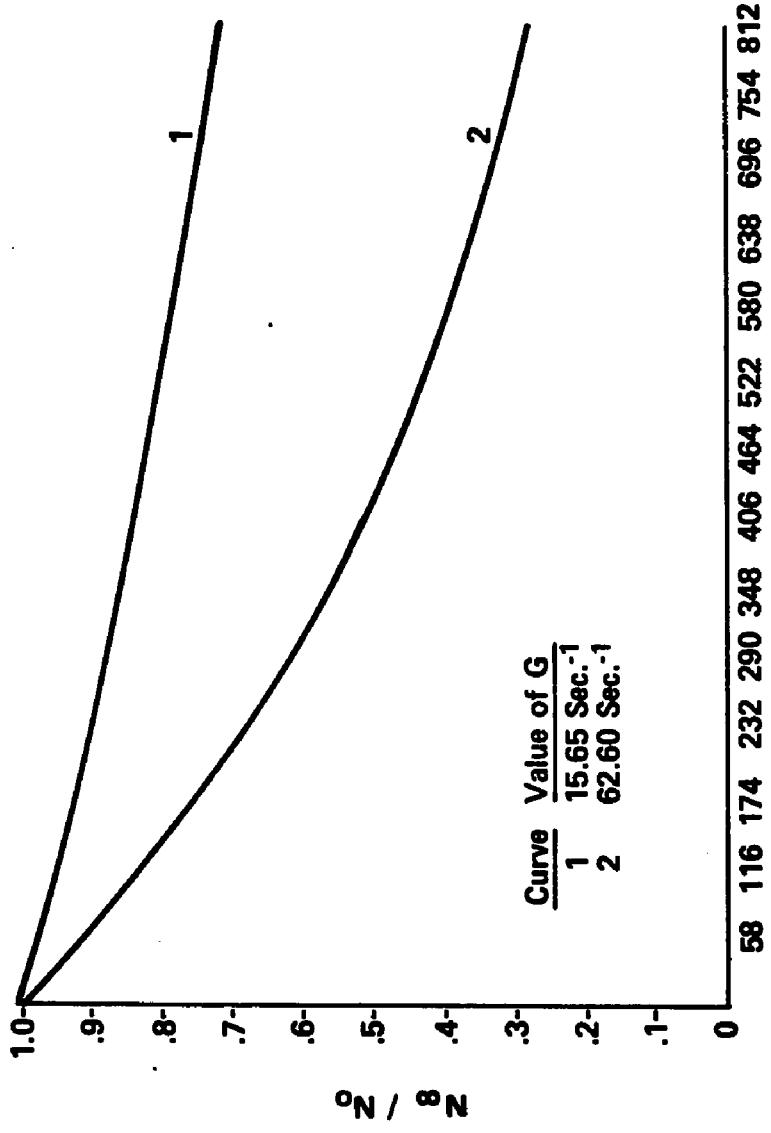

Figure 12. Plot of theoretical simulations of initially monodispersed particle size distributions for two distinct values of the rate of shear, G.

Therefore, in the case of shear rate we not only have a linear, multiplicative effect, but also the effects of polydispersity on σ^*_{ij} and on the total interaction barrier as well.

Effect of the radius of a singlet on the rate plot

Again multiples of actual experimental conditions were chosen for simulation purposes. Experimentally the radius of the singlet was taken as 1.01 μ. Figure 13 depicts this radius as well as that of a particle having a radius of 2.02 μ. Both simulations are of systems which were taken to be initially monodispersed. As in the previous case normalization could not be used since the radius appears as part of tau. Theoretically, the radius is a cubic factor in the rate of reaction. It is quite evident after perusal of Figure 13 that these predictions are born out. But in this case there are no striking effects due to polydispersity on σ_{ij} or in the total interaction barrier, since both systems are initially monodispersed. However, had the initial distributions of the systems been dissimilar and not monodispersed, then the additive effects of polydispersity would have been encountered. In this as well as the previous case, the relatively short time scale encountered for a major change in particle concentration should be noted.

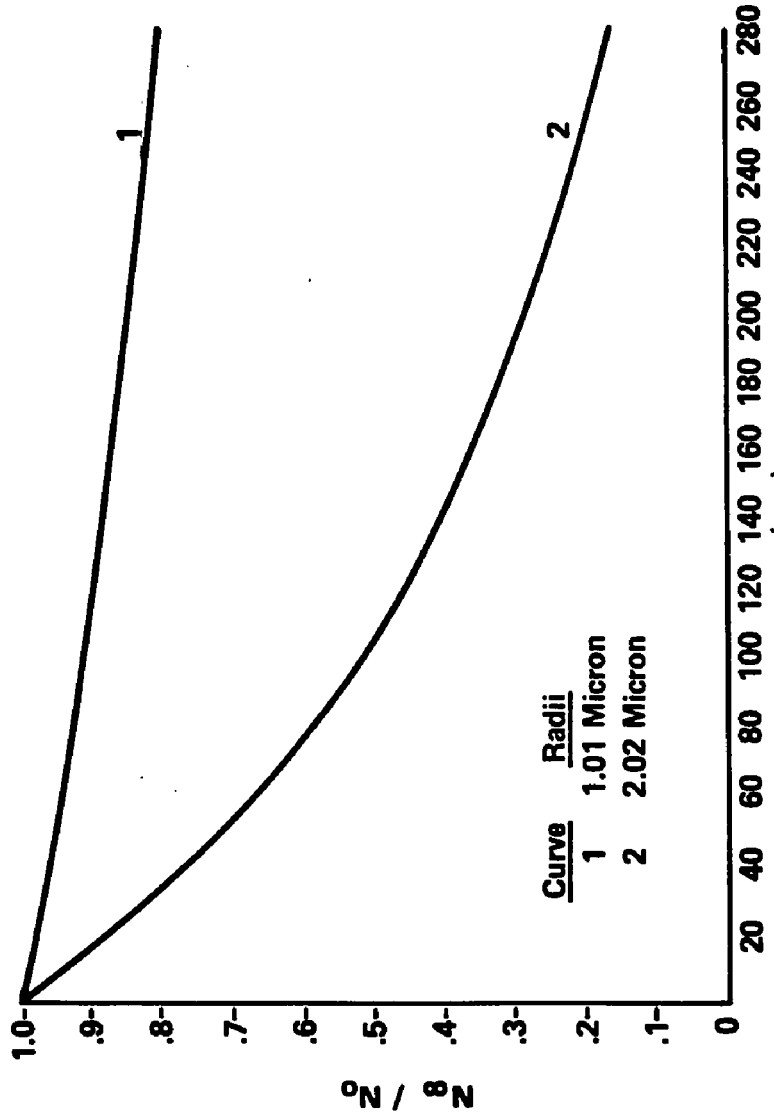

Figure 13. Plot of theoretical simulations of initially monodispersed particle size distributions for two distinct particle radii.

Effect of the total initial number of particles on the rate plot

The particle concentrations chosen for simulation study bracket those used during experimental kinetic studies. Figure 14 depicts theoretical simulations of initially monodispersed particle size distributions for two different particle concentrations, 5.0×10^6 and 1.5×10^7. All parameters in the simulations are the same except the initial number of particles. Again a dimensionless plot could not be used to visualize the results since N_0 (number of particles at time zero) is part of tau. The situation here parallels that found under the effects of the rate of shear. The effect of the greater number of particles is not only felt as a three-fold multiple but also in terms of a more rapidly proliferated polydispersed system. The data generated indicates again that the slopes (rates) at given times of equivalency are quite different. This again confirms that there is not only a linear multiplicative effect due to particle concentration, but also the effects of polydispersity on σ^*_{ij} and on the total interaction barrier as well.

Effect of alpha and epsilon on the rate plot

Initially two assumptions were made--that the flocs approximated spherical shape and that interaction energies would be similar for all particle collisions (i^{th} and j^{th})

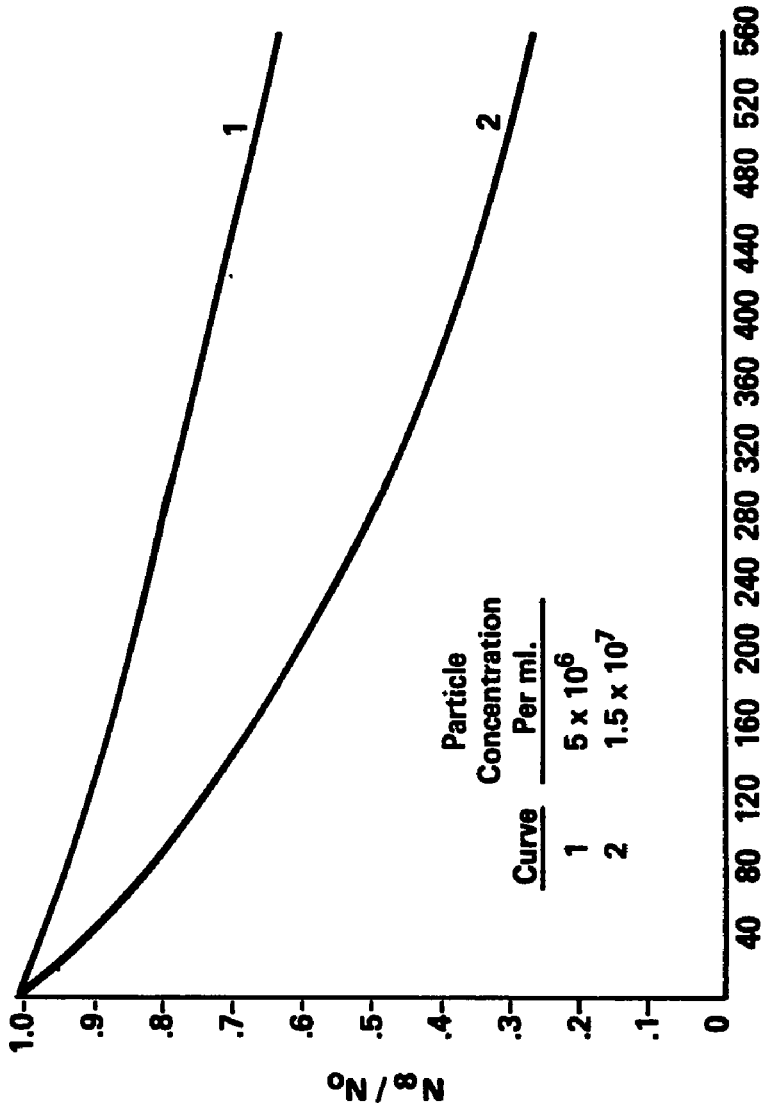

Figure 14. Plot of theoretical simulations of initially monodispersed particle size distributions for two different particle concentrations.

because the radii of curvature at the points of collision should be nearly the same for any two particles independent of floc size. Additionally, it was assumed that all collisions were 100 percent efficient, i.e., resulted in a new size particle. The former is not necessarily true since higher order X-mers could approximate many different geometrical configurations including rods, spheres, S-shaped and L-shaped forms. If the latter were not true, the radii of curvature at the points of collision between monomers for instance would not be the same as that between dimers or between monomer and dimer. Recognizing these possibilities, two modifying functions were developed. Epsilon (ε^*) was designated as a "shape factor" to make modifications in overall rate of reaction that reflect deviation from the spherical case. Alpha (α) was designated as the "collision efficiency" factor, and accounts for possible deviation from 100 percent collision efficiency of any i^{th} and j^{th} combination. Alpha accounts for the case where there is not a direct hit between the ith and j^{th} particles, but rather a glancing blow which does not result in the formulation of a new particle. Alpha is "s", the slip factor. See Appendix for equations.

Figure 15 depicts the effect of α on an initially 100 percent monodispersed particle size distribution of a maximum rate system. For these simulations, values of

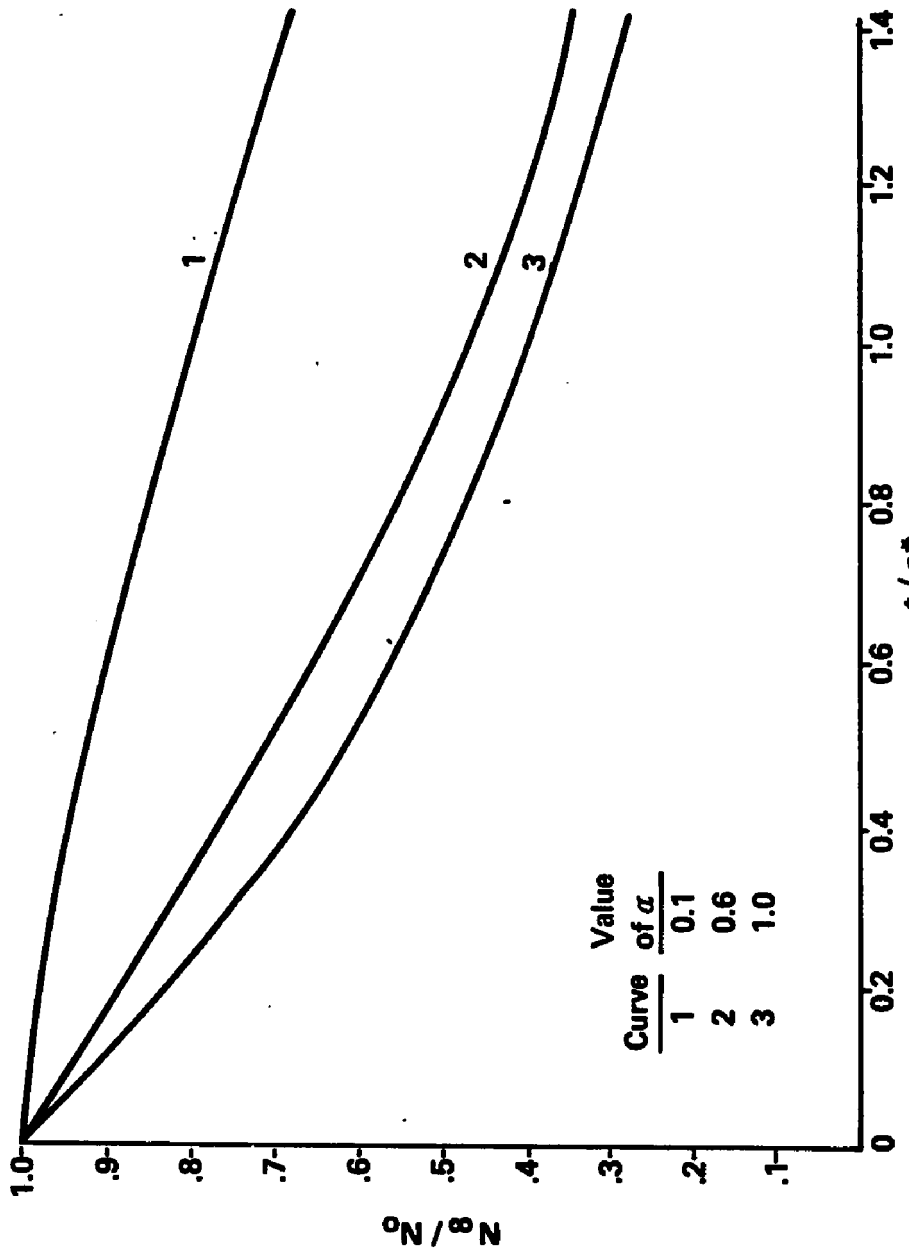

Figure 15. Normalized plot depicting theoretical simulations of an initially monodispersed particle size distribution with various values of Alpha.

α = 0.1, 0.6, and 1.0 (top to bottom) were chosen. Since the system was initially monodispersed it was decided to only modify the collision efficiency of the singlet-singlet collision. From the normalized plot one readily observes that with a reduction in efficiency of singlet-singlet collisions, there is a concomitant reduction in the overall velocity of the reaction. In addition there is also a change in the shape of the curve with the continued reduction of α. This is most probably due to the slower build up of larger sized particles which are generated after a period of time with the result that there is an apparent lag time before the reaction proceeds rapidly. It can be seen, however, that the main effect of reducing α is to decrease the overall reaction rate.

In contrast to this, ε^* has the effect of increasing the reaction rate dramatically for a relatively small increase. Figure 16 is the normalized plot of theoretical simulations of an initially monodispersed particle size distribution for three different values of ε^*. For these simulations, values of ε^* = 1.0, 0.8, and 0.6 (top to bottom) were chosen. It was shown by M. Vold (1959) that the volume of sedimented solid spheres does not coincide with, or necessarily approximate the volume of the coalesced spheres. In addition, the formation of

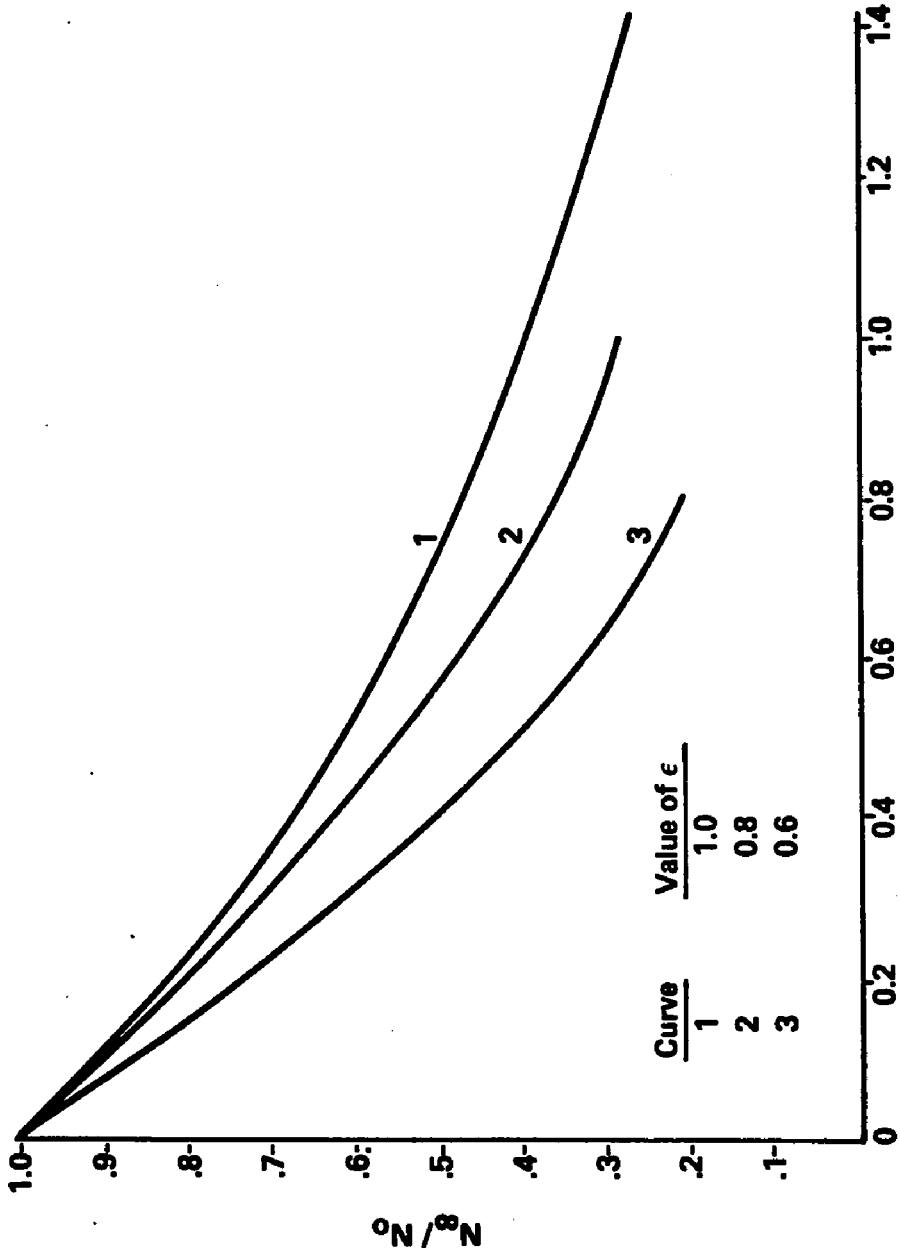

Figure 16: Normalized plot of theoretical simulations of an initially monodispersed particle size distribution for three different values of Epsilon.

geometric figures which do not at all approximate spheres will have a dramatic effect on the sweep-out volume of an agglomerate. This artifact exhibits its presence through the radius or volume of the agglomerate. Accounting for random irregular shapes would have been a formidable computational problem. Instead, using the work of M. Vold (1959), reasonable values for an agglomerate average ε^* could be chosen and used for all particles larger than monomers. Examination of Figure 16 shows the expected increase in reaction velocity with a decrease in ε^*. Since ε^* enters the volume calculation of an agglomerate in the divisor it must necessarily become smaller to make the volume larger. Epsilon equal to 0.8 is equivalent to multiplying the volume by 1.25, and an ε^* equal to 0.6 is equivalent to a volume multiplier of 1.67.

It should be apparent that a combination of α and ε^* will cause a cancelling out of one another's effects. Figure 17 is a normalized plot of theoretical simulations of an initially monodispersed particle size distribution for two different values of α and ε^*. In the top curve $\alpha = \varepsilon^* = 1$, and in the bottom curve $\alpha = 0.6$, and $\varepsilon^* = 0.8$. It is observed that α, through its effect on singlet-singlet collisions, holds back the reaction at early times; but at later times the effect of ε^* dominates over that of α as the number of

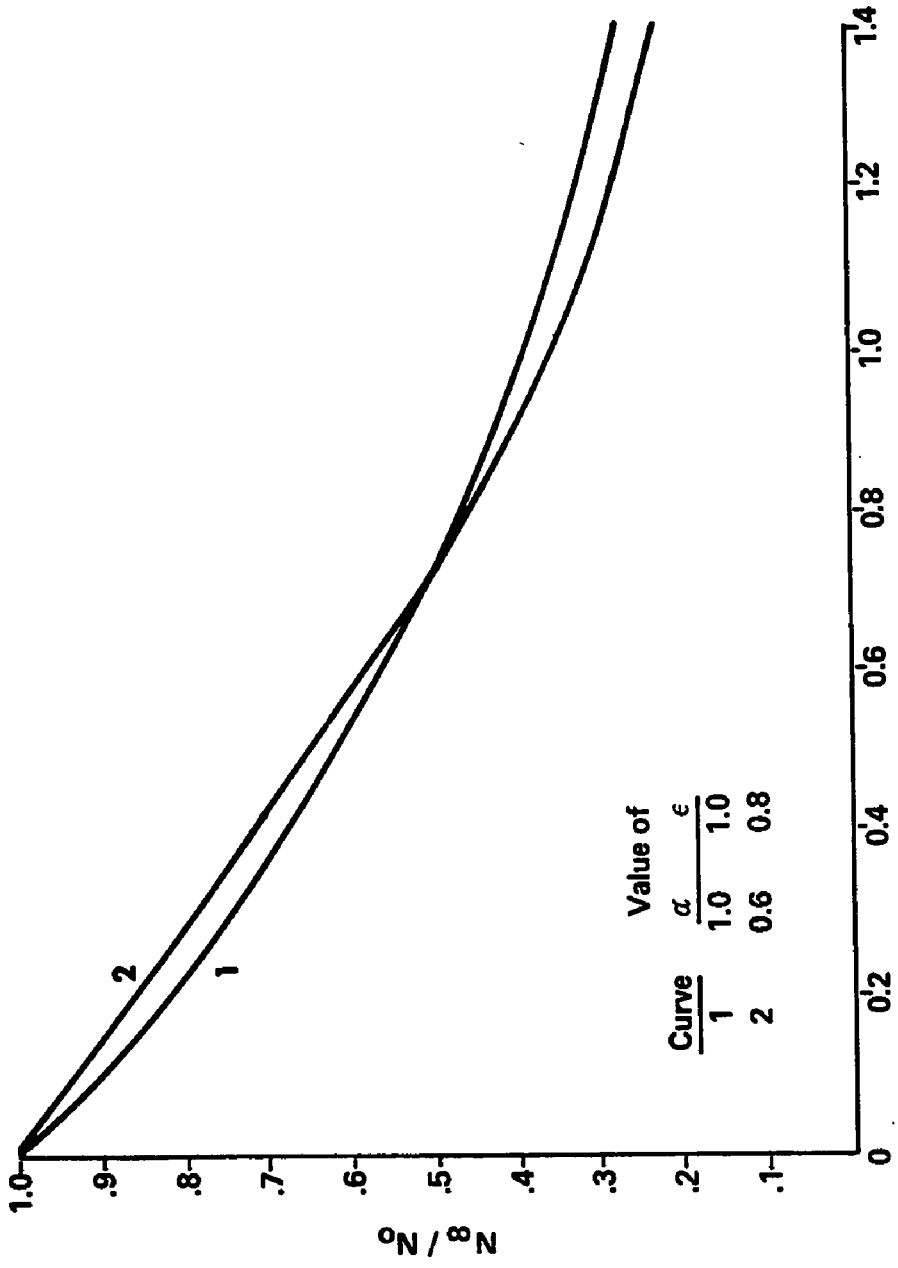

Figure 17. Normalized plot depicting theoretical simulations of an initially monodispersed particle size distribution for two different values of Alpha and Epsilon in each curve.

larger-sized particles becomes increasingly more significant.

It can be seen that there are an infinite number of possible combinations of α and ε^* for each particle size which would provide an infinite number of reaction rates, some being only subtly different from others.

KINETIC STUDIES

In this section, the results of the kinetic studies are described for a number of variables; initial particle size distribution, shear rates, and concentrations of electrolyte and quaternary ammonium compounds. These include baseline studies that demonstrate that the ln N_∞/N_0 versus time plot is an accurate method of treating the data. It will also be shown that the normalized plot yields valuable information on the rate process of various systems.

These experiments were intended to better define the physical significance and the limitations of the results obtained using the Coulter Counter method.

Theoretical Estimations of the Performance of the Shear Cell and Flocculating Particle System

Table V summarizes the estimated parameters of the particle system in water in the shear cell at 25°C and the relative contribution of laminar shear-induced flocculation to diffusion-controlled flocculation of a dilute monodispersed particle size system. The table is a useful approximation of the limiting conditions needed to ensure a laminar shear system and of the adjustment of conditions to study the particle suspension at initially different shear-controlled flocculation situations.

TABLE V

Calculated Parameters of the Particle System in the Shear Cell at 25°C and Relative Contribution of Laminar Shear-Induced Flocculation to Diffusion Controlled Flocculation

RPM	G ($sec.^{-1}$)	K^*/K	Percent Shear Control at t = 0
12.5	15.65	14/1	93
25	31.3	28/1	97
50	62.6	56/1	98

K^*/K was calculated from Equation 31 for particles in water at 25°C.

$$G = \frac{dv}{dr} = - \frac{2\Omega}{r^2} \left(\frac{R_b^2 \cdot R_c^2}{R_c^2 - R_b^2} \right) \tag{52}$$

Where v is the velocity; Ω the angular velocity; R_b and R_c are the radii of the cup and bob, respectively; and r is the radius from the turning axis to the midpoint between the cup and bob.

Table V points out that in each experimental situation, flocculation was predominantly controlled by laminar shear. For this reason the effects of diffusion-controlled flocculation could be ignored without introducing any significant error. This assumption also greatly reduces the complexity of subsequent calculations.

When examining the various ways of presenting kinetic data obtained from the couette cell, one is confronted with a number of choices. To compare a number of sets of data on the same plot the dimensionless (Equation 22) format has the advantage of eliminating differences such as N_0, G, and t which might preclude such a representation. When determining rate constants, the first order plot of ln N_∞/N_0 vs t has an advantage over the second order plot of $1/N_\infty$ vs t in that there is a dependence on the initial particle concentration when determining K^* theory. Both Swift and Friedlander and Curtis and Hocking chose the first order plot. When working with laminar shear-controlled systems, Bernstein used the second order plot for his work with diffusion-controlled systems. Both representations provide an accurate measure of the rate constant.

The data will be presented using the same format as Swift and Friedlander, and Curtis and Hocking. A direct comparison of rate constants between various

experimental runs is not possible since the initial number of particles at the beginning of each experimental run was not constant. Since particle concentration affects the rate of reaction, its effect must be negated when comparing runs. This was accomplished by comparing the experimental rate with the theoretical rate and determining the stability factor. Therefore, a comparison of stability factors (for a set of experimental conditions holding everything except initial number of particles constant) will be conducted.

Electrolyte Effects

Figure 18 depicts the effect of increased electrolyte (NaCl) concentration on the flocculation kinetics at constant shear rate. The reaction rate increases with increasing NaCl concentrations. At relatively early periods in time the curves appear linear. At later times, increased polydispersity causes sedimentation-flocculation, yielding false increases in the reaction rates. Upon comparing profiles of the 0.50 to 1.50 percent NaCl concentrations, the departure from linearity occurs sooner with the higher salt concentrations as the result of the faster rate of flocculation and accompanying polydispersity. Table VI presents some experimentally determined rate constants and apparent stability factors. Perusal of the rate data amplifies

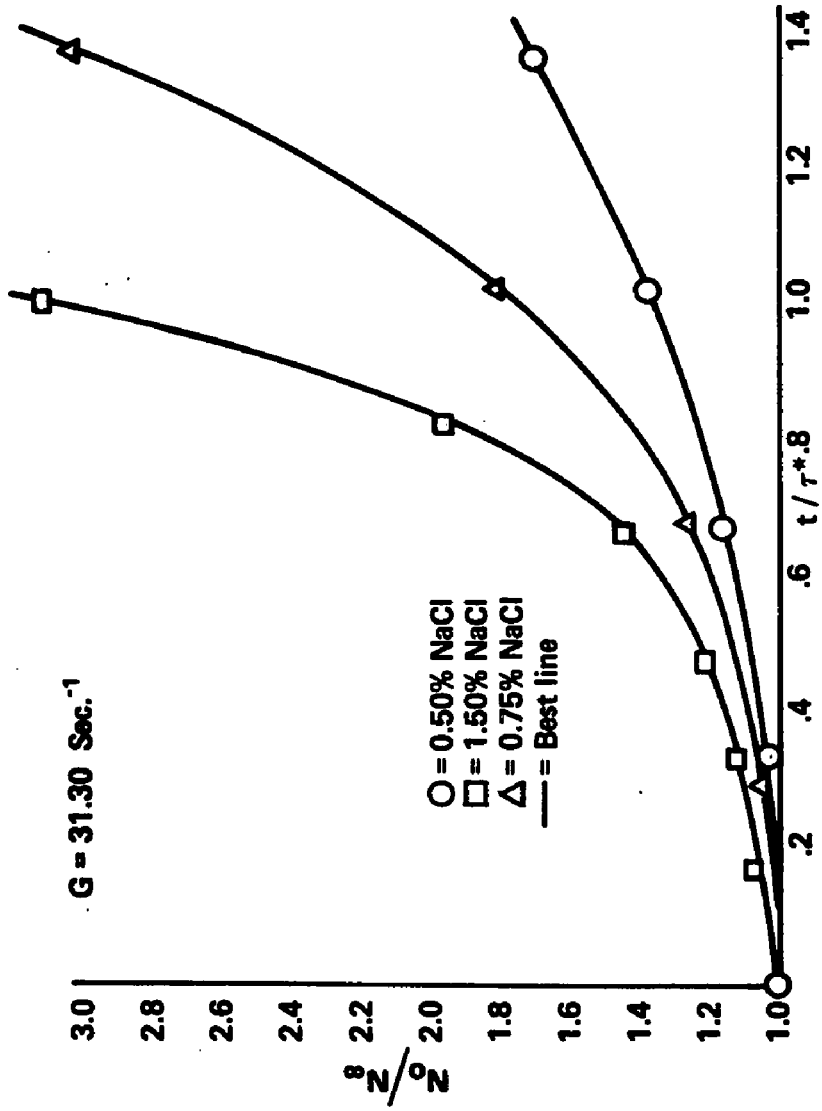

Figure 18. Normalized plot of various orthokinetic systems depicting the effect of salt concentration on the rate of reaction (modification of electrical double layer)

TABLE VI

Flocculation Rate Constants and Apparent Stability Factors $W^*_{app.}$

at Various Salt Concentrations at 25°C and G = 31.3

All rate constants are expressed as multiples of 10^{-4} sec.$^{-1}$

NaCl Concentration (percent)	Rate Constant		Initial No. of Particles x 10^6	$W^*_{app.}$
	Theory+	Found		
0.50	6.691	2.089	3.890	3.203
	7.325	1.847	4.259	3.966
0.75	6.980	2.084	4.058	3.348
	6.530	2.634	3.797	2.479
1.50	4.042	1.584	2.350	2.552
	7.255	2.915	4.218	2.489
	6.162	2.517	3.583	2.448

$$W^*_{app.} = \frac{\text{Maximum Theoretical Rate Constant}}{\text{Experimental Rate Constant}}$$

+Theoretical rate constants calculated from Equation 33 with $W^*_{ij} = 1.0$

the importance of the number of particles used during experimentation. The variance in the theoretical maximum rates is due to variance in particle concentration. There was also a corresponding fluctuation in the experimental rates.

As can be seen, for the range of particle concentrations used, a maximum reaction rate is approached at 0.75 percent NaCl. At 1.50 percent NaCl the maximum rate is insured as can be seen from the apparent stability factor data. There is also excellent agreement in the value of $W^*_{app.}$ once the maximum rate has been achieved. The variance in the $W^*_{app.}$ at the lower salt concentrations can be attributed to the variance in the initial number of particles. At the high salt concentration, slight differences in the number of particles in the system make no difference since there is an excess of electrolyte.

Surfactant Effects

Figures 19 and 20 depict the effect of the quaternary ammonium compound at two different rates of shear on the repulsive forces acting between latex particles. It is seen that there is virtually no difference in the reaction rates between systems with TTAB only, TTAB plus 1.50 percent NaCl, and 1.50 percent NaCl only. At the concentration of particles used, a 5×10^{-6} M TTAB

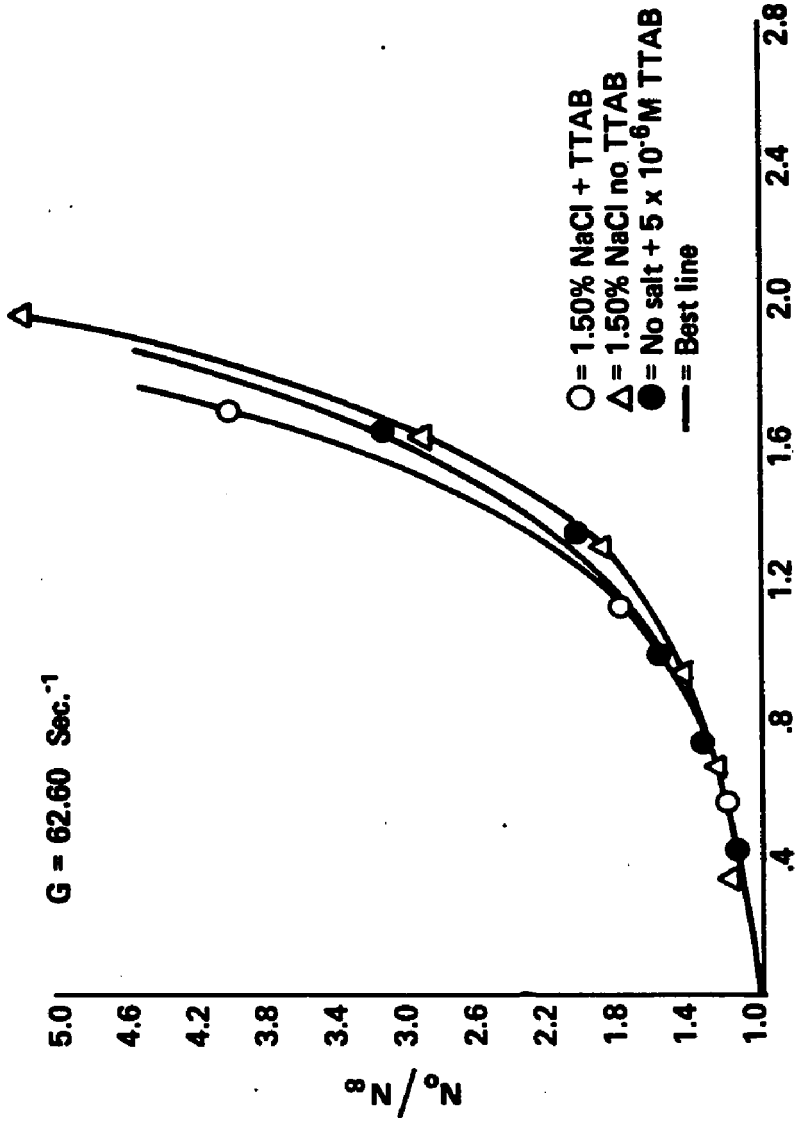

Figure 19. Normalized plot depicting the effect of quaternary ammonium compound on reaction rate (modification of surface charge density)

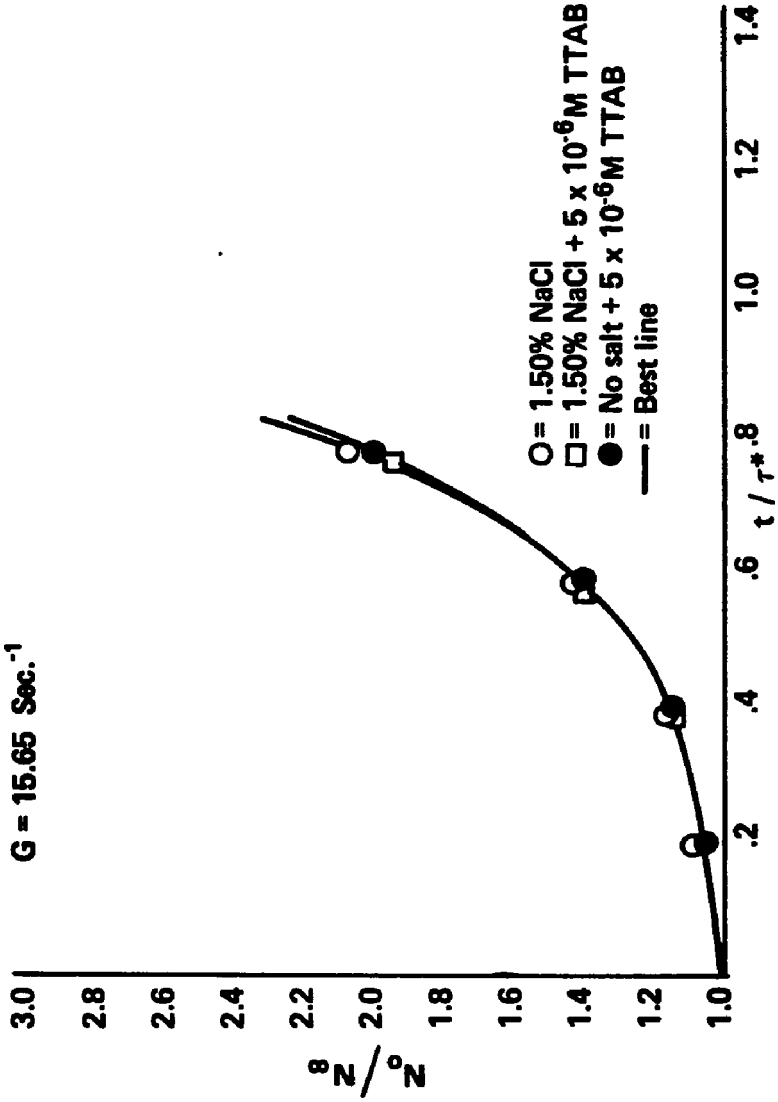

Figure 20. Normalized plot depicting the effect of quaternary ammonium compound on reaction rate (modification of surface charge density)

solution was sufficient to reduce the Helmholtz zeta potential to less than -2 mv as measured on the zeta meter. This low surface charge allowed for rapid coagulation. In a similar fashion the 1.5 percent NaCl reduced the electrical double-layer thickness to a minimum, allowing rapid coagulation. The combination of the two gave a reaction rate which was essentially the same as exhibited in the previous system thereby showing all systems to be at maximum rate conditions.

The data presented in Table VII reinforces the previous generalizations. Surfactant alone can reduce the repulsive energy to such low levels that maximum rates are achieved. Comparison of apparent stability factors (between systems containing both salt and surfactant and those containing only one or the other) shows all three systems to be in excellent agreement. By using both salt and surfactant one could be assured that the system was in fact "maximum rate". This is supported by the excellent agreement of the $W^*_{app.}$ values.

Rate of Shear Effects

In Figure 21 the influence of shear rate on the flocculation rate at constant salt concentration is readily observed. The curves are linear at initial time, and, thereafter, become increasingly curvilinear. It should be noted that in order to show the effects of rate

TABLE VII

Flocculation Rate Constants and Apparent Stability Factors $W^*_{app.}$

with and without Surfactant at 25°C and G = 31.3

All rate constants are expressed as multiples of 10^{-4} sec.$^{-1}$

NaCl Concentration (percent)	TTAB Concentration	Initial No. of Particles x 10^6	Rate Constant		$W^*_{app.}$
			Theory+	Found	
1.50	none	2.350	4.042	1.584	2.552
		4.218	7.255	2.915	2.489
		3.583	6.162	2.517	2.448
1.50	$5x10^{-6}$ M	3.563	6.128	2.461	2.490
		3.734	6.423	2.634	2.438
		3.816	6.563	2.496	2.630
none	$5x10^{-6}$ M	3.218	5.534	2.238	2.473
		3.437	5.912	2.340	2.562

$$W^*_{app.} = \frac{\text{Maximum Theoretical Rate Constant}}{\text{Experimental Rate Constant}}$$

+Theoretical rate constants calculated from Equation 33 with $W^*_{ij} = 1.0$

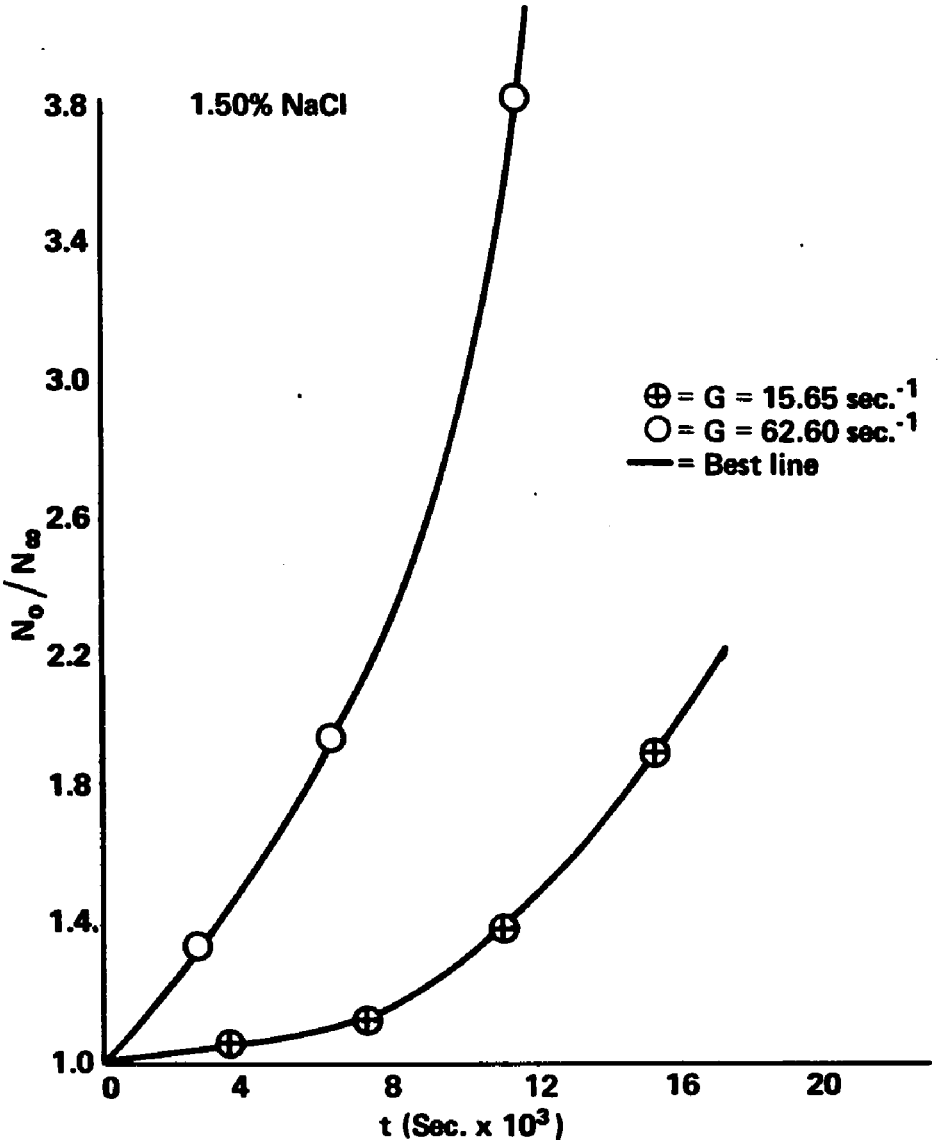

Figure 21. Plot showing the rate of shear effects on the rate of reaction

of shear one cannot use the usual dimensionless plot since tau tends to cancel out the effect of G. Therefore, these graphs were plotted as N_0/N_∞ versus t. It should be noted that there is an increase in the rate of shear; and with increasing rate of shear, linearity is lost more rapidly. This again emphasizes the necessity of an initially monodispersed particle suspension in order to maximize the duration of linearity. Because the reaction rate depends on the initial number of spheres present, a direct comparison of reaction rates is difficult. In order to make a reasonable comparison, the reaction rates for systems at two different rates of shear with similar initial particle concentrations are presented in Table VIII. The data certainly show that with increased rate of shear, there is increased reaction rate.

When examining Table VIII special notice should be made of $W^*_{app.}$ values. Keeping in mind that all systems are maximum rate, one would expect the $W^*_{app.}$ values to be in agreement. This is not the case. It, therefore, is reasonable to attribute the difference in $W^*_{app.}$ values to hydrodynamic slip, since the difference in shear rates is not enough to cause any significant deflocculation. This is especially true since this is initial rate data and the suspension consists predominantly of small aggregates which require relatively

TABLE VIII

Flocculation Rate Constants and Apparent Stability Factors $W^*_{app.}$

at Various Rates of Shear at 25°C with

NaCl Concentration = 1.50%

TTAB Concentration = 5×10^{-6} M

All rate constants are expressed as multiples of 10^{-4} $sec.^{-1}$

Rate of Shear ($sec.^{-1}$)	Initial No. of Particles x 10^6	Theory+	Found	$W^*_{app.}$
62.60	4.116	14.159	4.719	3.001
	4.496	15.467	4.961	3.118
	4.029	13.860	4.658	2.975
15.65	4.428	3.808	2.481	1.535
	4.309	3.705	2.585	1.433

$$W^*_{app.} = \frac{\text{Maximum Theoretical Rate Constant}}{\text{Experimental Rate Constant}}$$

+Theoretical rate constants calculated from Equation 33 with $W^*_{ij} = 1.0$

large forces to cause deflocculation as discussed in the literature review.

Particle Size Distribution Effects

Figures 22 and 23 show the effects of particle size distribution on the maximum rate of reaction at constant shear rates for systems employing similar initial concentrations of particles. Table IX lists the important parameters of the two systems.

In both examples particles were prepared in the usual fashion and then were allowed to flocculate in a thermostated beaker without stirring. An aliquot was removed and used to initiate each laminar shear-controlled experiment. In this fashion, as time elapsed, a progressively more polydispersed distribution could be obtained for the shear-induced flocculation experiments. The advantages of obtaining a polydispersed distribution in this fashion are twofold:

1. Starting with mostly monomers, the polydispersity could be confined to primarily monomers, dimers, and trimers.
2. Since all the particles came from the same system, experiment-to-experiment variation would be reduced (no unaccounted

TABLE IX

Important Parameters of Figures 22 and 23

	Figure 22				Figure 23			
Rate of Shear	31.3				62.6			
NaCl Concentration	1.5%				1.5%			
TTAB Concentration	5×10^{-6} M				5×10^{-6}			
Curve No.	Initial No. of Particles	Percent of Singlets	Doublets	Triplets	Initial No. of Particles	Percent of Singlets	Doublets	Triplets
1	3.56×10^{6}	94.2	4.7	1.1	4.12×10^{6}	89.4	6.0	2.5
2	3.59×10^{6}	79.0	13.1	6.7	3.69×10^{6}	77.2	14.3	5.6
3	3.24×10^{6}	69.8	17.2	9.8	3.41×10^{6}	66.9	16.2	10.9

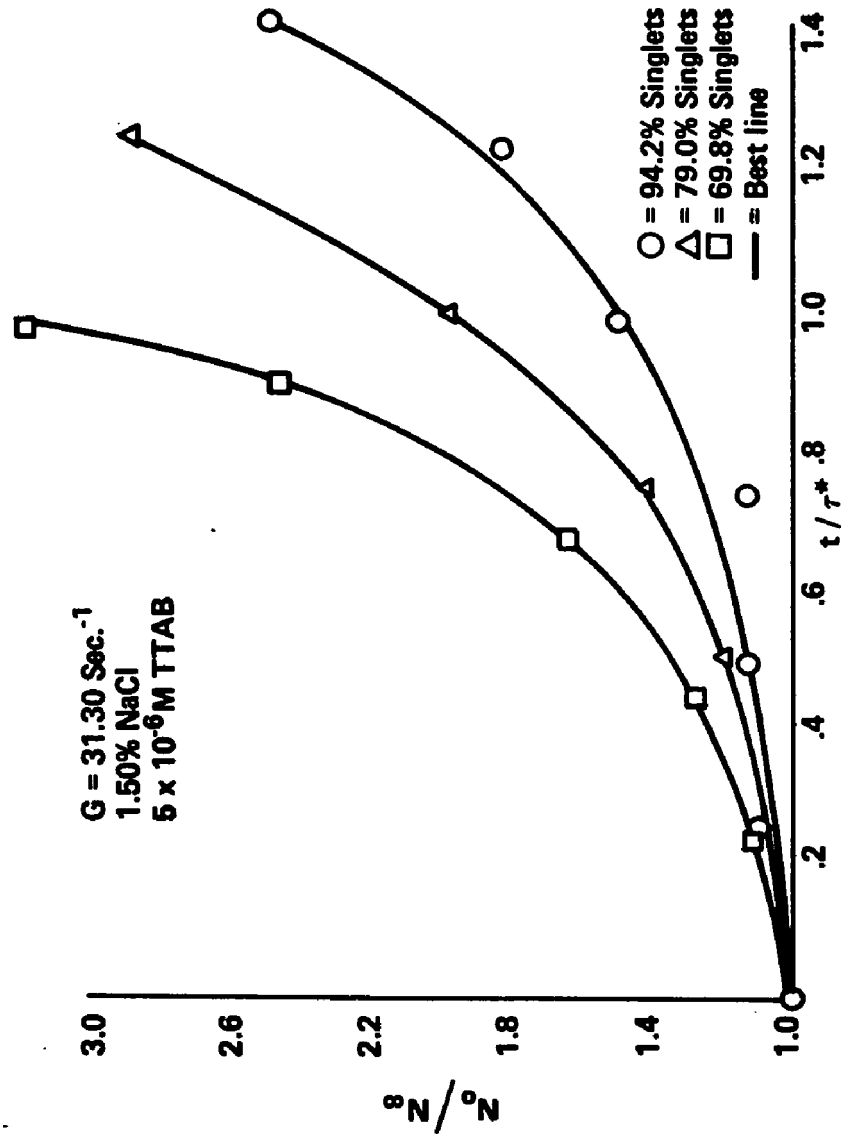

Figure 22. Normalized plot depicting the effect of polydispersity on the reaction rate of an orthokinetic system

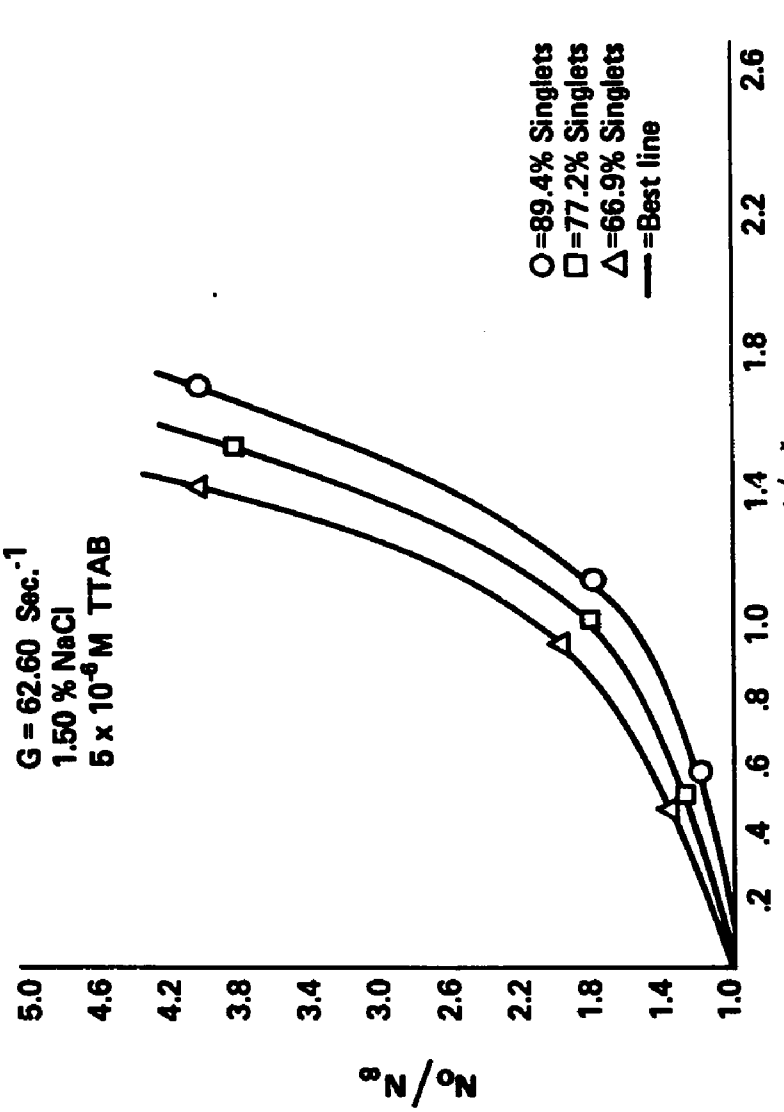

Figure 23. Normalized plot depicting the effect of polydispersity on the reaction rate of an orthokinetic system

large particles slipping in undetected).

From the figures it is apparent that the higher the concentration of monomers, the closer and longer the data approximate linearity. The more polydispersed the system, the more curvilinear the data, and the more quickly sedimentation-flocculation becomes an influencing factor in the rate of flocculation. As would be expected theoretically, an increase in polydispersity gives an increase in the rate of reaction. Some "one shot" experiments were also performed. In these cases particles were prepared as described above, but instead of taking a series of aliquots and performing a series of Couette flocculation experiments, just one aliquot was taken and one flocculation reaction performed. In these experiments the initial concentration of singlets fell within the ranges presented in Figures 22 and 23. In each instance the data fell into its proper ordered position. This indicated that the second of the two considerations listed above was not important and that the manner in which the particles were prepared precluded its occurrence. In addition, the methodology was shown to be reproducible.

Consideration was given to mixing latices of different diameters to study the polydispersity effect.

But, monodispersed solutions of latices of diameter greater than about 3-4 microns were not readily available. In addition, there are greater numbers of large particles serving as contaminants in dispersions of larger diameter latices. Since the capacity of the multichannel particle size analyzer was limited to a maximum size of 8-mers, it was deemed better to start with monomers and let them build into x-mers in a controlled fashion that would allow the viewing of the significant sizes contained in the suspension.

Table X presents flocculation rate constants at two different shear rates for systems which are progressively more polydispersed at initial times. In all cases increased polydispersity was concomitant with a corresponding increase in the experimental rate constant. The theoretical rate constants were calculated assuming that the systems contained suspensions of particles that were initially 100 percent monodispersed. As a result, the $W^{*}_{app.}$ is reduced as polydispersity increases. These experiments once again confirm the importance of knowing the most exact particle size distribution prior to initiating the reaction.

TABLE X

Flocculation Rate Constants and Apparent Stability Factors $W^*_{app.}$

at Various Rates of Shear for Different

Initial Particle Size Distributions at 25°C

NaCl Concentration = 1.50%

TTAB Concentration = 5×10^{-6} M

All rate constants are expressed as multiples of 10^{-4} $sec.^{-1}$

Shear Rate $sec.^{-1}$	Initial Percent of Singlets	Initial No. of Particles x 10^6	Rate Constant		$W^*_{app.}$
			Theory+	Found	
31.3	92.0	3.563	6.128	2.461	2.490
	77.0	3.587	6.169	2.789	2.212
	68.0	3.235	5.564	3.090	1.801
62.6	89.4	4.116	14.159	4.719	3.001
	77.2	3.686	12.681	6.116	2.074
	66.9	3.409	11.727	7.359	1.594

$$W^*_{app.} = \frac{\text{Maximum Theoretical Rate Constant}}{\text{Experimental Rate Constant}}$$

+Theoretical rate constants calculated from Equation 33 with $W^*_{ij} = 1.0$ assuming all particles are monomers.

Particle Density Effects

As mentioned previously, the density of the latex particles can manifest experimental artifacts. Figure 24 depicts these. The laminar shear-controlled case is linear at early times. At later times there is a loss of linearity. This loss of linearity manifests itself as an increase in the rate of reaction.

Subsequently, in time, there is increasing curvilinearity due to increasing polydispersity. However, there will come some point in time at which the flocs are sufficiently large enough for sedimentation and/or sedimentation-flocculation to become significant.

These various stages are exhibited by the figure. Loss of linearity depends on initial number of particles, the amount of initial polydispersity, the rate of reaction, and the rate of shear. The vertical lines in Figure 24 are arbitrary and are there to demonstrate the various stages during orthokinetic flocculation. A further discussion of the effects of polydispersity can be found in Appendix I.

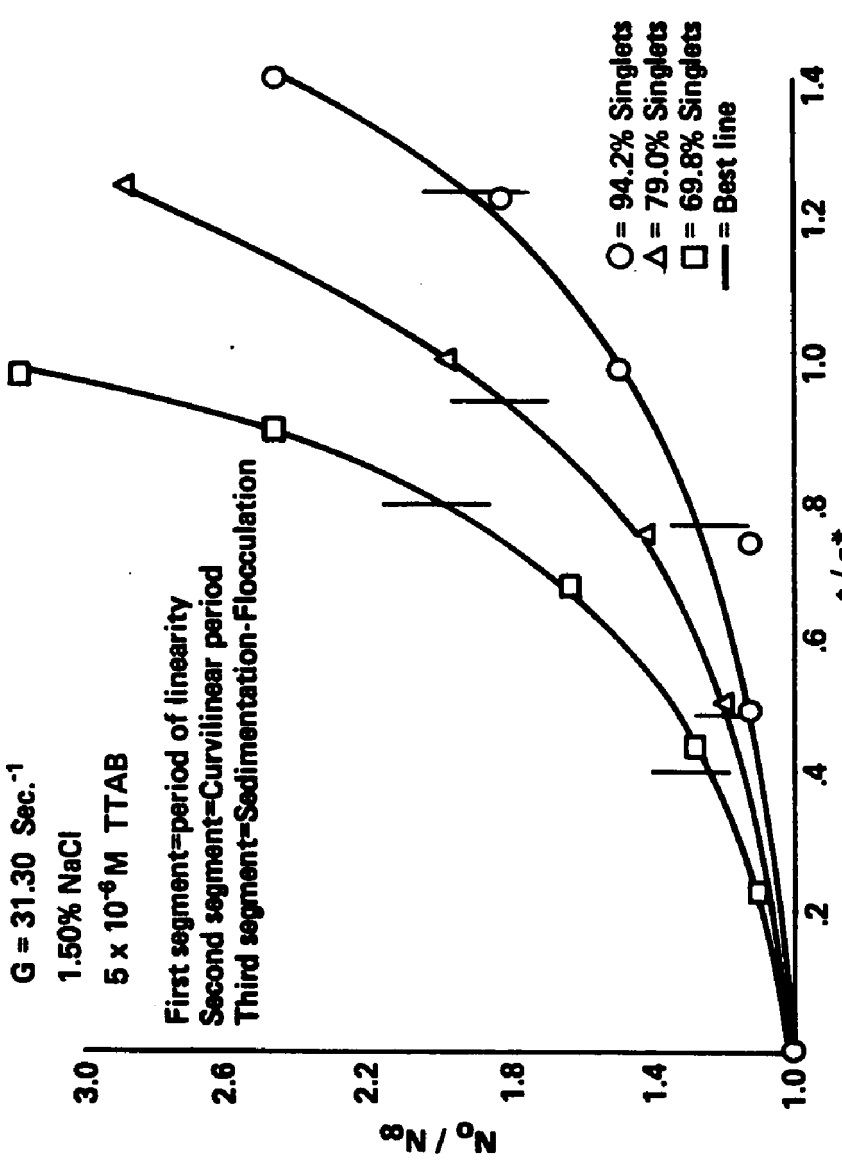

Figure 24. Normalized plot depicting the effect of particle density on experimental artifacts in orthokinetic reactions

Total and Individual Particle Size Distribution Changes with Time

Since an accurate determination of the total number of particles was necessary for any computation involving the particle size distribution, most experiments were performed using the graphical oscilliscope output from the RIDL analyzer. The RIDL's 400 channels could be easily broken down into about eight particle size classes. The data was treated by computing the number of particles in each class (N_i) and dividing this by the total number of particles in the system (N) as obtained from the total number of particles from the lowest threshold data taken from the Coulter Counter Model A at various times. A photograph was taken of the particle size distribution on the RIDL oscilliscope and was in turn integrated using a compensating polar planimeter. Figure 25 contains typical photographs of a particle size distribution at initial time (top) and at a short time later (bottom). It should be noted that the RIDL has provisions for expanding the scales horizontally and vertically to provide for more accurate integration.

The number of particles of a given size were determined with a knowledge of the total screen area, the scale on the ordinate and abscissa, the dilution factor, and the integrated area of the particle size under consideration.

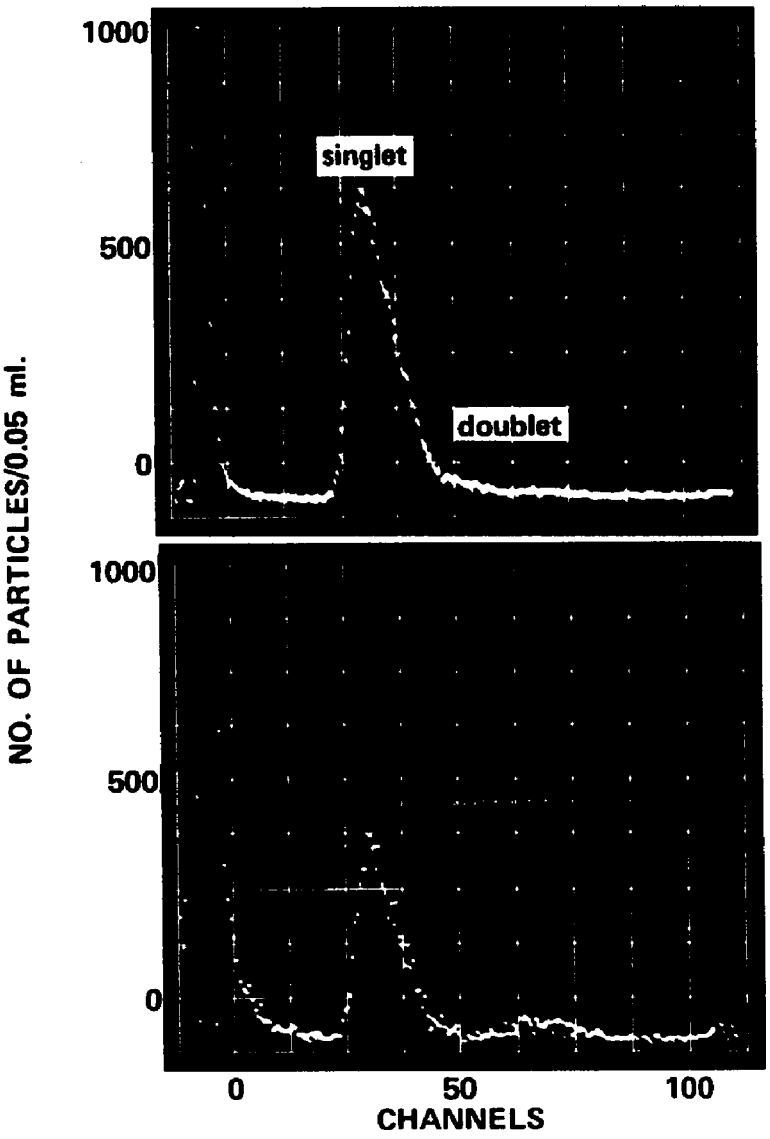

Figure 25. Pictures of differential particle distribution taken from the ocilloscope of the multichannel pulse height analyzer

Orthokinetic studies

The changes in the distribution of all particles, singlets, doublets and triplets with time in a 1.5 percent sodium chloride and $5x10^{-6}$ M TTAB medium are presented in Figures 26 and 27 as a function of two different shear rates. In both cases the data exhibit excellent agreement within experimental variation with the predicted rate of flocculation. Also notice that mass balance is maintained for approximately 1.2 to 1.4 units of dimensionless time. As will be noted in subsequent sections this is markedly different from the Taylor vortex case and very similar to the dimensionless time values found in the diffusion-controlled case. Determination of dimensionless time takes the rate of shear into account. If the shear rate were in error, then the loss of mass balance would not occur at the same dimensionless time if there were no other perturbations of the system. The fact that mass balance is lost at essentially the same dimensionless time for diffusion-controlled and laminar shear-controlled systems serves as a good internal check of the systems.

Effect of alpha and epsilon

A normalized plot of the total and individual particle size distribution with time in the maximum rate case for a laminar shear-controlled system with alpha

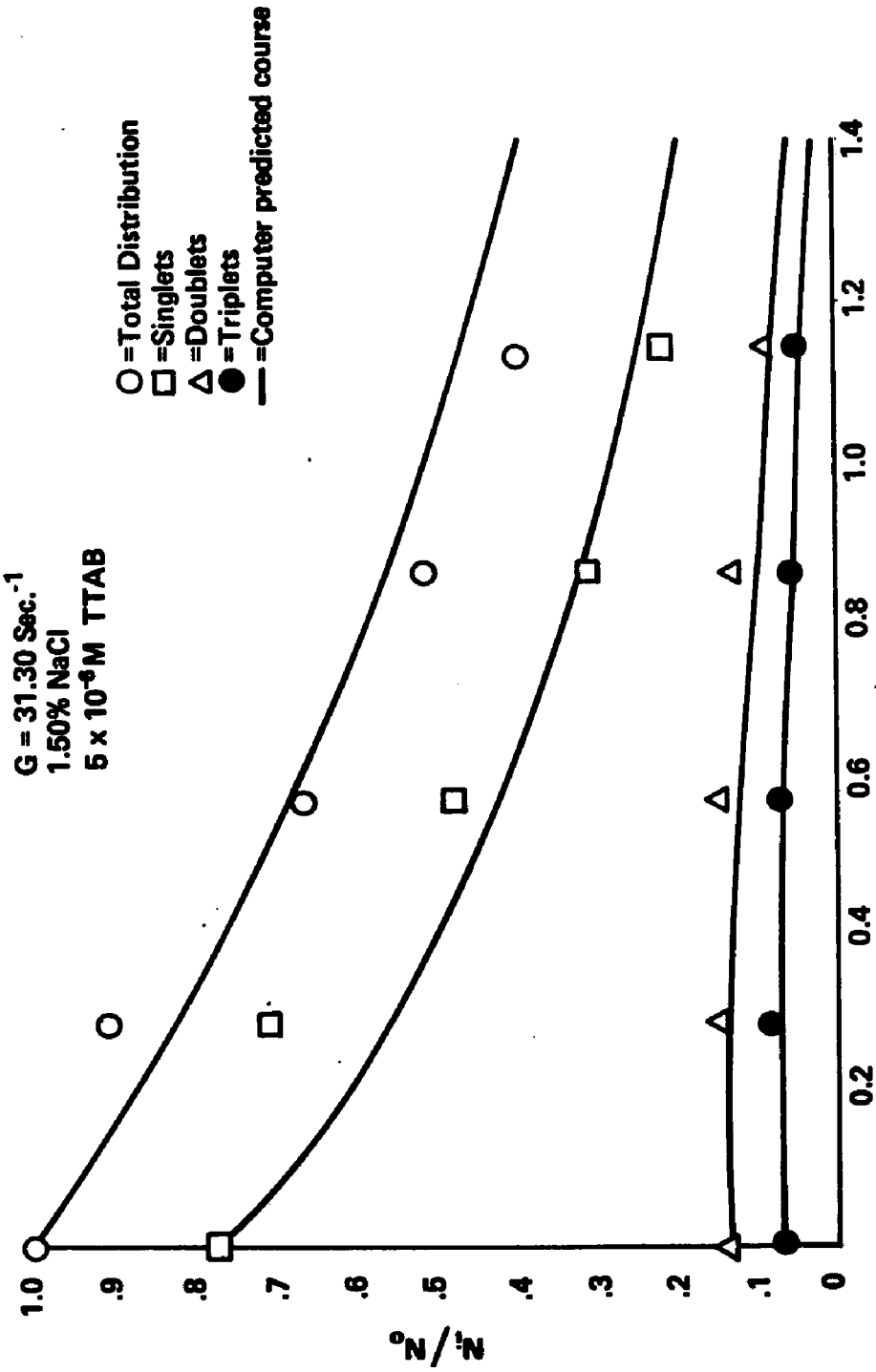

Figure 26. Normalized plot of the total and individual particle size distribution change with time in the maximum rate case for a laminar shear-controlled system

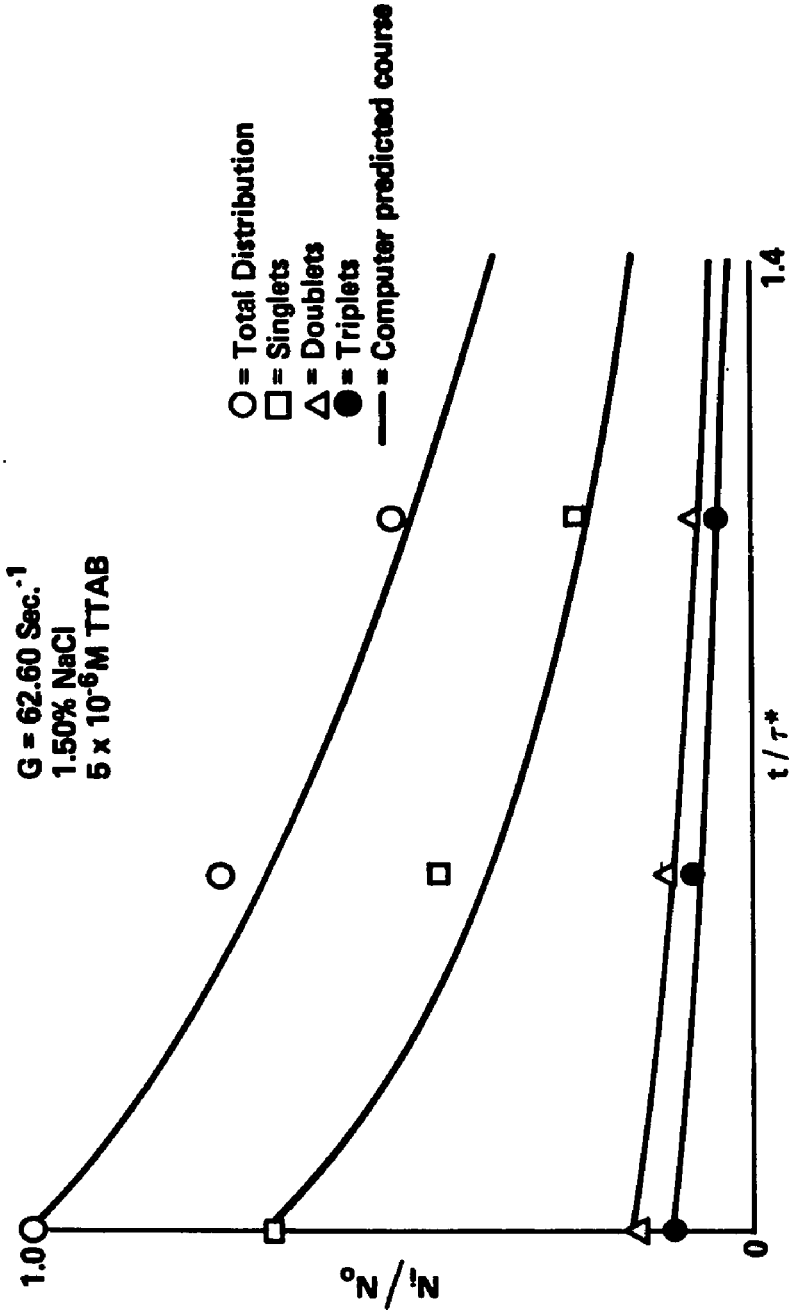

Figure 27. Normalized plot of the total and individual particle size distribution change with time in the maximum rate case for a laminar shear-controlled system

and epsilon variations is presented in Figure 28. The best overall fit of the data are to the computer generated curves with $\alpha = \varepsilon = 1$. Even with modest changes of epsilon the velocity of total and individual particles increases such that agreement between theory and experimental results is precluded.

Use of a modest alpha for the singlet-singlet interaction modifies the total and singlet particle predictions in a favorable way but greatly inhibits doublet and triplets unfavorably. The net effect was to slow everything down. Again it was found that a modification to the model did not aid in the prediction of experimental results, and that after all, the Smoluchowski model predicted experimental results quite accurately.

Effect of particle size distribution

Figures 29, 30, and 31 are normalized plots of the total and individual particle size distributions with time for maximum rate cases of laminar shear-controlled systems. The systems are increasingly more polydispersed at initial times. The effect of polydispersity can be seen most readily in doublet and triplet distributions, but in all cases each component of a more polydispersed system is changing more rapidly. Additionally, the good agreement between predicted and experimental results

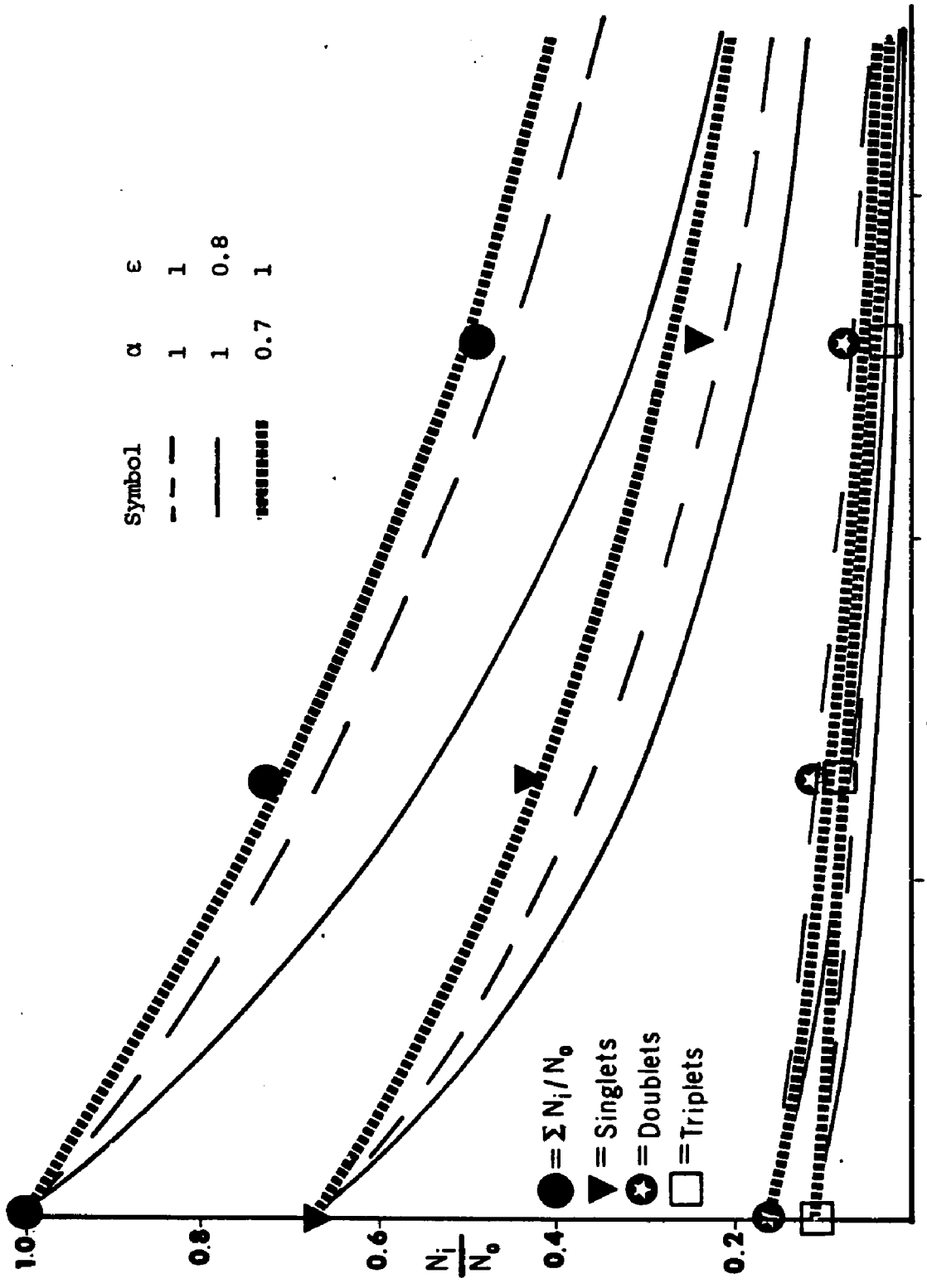

Figure 28. Normalized plot of the total and individual particle size distribution change with time in the maximum rate case for a laminar shear-controlled system with various alphas and epsilons.

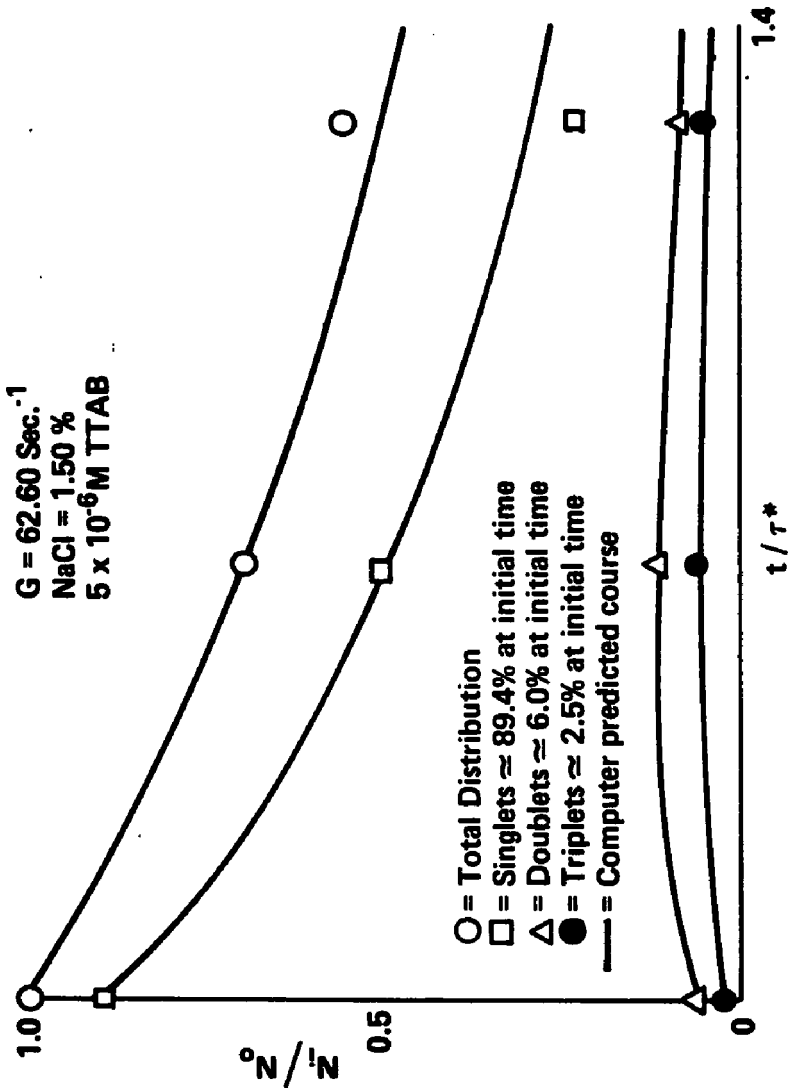

Figure 29. Normalized plot of the total and individual particle size distribution change with time in the maximum rate case for a laminar shear-controlled system

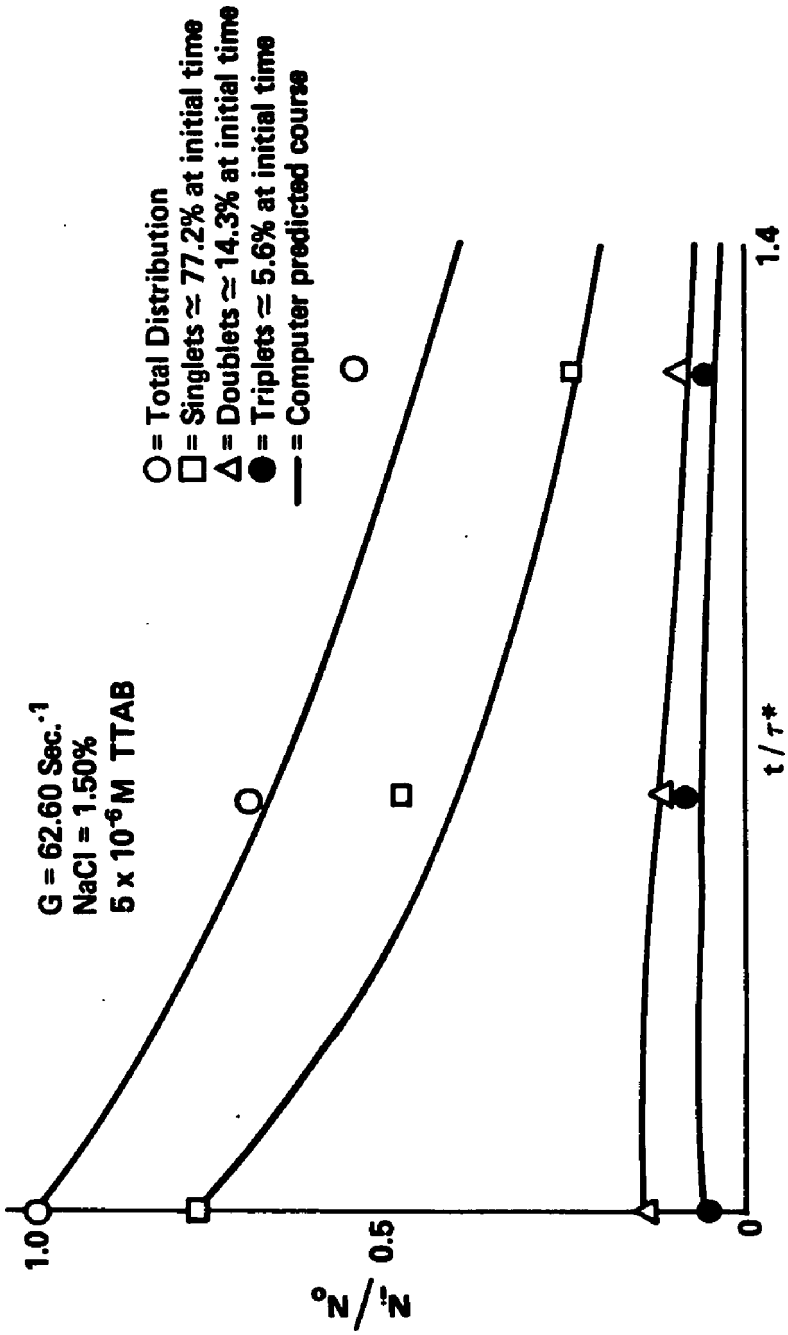

Figure 30. Normalized plot of the total and individual particle size distribution change with time in the maximum rate case for a laminar shear-controlled system

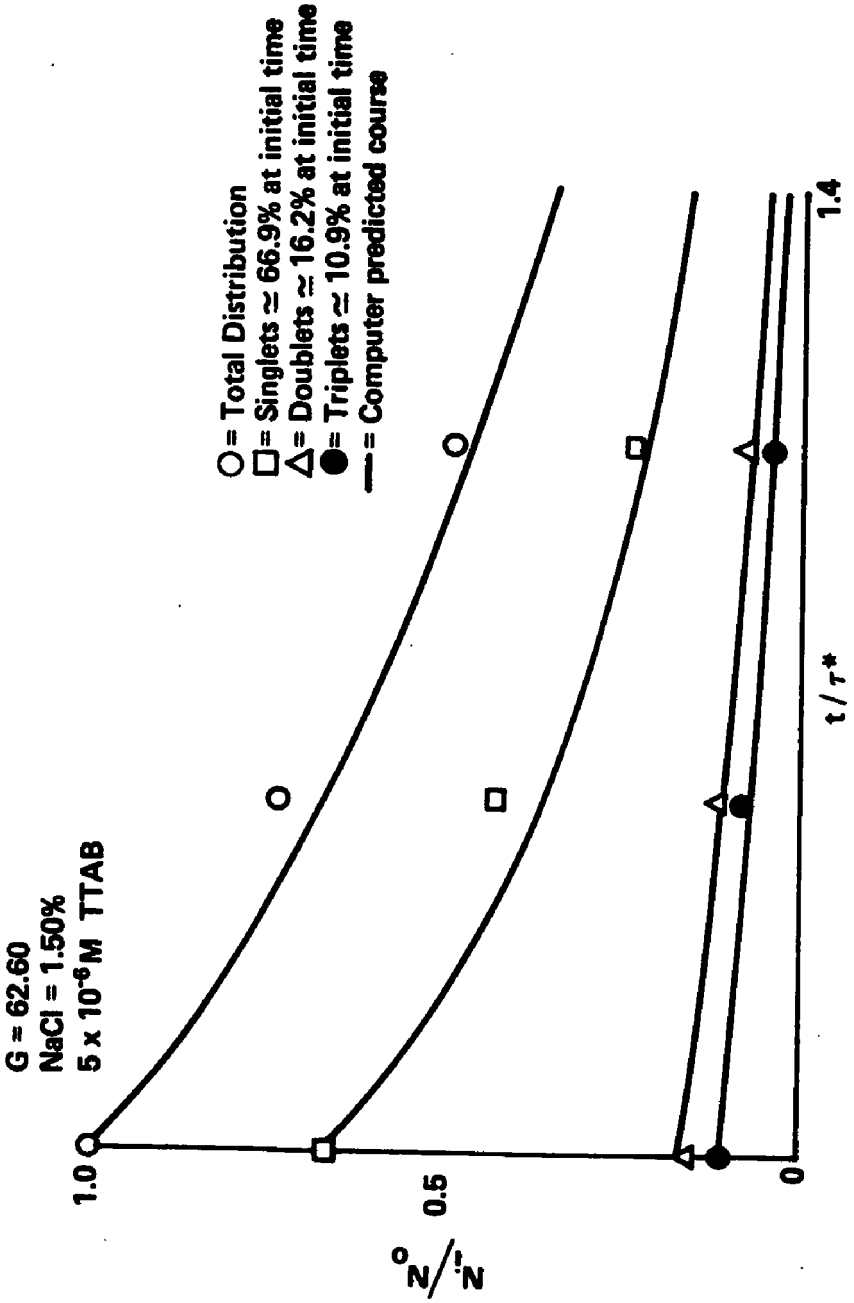

Figure 31. Normalized plot of the total and individual particle size distribution change with time in the maximum rate case for a laminar shear-controlled system

should be noted. This shows that the model is capable of handling complicated as well as singular systems.

THE TAYLOR SHEAR CELL

Introduction

During the literature review the marked differences between the hydrodynamics of a Couette cell and a Taylor shear cell were explored. Based on the review it was decided to investigate shear-induced flocculation under the influence of Taylor vortices and determine if the experimental results were consistent with experimental results from the Couette cell.

All apparati and experimental techniques were the same as those used for the Couette cell. The only exception being the Taylor cell itself, which is pictured in Figure 32. The dimensions of the cell (Table XI) were chosen to optimize the formation of Taylor vortices at low rpm's, while minimizing the reaction volume required. Motors of various speeds were used to rotate the bob via a shaft mounted in a double bearing clamp. The clamp prevented wobbling of the cup.

The data obtained using the Taylor shear cell was analyzed using the same methodology employed in the analysis of Couette cell data.

Finally, it was decided that two variables would be examined during the evaluation of the effect of Taylor vortices on the rate of reaction.

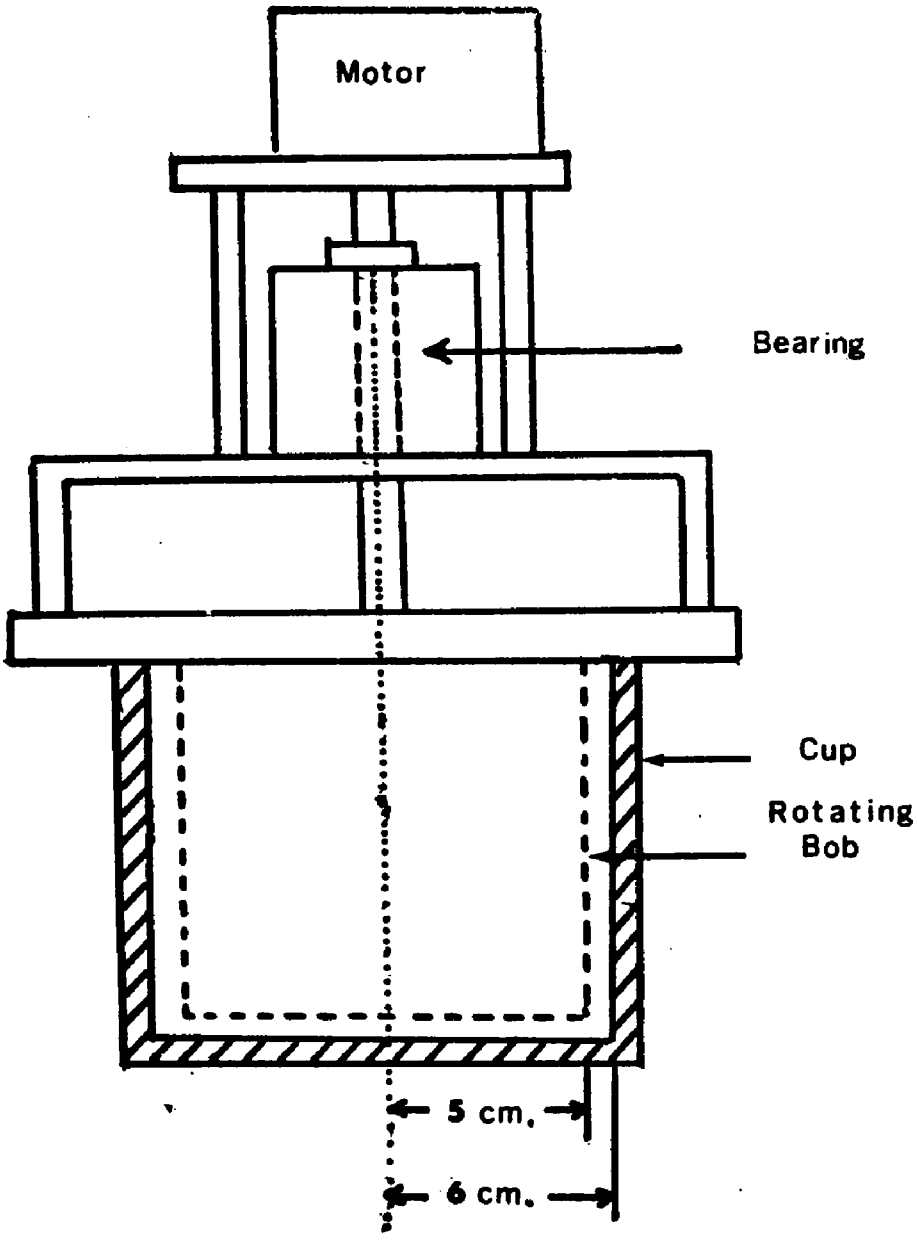

Figure 32. Shear Cell Producing Taylor Vortices

TABLE XI

Dimensions of the Taylor Shear Cell

Radius of the Cup	6.0 cm. ±0.01 mm.
Radius of the Bob	5.0 cm. ±0.01 mm.
Gap Between the Cup and the Bob	1.0 cm. ±0.01 mm.
Height of the Cup	10.0 cm.
Height of the Bob	9.9 cm.

Electrolyte Effects

Figure 33 depicts the effect of increased electrolyte concentration at a constant theoretical shear rate. The rate of shear was calculated assuming the shear was that of a laminar system using the equation in Table V. As in the Couette case, the reaction rate increases with increasing NaCl concentration. Also at early periods the curves are linear, and at later times become increasingly curvilinear as polydispersity increases.

Notice by comparison with a Couette system (Figure 18) that the vortex producing system with a theoretical G = 11.33 $sec.^{-1}$ is proceeding more rapidly than a laminar system with G = 31.30 $sec.^{-1}$ All the experiments were performed with monodispersed distributions and essentially the same number of particles. This comparison emphasizes the influence of Taylor vortices: to increase the volume average shear.

Rate of Shear Effects

In Figure 34 the influence of shear rate in the Taylor cell on the rate of flocculation at constant salt concentration is readily observed. Again we see the same curvilinear effects as noted above. Also in comparison with Figure 21 (Couette cell) we note that the kinetics of the vortex system is much more rapid. Note

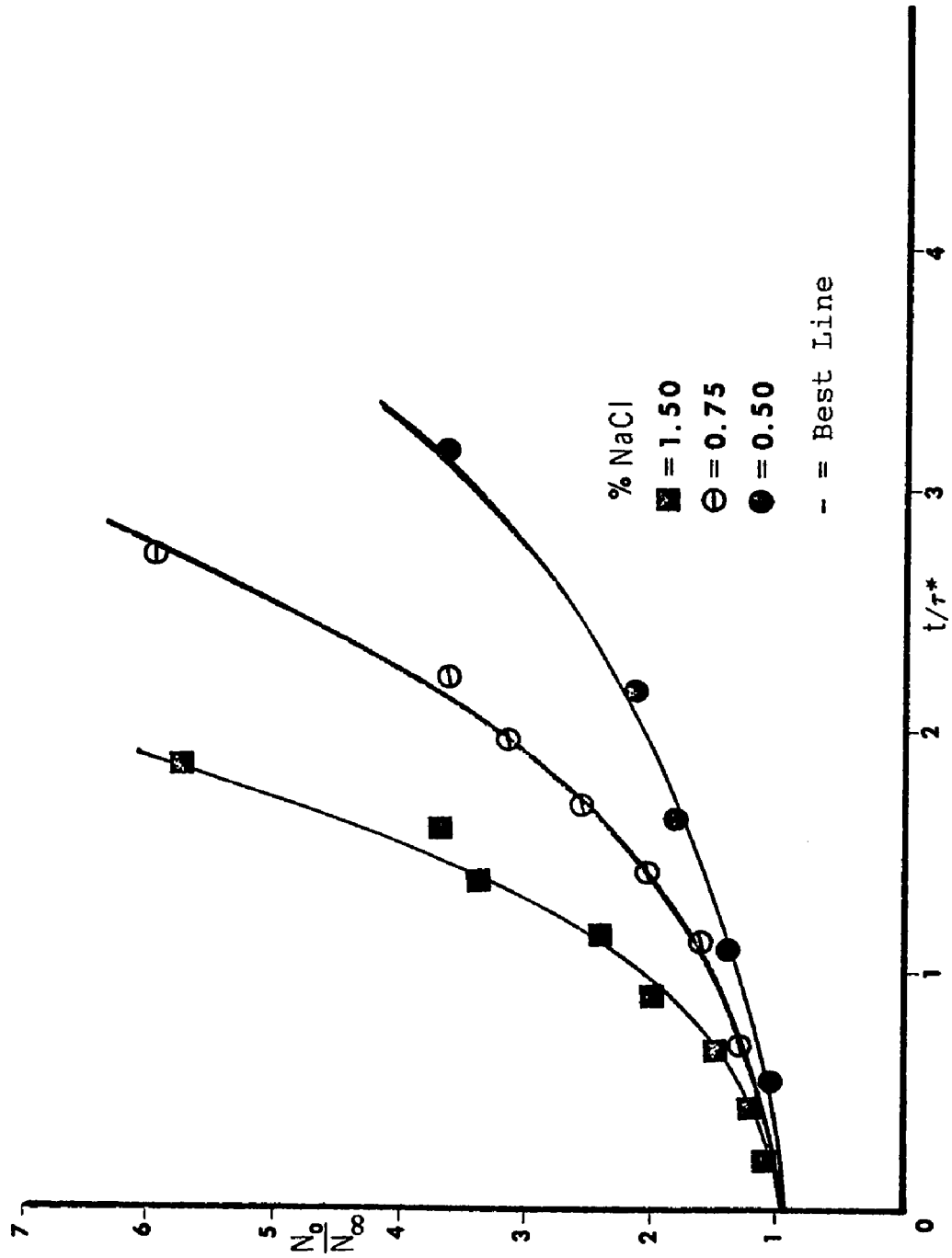

Figure 33. Normalized plot of various Taylor vortex systems depicting the effect of salt concentration on the rate of reaction

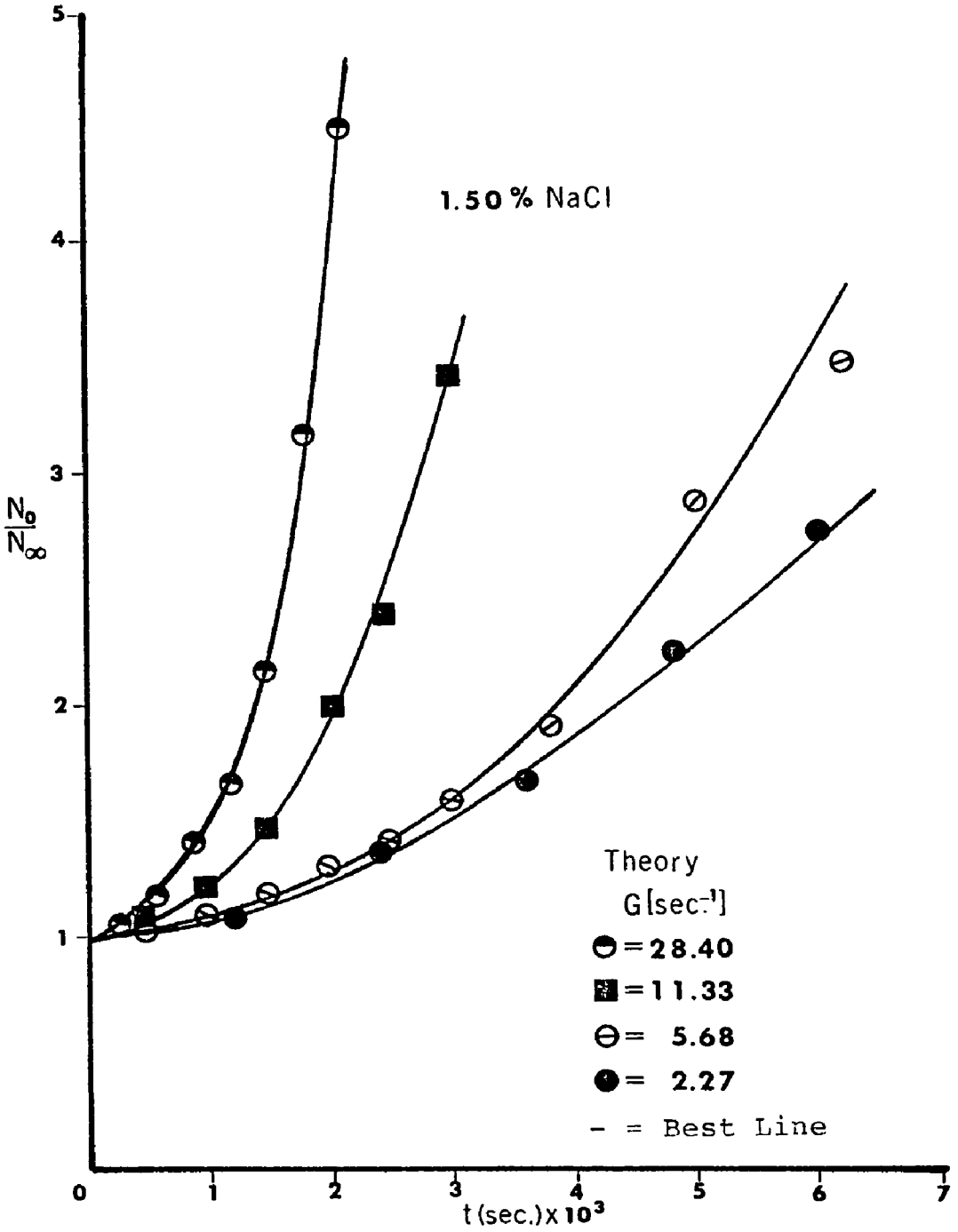

Figure 34. A plot depicting the effect of the theoretical rate of shear on the reaction rate of a Taylor vortex system

that there appears to be a jump in the velocity of the reactions after G = 5.68 $sec.^{-1}$ This is reasonable since at the lower two shear rates the systems are theoretically barely into the Taylor vortex producing region.

Again we have a strong indication that the volume average shear is actually much greater than the calculated rate of shear.

Total and Individual Particle Size Distribution Changes

Figure 35 represents an effort to take a closer look at the events in the Taylor shear cell using the computer program and RIDL techniques developed earlier.

The changes in the distribution of all particles, singlets, doublets, and triplets of latex particles (2.02 micron diameter) at 25°C and 1.50 percent sodium chloride concentration with time for the Taylor vortex shear-controlled system are shown in Figure 35. Examination reveals the experimental data is moving much more rapidly than the theoretical predictions even when using a stability factor of 2.50, which was experimentally determined. This is believed to be due to the increased volume average shear caused by the Taylor vortices. Subsequent manipulation of the theoretical predictions by the use of alpha and/or epsilon did not

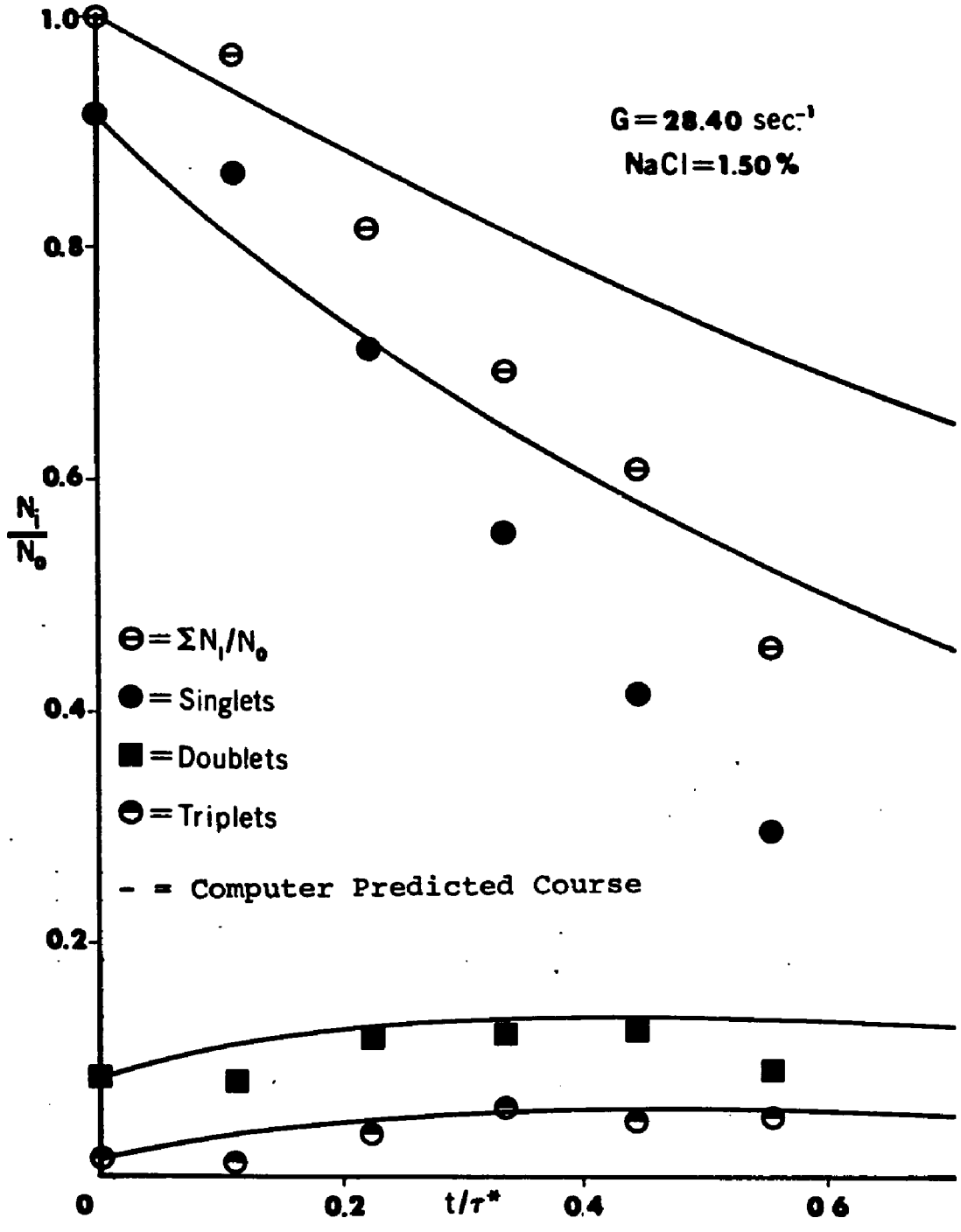

Figure 35. Normalized plot of the total and individual particle size distribution change with time in the maximum rate case for a Taylor vortex system

provide significantly better agreement between experimental and theoretical data.

It was also noted that when performing the experiments at maximum rate conditions a mass balance could only be maintained for a dimensionless time of approximately 0.6.

Fitting of the Data

In all experiments using the Taylor cell there was no correlation between experimental predictions and the data retrieved. It was felt that this was due to the inaccuracy of the shear rate used to make theoretical predictions. It is known that Taylor vortices increase the volume average shear and, therefore, using the theoretical rate of shear would produce inaccuracies. The predicted reaction velocities would be slow by the difference between the true rate of shear and the rate of shear used in the theoretical predictions. In an effort to model the data obtained from the Taylor cell a literature search was initiated to ascertain if a more accurate estimate of the true volume average shear could be obtained.

It was found that Debler et al. (1969) had performed experiments which might aid in the determination of a true volume average shear. They had accumulated torque data in the super critical regime of Taylor

instability. They demonstrated that after secondary flow commences there are multiple mode possibilities. They attempted to relate their own visual observations of azimuthal waves in secondary flow to their torque observations. They reasoned that simultaneous torque measurements and visual observations would establish more completely the torque-speed relationship for the particular modes which occurred. They determined the change in the torque-speed relationship after the onset of Taylor instability for a wide range of annulus gaps. The Taylor numbers for primary and secondary instability were obtained, and the features of the torque-speed relationship beyond the point of secondary instability were examined, but not unequivocally determined.

Using the data and tables presented by Debler et al., a probable shear rate of 82 $sec.^{-1}$ was calculated. It should be noted that in order to determine θ, the dimensionless moment, from Debler's data, it was necessary to extrapolate his data slightly. This may be the source of some error in the value of G obtained since θ is used to determine the dimensionalized moment, Φ, which in turn is used to calculate the shear rate.

In order to readily visualize the effect of G on the predicted rate plot the data cannot be plotted in the dimensionless form since G is part of τ. Therefore,

the data for the total particle size distribution is presented in N_∞/N_0 vs. τ format.

Figure 36 depicts various computer simulations versus data obtained from the Taylor cell. Disregarding simulation number 3 for the moment, it can be seen that there is an increasing reaction rate predicted with increasing shear rate at a constant W (2.858). The first simulation represents the predicted total rate based on the theoretical shear rate (no Taylor vortices present). It is evident that this prediction does not accurately fit the data since it is much too slow. The second prediction was determined using a shear rate of one-half that predicted by using Debler's data. It offers a reasonable fit to the early data. Simulation number 4 was made using the full Debler prediction of 82 for the rate of shear. It is faster than the experimental data, but it does offer a reasonable approximation to the last 3 data points. By far the best approximation is 3. It offers a reasonable fit to the data at all time intervals. For this simulation G is equal to 61.4, and the stability factor is 2.858. The value for W is the predicted collision efficiency taken from the work of Curtis and Hocking (1970) which will be discussed in the first appendix. This value of the stability factor is in good agreement with the data reported in previous sections for equivalent laminar shear rates (G = 62.6). Comparing

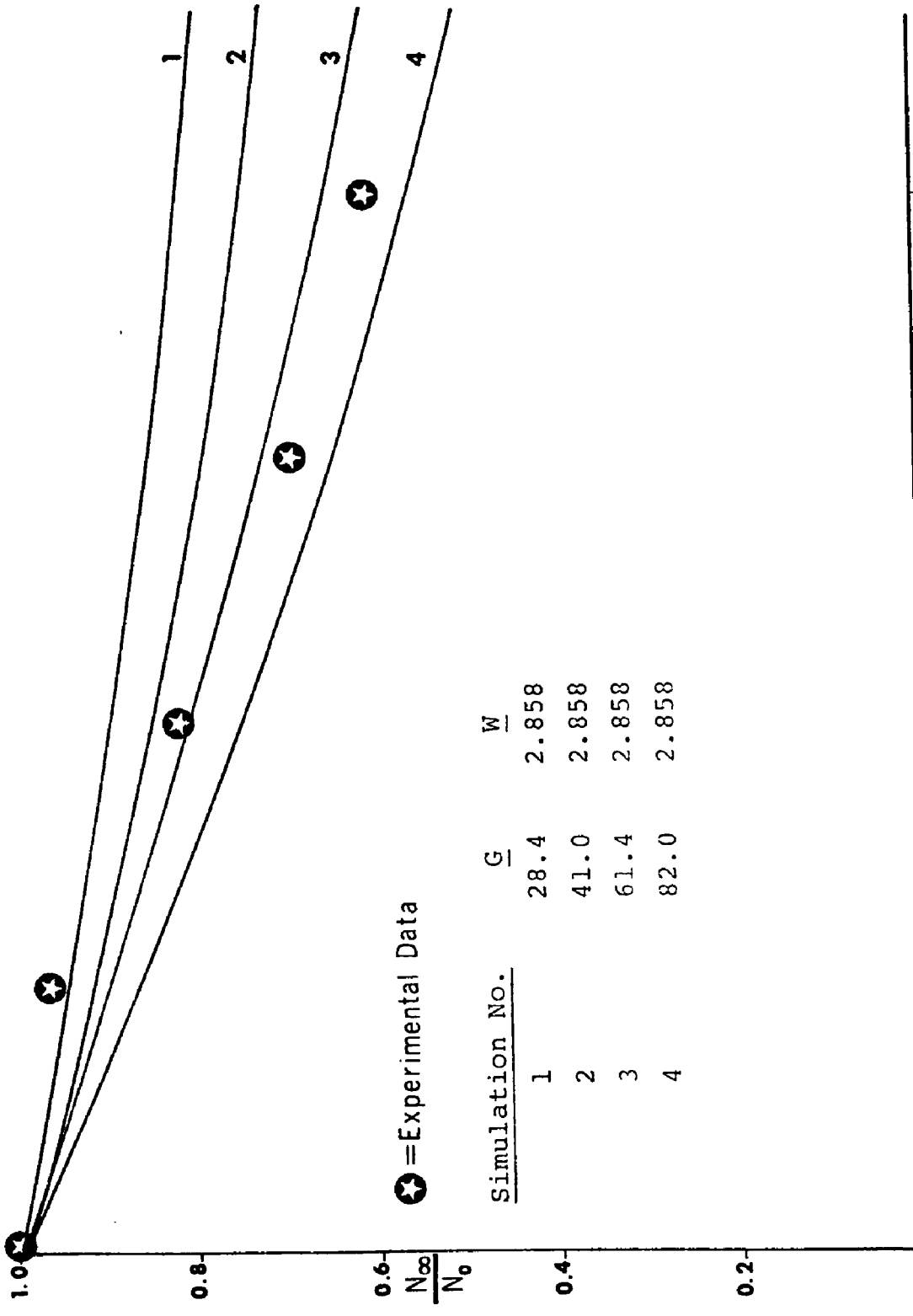

Figure 36. Plot of various computer simulations versus experimental data obtained from the Taylor shear cell

theoretical rate constants (using these final values of W and G) with experimentally determined rate constants revealed them to be consistently within 15 percent of one another.

Further validity can be afforded to the choice of the shear rate if one were to examine the point in dimensionless time at which mass balance is lost. For diffusion-controlled and laminar shear-controlled systems this is approximately 1.3 t/τ. For the Taylor vortex system it is approximately 0.5 to 0.6 t/τ. Taking a ratio of the diffusion-controlled value to the Taylor and multiplying by the theoretical shear rate for the Taylor cell gives a new shear rate which could be 61.4 if the correct values were chosen. Therefore, we have two independent means of converging on a reasonable value for the rate of shear.

It is important that even while under the influence of Taylor vortices the rate of flocculation of the system can be reasonably predicted using the Smoluchowski equations provided judicious values for the rate of shear and collision efficiency can be determined.

DIFFUSION-CONTROLLED FLOCCULATION

Introduction

At the conclusion of the literature review it was apparent that flocculation under perikinetic conditions was well documented and, by comparison, less complicated than orthokinetic flocculation. For these reasons it was decided to use diffusion-controlled studies to serve as a baseline for experimental methodology and as a tool to factor out the experimental artifacts (considerations in present approach to the problem) that so readily creep into flocculation studies.

In addition, diffusion-controlled systems could be used to generate polydispersed particle systems for orthokinetic studies. The advantage of using a perikinetic reaction to generate a polydispersed system is that the degree of polydispersity could be confined to the smaller end of particle sizes without also having many larger particles. This difference is inherent in the difference in mechanism between perikinetic and orthokinetic reactions.

All apparatus and experimental techniques were the same as those used for the couette cell, with the following exceptions:

1. Diffusion-controlled experiments were conducted in glass water-jacketed beakers (Figure 37) thermostated at 25°C.
2. Reaction samples were taken at a point which was concomitantly in the center of the beaker, as well as, at the midpoint of the column height.

Analysis of the data was slightly different from orthokinetic systems. All rate constants were determined by least squares regression analysis of the $1/N_{\infty}$ vs. t. Identical rate constants could be obtained from either type plot. The values obtained were initial values (up to 8 hours for diffusion-controlled experiments) and do not reflect the deviations at longer times due to sedimentation-flocculation.

Electrolyte and Surfactant Effects

Table XII shows some of the results of perikinetic flocculation studies with varying amounts of salt and TTAB. The effect of the TTAB is to render the particle

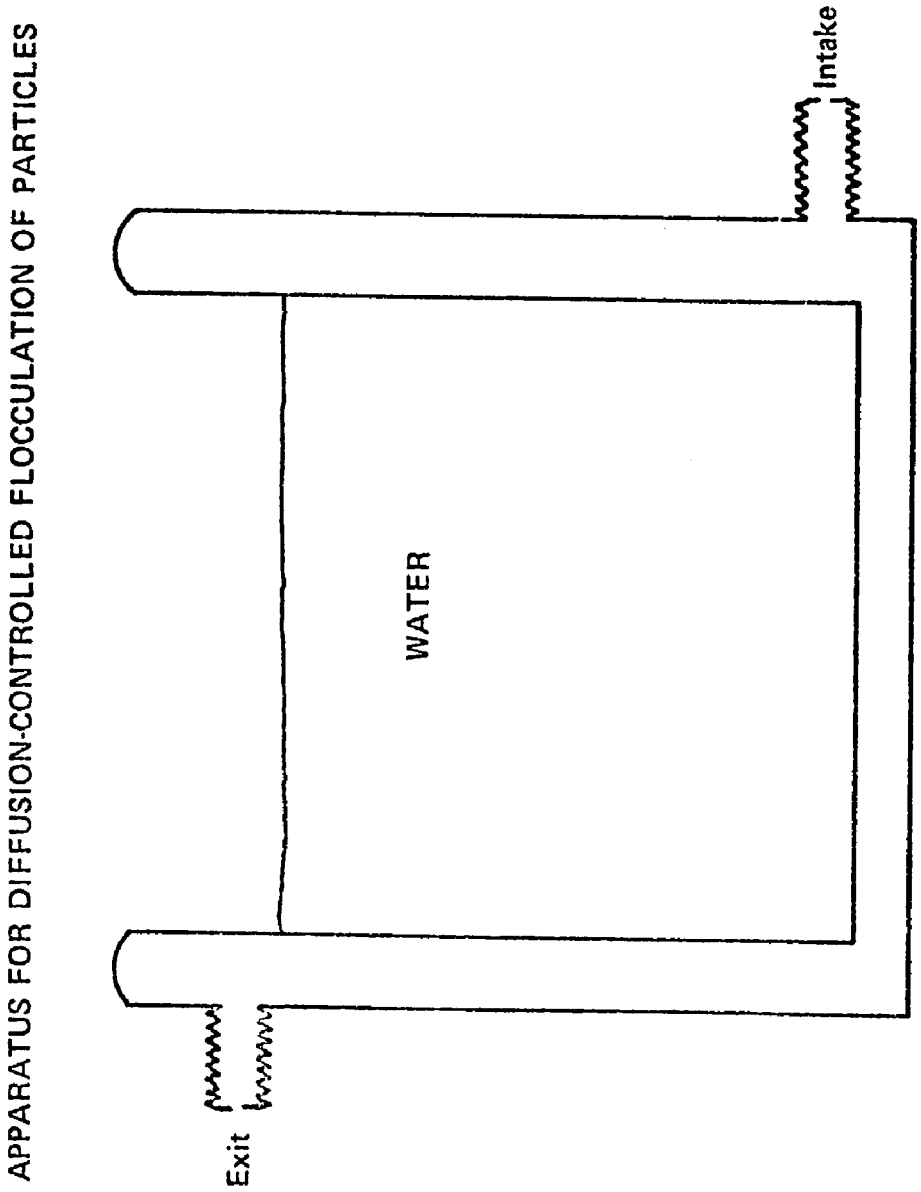

Figure 37. Apparatus for Diffusion-Controlled Flocculation of Particles

TABLE XII

Rate Constants Obtained from
Various Perikinetic Systems

% Sodium Chloride	5×10^{-6} M TTAB	Rate Constants (10^{-12} cm.^{3} sec.$^{-1}$) Experimental	Theory
1.50	none	3.00	5.96
1.50	none	3.08	
1.50	none	3.10	
		3.06 avg.	
0.75	none	3.07	
0.75	none	3.00	
		3.04 avg.	
0.50	none	2.38	
0.50	none	2.30	
0.50	none	2.28	
		2.32 avg.	
1.50	yes	3.05	
1.50	yes	3.15	
		3.10 avg.	
0.75	yes	3.08	
0.50	yes	3.12	
none	yes	3.06	
none	yes	3.20	
		3.13 avg.	

surface charge towards zero and the salt reduces the electrical double layer towards zero.

It is easy to see the excellent reproducibility of results from experiment to experiment. It can also be seen that at 0.75 percent sodium chloride concentration the system was essentially a maximum rate system. Also, the TTAB so effectively reduces the surface charge that little or no salt is needed to achieve a maximum rate system.

These data agree with the kinetic data presented by Bernstein, Higuchi, and Swift and Friedlander as previously noted in the literature review.

Figure 38 shows the Smoluchowski type plot in dimensionless form for the total change in the particle size distribution with time for the diffusion-controlled system. Pictorially, as expected, the rates of flocculation increase with increasing concentrations of sodium chloride in the absence of TTAB. A maximum experimental rate is achieved beyond 0.75 percent sodium chloride concentration and is smaller than the theoretical maximum rate constant predicted by the classical Smoluchowski theory by a factor of about 1.9. Although not depicted in Figure 38, as time progressed sedimentation flocculation caused a loss of particles which caused the data plot at later times to be concave upward. This erroneously indicated an increase in the

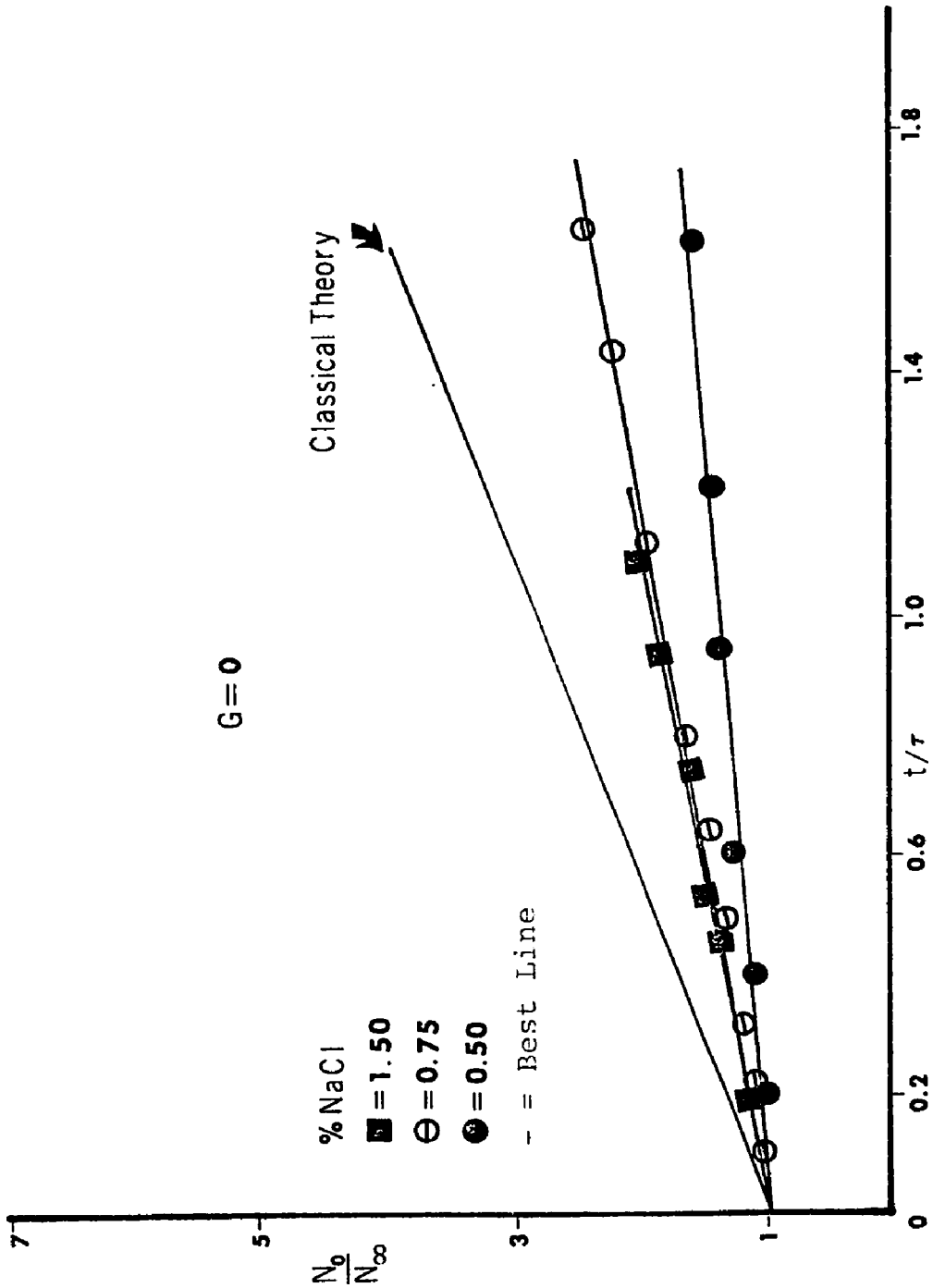

Figure 38. Normalized plot of various perikinetic systems showing the effect of salt concentration on the rate of reaction

flocculation rate. This effect can be seen in Figure 39. The erroneousness was proven by performing a simple mass balance check. After reading the sample it was sonified as described earlier and read again. Deviation from the concentration of particles at the beginning of the experiment showed the loss of mass balance.

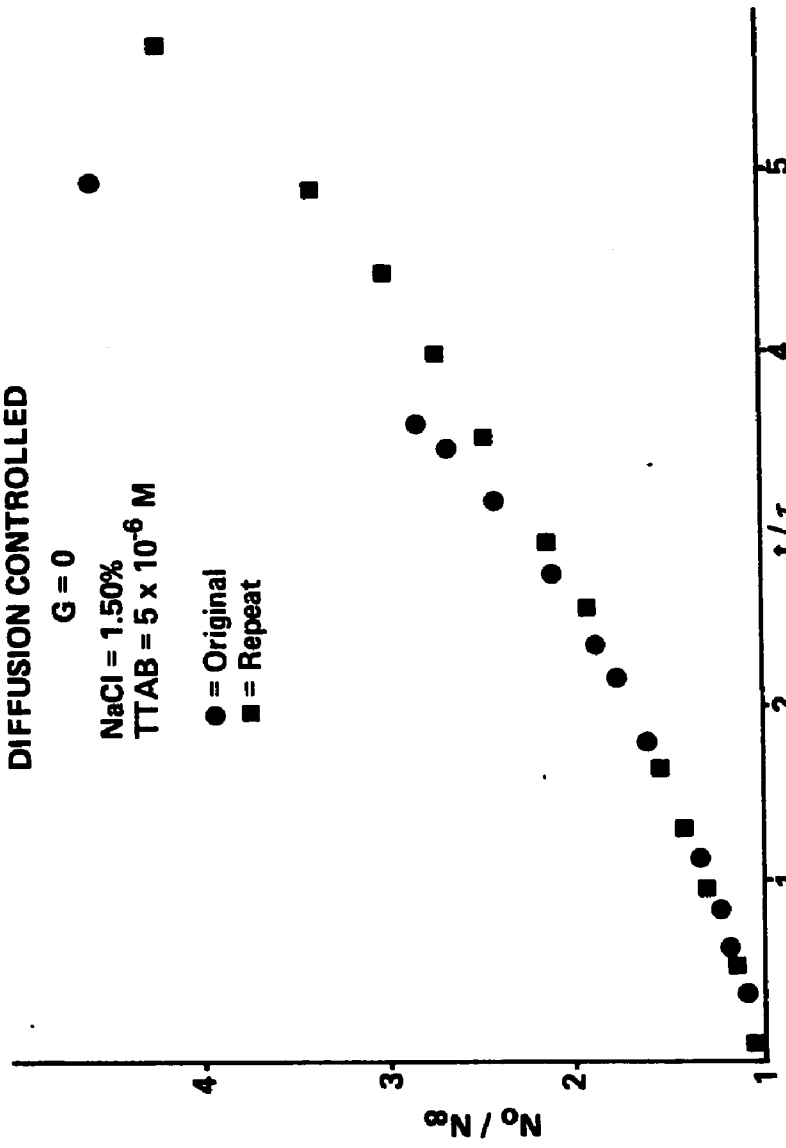

Figure 39. Normalized plot depicting the effect of particle density on experimental artifacts in perikinetic reactions

Total and Individual Particle Size Distribution Changes

Using the work of Suzuki, et al. (1969) a computer program was developed for the simulation of diffusion-controlled reactions. The same general considerations went into the development of this program as went into the development of the laminar shear simulating program.

The program was used to compare theoretical predictions of time course diffusion-controlled reactions with actual experimental data.

The changes in the distribution of all particles, singlets, doublets and triplets of the latex spheres at 25°C and 1.50 percent sodium chloride concentration with time, for the rapid diffusion-controlled situation are shown in Figure 40. There is excellent agreement between the experimental data and computer predictions of the fundamental Smoluchowski equation for flocculation by Brownian collision. The value used for the stability factor was the average stability factor determined experimentally for the rapid system, 1.94. A check on the mass balance was performed at each data observation. It was found that mass balance was maintained until a dimensionless time of approximately 1.3, equivalent to about 350 minutes, after which the loss of all particles with time due to sedimentation

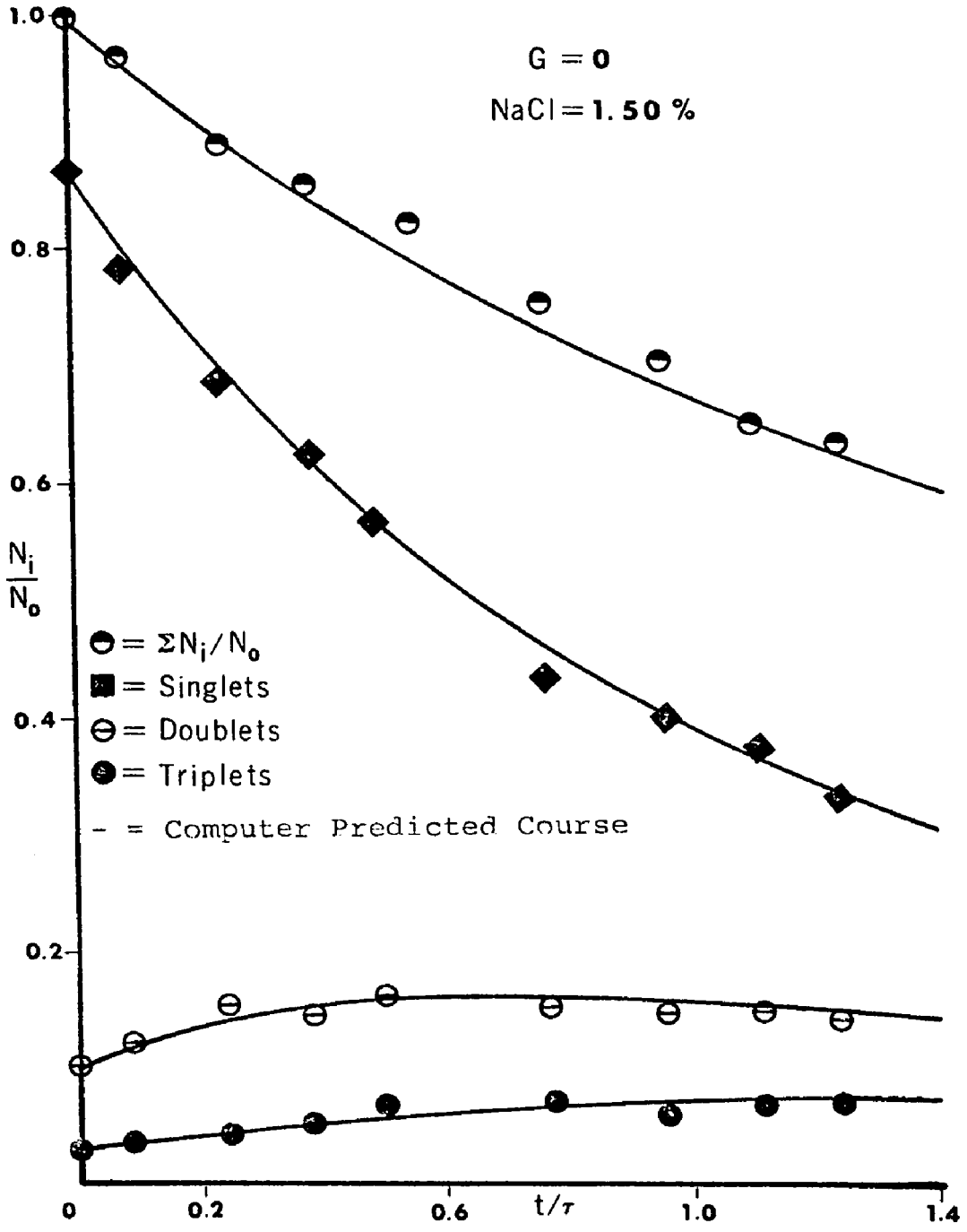

Figure 40. Normalized plot of the total and individual particle size distribution changes with time in the maximum case for a diffusion-controlled system

became increasingly significant. Again, as in the shear case there is an excellent fit of the data to the model without the use of a modifying function, such as epsilon.

Comparison of Orthokinetic and Perikinetic Systems

When reviewing the literature it was apparent that the work of Swift and Friedlander (1964) was very important. The authors made the assumption that the stability factor in the maximum rate diffusion-controlled case was equivalent to that of the couette case at maximum rate. Perhaps not so fortuitously, the experimental conditions chosen lead them to believe that their assumption was correct. It now seems clear that based upon the theoretical considerations presented in the literature review and the data in this dissertation that their assumption is valid only under special conditions, such as: Maximum reaction rate under diffusion-controlled conditions compared with a Couette reaction at a rate of shear which produces the same nominal stability factor. This is extremely important because it underscores the basic fact that the processes of aggregation in the two systems are physically different. Although the electrical considerations of attraction and repulsion are the same, the orthokinetic hydrodynamics are markedly

different because of the trajectories and particle-particle pressures.

DISCUSSION

General

While the experimental and the theoretical portions of this study would individually stand on their own, it is felt that the combination offers a unique and powerful handle in investigating the many factors that comprise the flocculation process. These techniques have made it possible for the first time to systematically study the particle size distribution changes with time of laminar shear-controlled systems in which various particle-particle interaction functions may be examined both theoretically and experimentally. Also, these approaches have permitted the critical evaluation of methods for treating flocculation kinetics, viz., the ln N_∞/N_0 versus time plots.

Clarification of the Literature and Future Studies

Although there were little experimental data pertaining to flocculation in a laminar shear field, a significant amount of theoretical literature existed. The work presented in this dissertation supports the theoretical findings culminated by Curtis and Hocking, and further explains the experimental findings of Swift and Friedlander. In addition, a more critical examination

of flocculation processes in a laminar shear field were obtained by examining not just the total or overall rate process, but for the first time by studying the rate processes of individual particle sizes. These studies indicated that shape factors, and individual collision efficiencies do not readily provide a better fit of experimental data (relatively monodispersed particle size distributions) to simulated predictions of initial rate data using Smoluchowski's equations. Further, it appeared that the study of shape factors and collision efficiencies would lead to an infinite number of combinations, all of which would possess various subtileties.

By virtue of experimental design these studies were limited to initial rates due to sedimentation of the latices. The latices were a logical choice for baseline studies since they allowed for the most accurate evaluation of the particle size distribution. A logical next phase of investigation would be the flocculation and/or coalescence of emulsions in a laminar shear field. Although initial distributions would be more dispersed, if accounted for, their predicted time course should be predicted by the model as shown for polydispersed latex systems. The emulsion systems would have the advantage of a more closely matched density between suspending medium and suspended

particles, thereby allowing for evaluation of experiments of longer duration. In these systems particle shapes and collision efficiencies may be of much more importance.

Application to Pharmaceutics

It is felt that the methodology developed in this dissertation is unique because it not only provides a method of testing long standing theory, but also establishes an uncomplicated system for the stability testing of suspensions and possibly emulsions. Using this system, the industrial scientist could conceivably custom fit the flocculation characteristics of a drug product to the shelf life needs of the company. The apparatus could also be used as a control tool in the manufacture of suspensions or emulsions because of its ease of use and the rapidity with which results can be obtained.

Theoretical Considerations of Curtis and Hocking

In the body of the dissertation the work of Curtis and Hocking (1970) was cited. Now the importance of their work will become even more evident. Their calculation of the "collision efficiency" or W along with an accurate assessment of the shear rate will allow a rigid test of the ability of the Smoluchowski theory to model experimental results.

They reasoned that if the particles always moved within the undisturbed shear velocity, any one particle would collide with another of given size if it were within a cylinder of radius normal to the sum of the radii of the particles, with its axis parallel to the flow of direction. Furthermore, the cross-sectional area within which the particle lies if collision occurs when allowance is made for the effect of hydrodynamics and London forces, as a fraction of the geometrical cross-section, is the collision efficiency for particles of the two sizes. They took the comparatively simple case for two equal spherical particles.

What this means is that Curtis and Hocking took a very critical look at what might be called a slip factor. Figure 41 is a depiction of the physical significance of a slip factor, which is dependent on the shearing

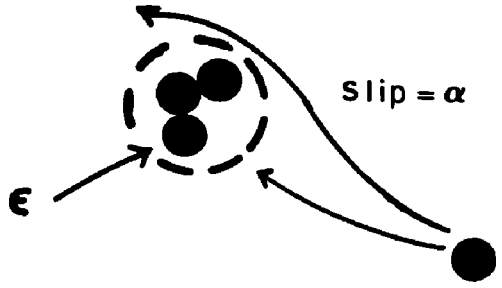

Figure 41. The slip of one particle around an aggregate

motion on the particles, which drags them along in the fluid, the hydrodynamic forces which result from the translation and rotation of two particles immersed in the fluid, and the London forces of attraction. All of these affect the trajectories of the particles. With a knowledge of the system parameters, a reasonable value for A ($2x10^{-14}$ ergs, as pointed out by Curtis and Hocking), and the second curve in Figure 2 of their paper, a reasonable estimate of the theoretical collision efficiency could be determined for systems at various rates of shear. The values obtained were 2.858 and 2.674 for monodispersed systems with corresponding shear rates of 62.60 and 31.30, respectively. As can be seen, these predicted values are very close to the experimental values reported in Tables VII and VIII.

The closeness of the predicted and experimentally determined stability factors would indicate that:

1. Our understanding of the physical process of flocculation in a laminar shear field has been enhanced since the theoretical considerations of Curtis and Hocking have been confirmed.
2. The explanation presented to account for Swift and Friedlander observations is correct.

3. Using the Curtis and Hocking methodology to determine the stability factor and the Smoluchowski equations, one could accurately predict the time course of flocculation in a laminar shear field.

APPENDIX I

Theoretical and Experimental Considerations of Extraneous Factors in Laminar-Shear Induced Flocculation Studies

In the body of the dissertation it was stated that sedimentation and/or sedimentation-flocculation was the cause of the rapid loss of mass balance experienced during experimentation. Now we will examine both situations more closely.

If sedimentation-flocculation were the cause of mass balance loss, then it should be possible to detect an unusually rapid loss of particles while maintaining mass balance. Additionally, sedimentation or sedimentation-flocculation would eventually cause a loss of particles without the maintenance of mass balance when sampling at a constant depth.

Sedimentation of a monodispersed particle size distribution can be pictured as a dropping curtain. Once the curtain begins to pass the sampling point, there is an artificial loss of particles.

In the case of sedimentation-flocculation there is the above effect as well as increased flocculation due to the "sweeping-out" effect of the sedimenting agglomerate.

In actuality the particle size distributions were not monodispersed. They contained small percentages of larger sized particles. Further, an increase in the rate of flocculation depends on the difference in sedimentation velocity of different particles and is only present when

the system is polydispersed. This case has been analyzed by Muller (1928). A significant effect on the perikinetic rate is only found when the radius ($r_{crit.}$) of the sedimenting particles is larger than:

$$r_{crit.} \geq \left(\frac{40kT}{\pi gd}\right)^{\frac{1}{4}} \tag{53}$$

where k is the Boltzman constant; T the absolute temperature; $\pi = 3.1415$; g is acceleration due to gravity; and d the density difference between the latex and the medium. For the systems studied, at 25°C, this value is 3.07 microns, based upon a density difference, d, of 0.06 g cm^{-3}. Since the latex particles are 1.01 microns in radius, the effect becomes significant for 4-mers and larger particles.

In the case of Couette flow the effects of sedimentation could be modified by a centrifugal force. Effects of centrifugal force can be calculated using a standard physics textbook equation.

$$F_c = m \frac{v^2}{r} \tag{54}$$

Where F_c is the centrifugal force, v is the velocity; m is the mass (assumed to be one); and r is the distance from the axis of rotation to a point in the annulus.

Comparison of F_c to g shows that the maximum centrifugal force developed is less than 1/10 that of gravity.

In summation, the effect of centrifugal forces are less than the effect of gravity (sedimentation) which is initially less than the effect of diffusion, which in itself is nearly insignificant as compared to the rate of shear in an orthokinetic reaction.

Based on the above, the fact that the system is initially essentially monodispersed and that a rapid loss of particles while maintaining mass balance could not be detected, one concludes that the loss in mass balance was most probably due to sedimenting particles some time after initiation of the reaction. This effect could be delayed by sampling deeper into the system. But, here too, there are limitations. One cannot sample too close to the bottom of the apparatus because there is the possibility of anomalous hydrodynamic flow near the base of the cell. Therefore, prudent procedure dictates that the sampling be performed as far away from the bottom of the cell as possible.

Now we will examine Figure 42 and Table XIII. Both are typical of the data accumulated with the Couette cell. Figure 42 depicts the entire duration of an experiment. Table XIII lists the found mass balance of each sample taken during the experiment. A comparison of the two shows that so long as mass balance is maintained, there is good agreement between the model predictions and the experimental data. Mass balance in

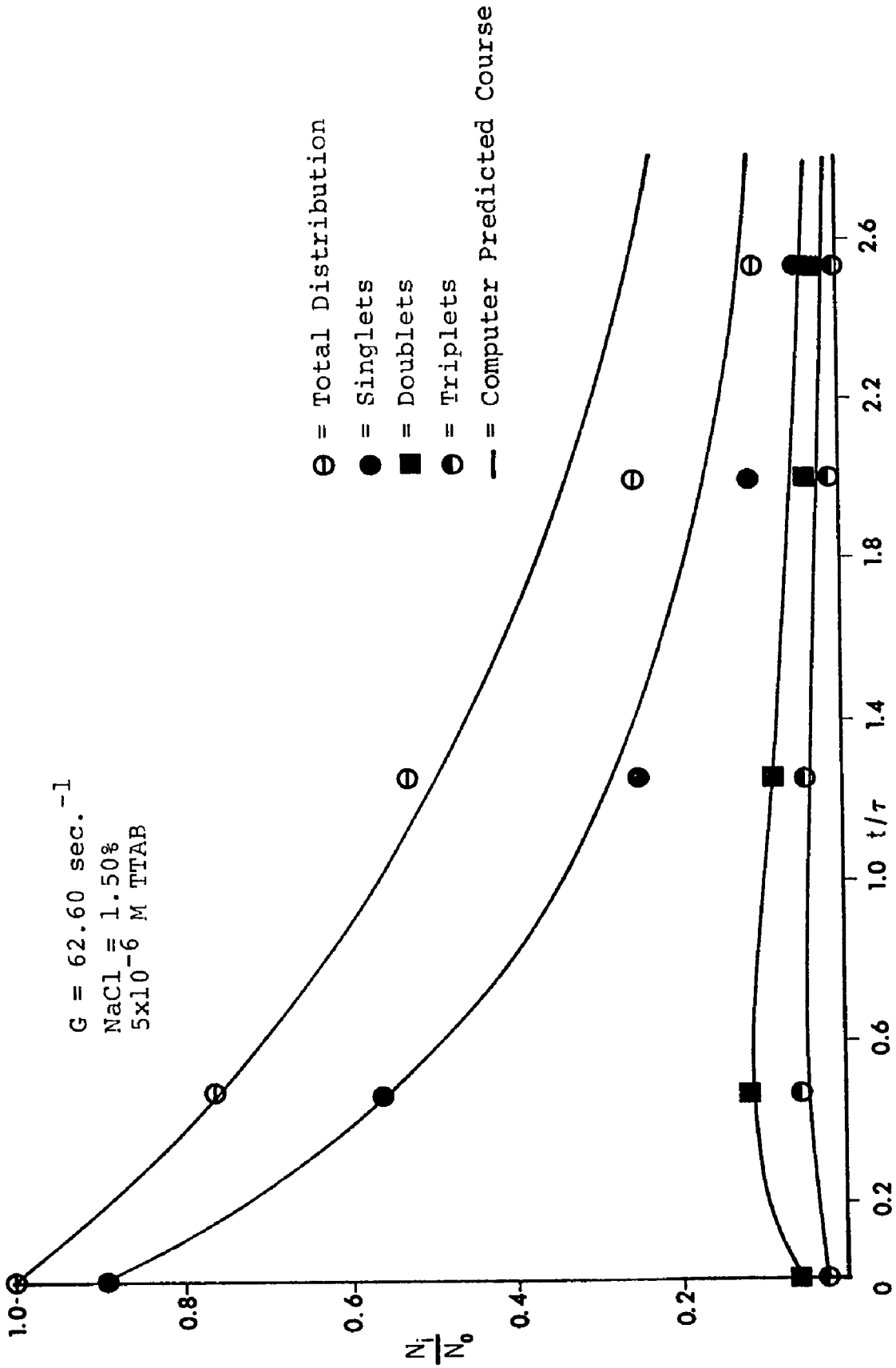

Figure 42. Normalized plot of the total and individual particle size distribution change with time in the maximum rate case for a laminar shear-controlled system depicting the loss of mass balance.

TABLE XIII

Mass Balance at Each Sample Interval

for the Laminar Shear-Controlled Experiment

Pictured in Figure 42

Sample Number	Mass Balance as a Percent of Original Number of Particles
Original	100
1	97
2	101
3	86
4	74

the computer program was maintained by choosing a sufficiently large number of particle size classes. It is assumed that since there is good agreement between the experimental and model predictions at early times, that sedimentation-flocculation does not have a significant effect on initial reaction rates.

Finally, at later times, mass balance is lost experimentally after the combined percentage of singlets, doublets, and triplets falls below 40 percent. This is logical since the system would now contain many large particles, all of which are sedimenting (falling beneath the sampling window) and most probably experiencing some degree of sedimentation-flocculation.

APPENDIX II

Additional Considerations Pertaining to the Taylor Vortex System

Figure 35 presented some interesting data which was consistent throughout the Taylor system studies. The data indicated a lag time for a dimensionless time interval of approximately 0.1. One might consider that the lag time is a function of the fact that the data was forced through an N_i/N_o value of 1.0 by the nature of the data put. A sample of the suspension was taken just prior to initiation of the experiment, and the analysis of this sample was given to the computer to use as the initial particle distribution at dimensionless time zero.

It was postulated that a lag time could be substantiated by introducing (as the original particle size distribution) the particle size distribution at some later time in the experiment, and then determine if model predictions and experimental data were in agreement. Choice of later time data had to be limited to the first (preferably) or second sampling after initiating the experiment due to the limitation of being able to identify only up to 8-mers on the apparatus.

Of course, starting with data point two or three did eliminate the lag-type hump in the experimental data. But, using later time data as an initiating

point in the computer program did not provide a better fit of the theoretical model to the experimental data. The experimental rates of reaction were still much faster than the model predictions.

Finally, let us take a closer look into the problem of hydrodynamics in the Taylor cell, so that we might have a better appreciation for the complexity of the motion therein, and the ultimate problem of defining the flocculation kinetics in such an environment.

The two-dimensional shear flow that is closely simulated in the Couette apparatus has a velocity distribution $u = ay$, in which the coordinate y is perpendicular to the direction of the velocity u and the symbol a denotes a constant. The shear rate is the derivative of u with respect to y for such two-dimensional flows. Consequently, the constant a is called the shear rate for the particular velocity distribution under discussion. This constant is useful because it specified the relative velocity of one fluid particle with respect to another. Now this relative velocity is assumed to be nearly that of the suspended particles. For large values of the shear rate, there is a large relative velocity of particles in the fluid. It is this relative velocity that enhances flocculation since the probability for collisions is increased thereby.

For laminar flows it is assumed that the shear stresses that are induced in a fluid by a particular velocity distribution are directly proportional to the shear rate. The proportionality constant is the viscosity of the fluid. When a test apparatus is operating so that Couette flow is obtained, the torque that is exerted on either of the co-axial cylinders is directly proportional to the shear rate. Thus the higher the torque on the cylinders, the higher will be the relative velocities in the annulus with an increased probability for collision and flocculation. If the inner cylinder rotates instead of the outer one, Taylor cells can occur. If they do, the velocity distribution is much more complex than that for Couette flow. One notes experimentally that the torque on the cylinder increases.

If one were to examine the problem completely, one would determine after a lengthy and difficult numerical calculation the value of the shear rates for this three-dimensional flow. With this knowledge the relative velocities of suspended particles could be inferred, and this information included in a difficult unattempted model, to determine collision probabilities.

If, instead of such an analysis, one were to take the values of the torque that are measured when Taylor cells appear, and divide by the proportionality constant,

the viscosity of the fluid, it would be concluded that the shear rate so calculated had increased significantly due to the occurrence of the secondary motions in the Taylor cells. However, such an estimation is likely to be misleading. Because the three-dimensional motions within these cells will change the distribution of relative velocities throughout the cells, the probability for particle collision could be decreased from the value that might be expected from the apparent increase in the shear rate. This is because the cellular motion will bring particles from the neighborhood of the outside of the annulus where they are moving slower than those in the middle of the gap (i.e., half-way from the inner radius to the outer radius) to the neighborhood of the inner cylinder. Here they will be moving faster than those at the middle of the gap. Thus the particles are speeding up and slowing down as they move around in the annulus.

As has been just indicated, such motions could, in principle, be used to predict a collision efficiency. But these motions are not the ones that were used by Curtis and Hocking, or in any of the two-dimensional shear theories. Lacking the existence of such a theory, the author attempted to place in perspective the data taken while Taylor cells were present. He did this by

weighing the value of the shear rate that was estimated from the torque data of Debler, et al for similar situations.

APPENDIX III

Sample Calculations Plus Discussion of the Modification of Smoluchowski's Basic Equation to Include Alpha and Epsilon

On the following pages are some sample calculations to further clarify the generation of certain key parameters.

$\underline{\tau}$

Equation 13 defined tau as:

$$\tau = \frac{3\eta}{4kTN_0}$$

and typical values for the constants and variables would be:

$$\tau = \frac{3\ (0.8987\text{x}10^{-2})}{(4)(1.38\text{x}10^{-16})(298)(1\text{x}10^{7})} = 16{,}390 \text{ sec.}$$

$\underline{\tau^*}$

Defined by Equation 21,

$$\tau^* = \frac{3}{16Ga_i^3N_0}$$

and a typical calculation would be:

$$\tau^* = \frac{3}{(16)(62.60)(1.01\text{x}10^{-4})^3(1\text{x}10^{6})} = 2{,}907 \text{ sec.}$$

$\underline{G}$

The rate of shear in a Couette cell can be calculated using Equation 52

$$G = \frac{dv}{dr} = -\left(\frac{2\Omega}{r^2}\right)\left(\frac{R_b^2 \cdot R_c^2}{R_c^2 - R_b^2}\right)$$

$\Omega = 2\pi$ (revolutions per second)

at 50 revolutions per minute

$$\Omega = 2\pi\left(\frac{50}{60}\right)$$

and

$$G = - \left(\frac{2(2)(3.1415)(50/60)}{(9.6)^2}\right)\left(\frac{(9.2)^2(10)^2}{(10)^2-(9.2)^2}\right)$$

$$= \left(\frac{10.48}{92.16}\right)\left(\frac{8464}{15.36}\right)$$

$$= (0.11372)(551.04)$$

$$= 62.6$$

Alpha and Epsilon

The alpha and epsilon values both appear in the calculation of the $\sigma^*(ij)$ term. Assuming that all particles are spherical, and they aggregate into spheres of an equivalent volume, the size of a particle can be described as a multiple of a primary particle:

$$v_i = iv_1 \tag{55}$$

$$a_i = i^{\frac{1}{3}} a_1 \tag{56}$$

where v_i and a_i are the respective volume and radius of the ith size particle and the v_1 and a_1 refer to the singlet particle. In this manner one can develop Equation 42

$$\sigma^*_{ij} = \frac{1}{8} \quad (i^{\frac{1}{3}} + j^{\frac{1}{3}})^3$$

The equivalent volume of the ith or j^{th} size particle can be modified by dividing the appropriate term by $\varepsilon_i^{*\frac{1}{3}}$ or $\varepsilon_j^{*\frac{1}{3}}$ respectively. Equation 42 becomes:

$$\sigma^*_{ij} = \frac{1}{8}\left(\left(\frac{i}{\varepsilon^*_i}\right)^{\frac{1}{3}} + \left(\frac{j}{\varepsilon^*_j}\right)^{\frac{1}{3}} \right)^3$$

During the computational process the particular alpha value is a multiple of the corresponding σ^*_{ij} value as a matter of convenience. Examining Equation 46 the

elegance of this maneuver becomes more evident:

$$\frac{dY_k^*}{dX^*} = \sum_{\substack{i=1 \\ j=k-1}}^{i=k-1} \frac{\sigma_{ij}^* Y_i^* Y_j^*}{W_{ij}^*} - 2 \sum_{i=1}^{\infty} \frac{\sigma_{ik}^* Y_i^* Y_k^*}{W_{ik}^*}$$

Assuming the σ_{ik}^* size is being acted on by alpha, (reduced) then the overall effect is a reduction in the rate of loss of the kth size particle.

APPENDIX IV

Tabulated Data for

All Computer Simulations

On the following pages is a tabulation of the data that was entered into the computer for simulation runs using the Smoluchowski model with and without the alpha and/or epsilon variations.

TABLE XIV

Parameters Used for Model Simulations

Figure No.	Curve No.	% of Particle Sizes (x-mer)									
		1	2	3	4	5	6	7	8	9	10
9	1	100.0									
	2	100.0									
10	1	90.0	6.85	1.00	0.50	0.50	0.25	0.25	0.25	0.20	0.20
	2	80.0	10.85	3.50	2.00	2.00	0.50	0.50	0.25	0.20	0.20
	3	70.0	15.85	6.00	3.00	3.00	0.75	0.75	0.25	0.20	0.20
11	1	100.0									
	2	100.0									
	3	100.0									
12	1	100.0									
	2	100.0									
13	1	100.0									
	2	100.0									
14	1	100.0									
	2	100.0									
15	1	100.0									
	2	100.0									
	3	100.0									
16	1	100.0									
	2	100.0									
	3	100.0									
17	1	100.0									
	2	100.0									

TABLE XV

Parameters Used for Model Simulations

Figure No.	Curve No.	% of Particle Sizes (x-mer)									
		1	2	3	4	5	6	7	8	9	10
26		77.0	13.1	6.7	2.1	1.7					
27		66.9	16.2	10.9	3.5	1.4	0.6	0.5			
28	1	89.4	6.0	2.5	1.2	0.9					
	2	89.4	6.0	2.5	1.2	0.9					
	3	89.4	6.0	2.5	1.2	0.9					
29		89.4	6.0	2.5	1.2	0.9					
30		77.2	14.3	5.6	1.9	1.0					
31		66.9	16.2	10.9	3.5	1.4	0.6	0.5			
35		87.7	6.0	3.6	1.7	1.0					
36	1	87.7	6.0	3.6	1.7	1.0					
	2	87.7	6.0	3.6	1.7	1.0					
	3	87.7	6.0	3.6	1.7	1.0					
	4	87.7	6.0	3.6	1.7	1.0					
*40		86.8	8.1	3.1	1.5	0.5					
42		89.4	6.0	2.5	1.2	0.9					

*These additional parameters were required for the diffusion-controlled system:
Viscosity = 0.8937 centipoises; Absolute Temperature - 298°K;
Boltzmann Constant = 1.38044×10^{-16} erg. $deg.^{-1}$

TABLE XVI

Parameters Used for Model Simulations

Figure No.	Curve No.	Initial No. of Particles	Radius of Singlet	W	ε^*	$\alpha_{1,1}$	G $sec.^{-1}$
9	1	$5x10^7$	1.01	1.0	1.0	none	31.30
	2		2.02				
10	1	$5x10^6$	1.01	1.0	1.0	none	31.30
	2						
	3						
11	1	$5x10^7$	1.01	4.0	1.0	none	31.30
	2			2.0			
	3			1.0			
12	1	$5x10^7$	1.01	1.0	1.0	none	15.65
	2						62.60
13	1	$5x10^7$	1.01	1.0	1.0	none	31.30
	2		2.02				
14	1	$5x10^6$	1.01	1.0	1.0	none	31.30
	2	$1.5x10^7$					
15	1	$3.7x10^7$	1.01	1.0	1.0	0.1	31.30
	2					0.6	
	3					1.0	
16	1	$3.7x10^7$	1.01	1.0	1.0	none	31.30
	2				0.8		
	3				0.6		
17	1	$3.7x10^7$	1.01	1.0	1.0	1.0	31.30
	2				0.6	0.8	

TABLE XVII

Parameters Used for Model Simulations

Figure No.	Curve No.	Initial No. of Particles	Radius of Singlet	W	ε^*	$\alpha_{1,1}$	G $sec.^{-1}$
26		4.2×10^6	1.01	2.49	1.0	none	31.30
27		4.0×10^6	1.01	1.59	1.0	none	62.60
28	1	4.9×10^6	1.01	3.00	1.0	1.0	62.60
	2				0.8	1.0	
	3				1.0	0.7	
29		4.9×10^6	1.01	3.00	1.0	none	62.60
30		4.7×10^6	1.01	2.07	1.0	none	62.60
31		4.0×10^6	1.01	1.59	1.0	none	62.60
35		2.4×10^6	1.01	2.50	1.0	none	28.40
36	1	2.4×10^6	1.01	2.86	1.0	none	28.40
	2						41.00
	3						61.40
	4						82.00
*40		9.6×10^6	1.01	2.09	1.0	none	0
42		4.9×10^6	1.01	3.00	1.0	none	62.60

*These additional parameters were required for the diffusion-controlled system:

Viscosity = 0.8937 Centipoises; Absolute Temperature = 298°K;
Boltzmann Constant = 1.38044×10^{-16} erg. $deg.^{-1}$

BIBLIOGRAPHY

Albers, W., and Overbeek, J. Th. G., J. Colloid Sci., 15, 489 (1960)

[a]Bernstein, D. F., Higuchi, W. I., and Ho, N. F. H., J. Pharm. Sci., 60, 690 (1971)

[b]Bernstein, D. F., "The Kinetics of Coalescence of Dilute Oil-in-Water Emulsions." Ph.D. Dissertation, University of Michigan, 1971

Bird, R. B., Curtis, C. F., and Lightfoot, E. N., "Transport Phenomina," J. Wiley & Sons, New York, New York, 1960

Brenner, H., Chem. Engng. Soc., 16, 242 (1961)

Clay, P. H., Proc. Roy. Acad. Sci. (Amsterdam), 43, 852,979 (1940)

Curtis, A. S. G., and Hocking, L. M., Trans. Faraday Soc., 66, 1381 (1970)

Dean, W. R., and O'Neill, M. E., Mathematika, 10, 13 (1963)

Debler, W., Füner, E., and Schaaf, B., Proc. Twelfth Int. Cong. of Applied Mech., 158 (1969)

Frens, G., Engel, D. J. C., and Overbeek, J. Th. G., Trans. Faraday Soc., 63, 418 (1967)

Goldman, A. J., Cox, R. G., and Brenner, H., Chem. Engng. Sci., 21, 1151 (1966)

Hauser, E. A., and Niles, G. E., J. Phys. Chem., 45, 954 (1941)

Higuchi, W. I., Okada, R., and Lemberger, A. P., J. Pharm. Sci., 51, 683 (1962)

Higuchi, W. I., Okada, R., Stelter, G. A., and Lemberger, A. P., J. Pharm. Sci., 52, 49 (1963)

Ho, N. F. H., Suzuki, A., and Higuchi, W. I., J. Pharm. Sci., 59, 1125 (1970)

Ho, N. F. H., Toguchi, H., and Higuchi, W. I., J. Pharm. Sci., 62, 851 (1973)

Hogg, R., Healy, T. W., and Fuerstenau, D. W., Trans Faraday Soc., 62, 1638 (1966)

Honig, E. P., Roeberson, G. J., and Wiersma, P. H., J. Colloid Interf. Sci., 36, 97 (1971)

Hul, H. J., van den and Hoff, J. W., van der, J. Colloid Interf. Sci., 28, 336 (1968)

Jeffrey, G. B., Proc. Lond. Math. Soc. (ser. 2), 14, 327 (1915)

Jones, J. E., and Levine, S., J. Colloid Interf. Sci., 30, 241 (1969)

Kruyt, H. R., "Colloid Science," Vol. 1, Elsevier Publishing Co., Amsterdam, The Netherlands, 1952, p. 278

Langstroth, G. O., and Gillespie, T., Can. J. Chem., 29, 201 (1951)

Lemberger, A. P., and Mourad, N., J. Pharm. Sci., 54, 229 (1965)

Levich, V. J., "Physical Chemical Hydrodynamics," Prentice Hall, Englewood Cliffs, New York, 1962

Lin, C. J., Lee, K. J., and Sather, N. F., J. Fluid Mech., 43, Part 1, 35 (1970)

Manley, R. St. J., and Mason, S. G., J. Colloid Sci., 7, 354 (1952)

Mason, S. G., and Manley, R. St. J., J. Colloid Sci., 7, 354 (1952)

Mason, S. G., and Manley, R. St. J., Can. J. Chem., 33, 763 (1955)

Mason, S. G., and Trevelyan, B. J., J. Colloid Sci., 6, 354 (1951)

Mathai, K. G., and Ottewill, R. H., Trans. Faraday Soc., 62, 759 (1966)

[a]Matthews, B. A., and Rhodes, C. T., J. Colloid Interf. Sci., 28, 71 (1968)

[b]Matthews, B. A., and Rhodes, C. T., J. Pharm. Sci., 57, 557,569 (1968)

Matthews, B. A., and Rhodes, C. T., J. Colloid Interf. Sci., 32, 332 (1970)

Maude, A. D., Br. J. Appl. Phys., 12, 293 (1961)

Muller, H., Kolloidchem. Beih., 27, 223 (1928)

Muller, V. M., Colloid J. (USSR), 31, 340 (1969)

O'Neill, M. E., Mathematika, 11, 67 (1964)

Saffman, P. G., and Turner, J. S., J. Fluid Mech., 1, 16 (1956)

Schlichting, H., "Boundry Layer Theory," McGraw-Hill, New York 1968

Schultz-Grunow, F., Zeitschrift fur Angewandte Mathematik und Mechanik, 39, 101 (1959)

Shinnar, R., and Church, J. M., Ind. Eng. Chem., 52, 253 (1960)

Smoluchowski, M. von, Physik. Z., 17, 557, 585 (1916)

Smoluchowski, M., von, Z. Physik. Chem. (Leipzig), 92, 129 (1917)

Spielman, L. A., J. Colloid Interf. Sci., 33, 562 (1970)

Stimson, M., and Jeffrey, G. B., Proc. Roy. Soc. A, 111, 110 (1926)

Suzuki, A., Ho, N. F. H., and Higuchi, W. I., J. Colloid Interf. Sci., 29, 552 (1969)

Swift, D. L., and Friedlander, S. K., J. Colloid Interf. Sci., 19, 621 (1964)

Taylor, G. I., Trans. Roy. Soc., A223, 289 (1923)

Vermeulen, T., Williams, G. M., and Langlois, G. E., Chem. Eng. Progr., 51, 85 (1955)

Verwey, E. J. W., and Overbeek, J. Th. G., "Theory of the Stability of Lyophobic Colloids," Elsevier Publishing Co., New York, New York 1948

Vold, M. J., J. of Colloid Sci., 14, 168 (1959)

Wakiya, S., J. Phys. Soc. Japan, 22, 1101 (1967)